Parametric Analysis and Semi-Active Control of Automotive Suspension Systems

by

LAM Hiu Fung

A Thesis Submitted in Partial Fulfillment

of the Requirements for the Degree of

Master of Philosophy

In

Mechanical and Automation Engineering

June 2001

ABSTRACT

In the environment of a moving vehicle, ride quality is concerned with the sensation or feel of the passenger. Vibration in today's increasingly high-speed vehicles including automobiles severely affects their ride comfort and safety. To improve the ride comfort, effective vibration control of suspension systems is very important. In this study, a semi-active device called magneto-rheological (MR) damper is selected since it can provide high controllable force for vibration suppression. Moreover, the semi-active system is more stable, consumes less power and less complexity comparing to the active system. The objective of this thesis is to study the characteristics of the Two Degree-of-Freedom (2DoF) quarter car models, and develop an effective semi-active automotive suspension system. In this study, there are four reference systems, which are passive, skyhook, groundhook, and hybrid suspension systems. Based on the analysis of those four systems, the influences of the parameters on each system are discussed. Comparing those systems, the optimal system and parameters are identified and this optimal system is selected as the reference model for the sliding mode controller. Considering loading uncertainty, this controller is used in the automotive suspension systems with MR dampers in order to improve the passenger's comfort and safety. In order to show the effectiveness of the controller, the controller with the optimal reference model is compared with other controllers. The transmissibility analyses and simulation results for three kinds of road excitations are used to evaluate the performance of those control systems. The vibration responses are evaluated in both time and frequency domains.

Compared to the passive system, the acceleration of the sprung mass is significantly reduced for the system with a controlled MR damper. Under random excitation and the road elevation profile, the ability of the MR fluid damper to reduce both peak response and root-mean-square response is also shown. The performances of different reference models for the sliding mode controller are also presented. The results of this study can be used to develop guidelines to effectively integrate automotive suspensions with MR dampers.

摘要

行車質素就是乘客在車輛行駛時的感覺或感受。由於現今車輛的馬力及速度不斷增加，其所造成的振動嚴重地影響了行車安全與舒適性。爲了改善行車質素，有效的懸掛振動控制系統是必須的。與主動控制系統相比，半主動控制系統具有高可靠性，而且不需要特別大的能量消耗，因此本文選用了一種名爲磁流變阻尼器 (magneto-rheological damper) 之半主動控制器件作爲懸掛系統中的重要部份。

本研究的目的就是通過對一個雙自由度的車輛模型之特性的研究以建立一個高效率的車輛懸掛系統。本文研究了四種懸掛系統，分別有被動、連天、接地和混合系統。根據這四種系統之分析，了解不同的參數對整個系統之影響。從以上系統之比較，可找出最優之系統及其參數，並以之作爲滑模控制 (sliding mode control) 中的參考模型。

在本文中，考慮載荷具有不確定性，同時要改善行車安全與舒適性，因此建立了一個滑模控制器以應用於配備磁流變阻尼器之車輛懸掛系統。爲了研究控制系統的性能，應用不同之參考模型之滑模控制器會被作出比較及分析。同時爲了測試懸掛系統的性能，分別在時間域和頻率域對三種不同的路面激勵下的系統的傳導特性和響應特性進行了仿真分析。

與被動控制系統相比，通過安裝受控的磁流變阻尼器，負載質量的加速度和位移均大幅度被減低。在隨機及現實路面的激勵中，磁流變阻尼器也同時表現了對峰值響應和方根平均值響應的減振能力。同時，本文亦給出了應用不同之參考模型之滑模控制器之性能。我們發展的裝置和原理將對汽車工業在設計新的懸掛系統，或者在提升現有的懸掛系統時，具有很高的參考價值及引導作用。

ACKNOWLEDGEMENTS

I would like to express my most sincere thanks to my advisor, Prof Liao Wei-Hsin, for all his help during the past two years. His guidance and encouragement were vital elements in the completion of this work.

I would also like to thank Prof Huang Jie and Prof. Li Wen-Jung for serving on my graduate committee members as well as other faculty members for their patient instruction throughout my academic study at The Chinese University of Hong Kong.

Moreover, I would like to express my thanks to my close colleagues, Cedric K. H. Law, Mark S. K. Lau, H. C. Lo (Chun), He Yong and Dr. D. H. Wang for supporting me and working with me in many long lonely nights.

Finally I would like to thank my father and mother, K. P. Lam and C. L. Ip, my brothers, Raymond H. W. Lam and Jimmy H. M. Lam (M&Lam) for all their love and support during my study at CUHK.

TABLE OF CONTENTS

LIST OF FIGURES

LIST OF TABLES

Chapter 1

INTRODUCTION

When you were driving a car, or taking a bus, or sitting on a train, did you feel anything special? Vibration, it is an unwanted thing during traveling for most people. However, have you ever imagined that you can do anything you want stably when you are traveling? For example, you can take a bath in a train. You can sleep in a bus as comfortable as on your bed. Our objective is to eliminate the vibration for a moving vehicle in this dissertation work. Before we discuss how to achieve this goal, some background about this thesis is provided. Controllable suspension systems including the models of suspension systems, controllable devices and vibration control methods are introduced. Previous researches will be presented in the literature review. The motivation and objective of this research will also be stated. Finally, the outline of this thesis will be described at the end of this chapter.

1.1 Controllable Suspension System

In a moving vehicle, passengers often feel uncomfortable due to the vibration of the vehicle body. A suspension system is mainly used to isolate the vehicle body with the passengers from road disturbances. It reduces the displacement and acceleration of the vehicle body. To improve the ride comfort, effective vibration control of the vehicle suspension system is very important.

In this study, controllable suspension systems are considered. This controllable system includes three main parts. They are system model, controllable device, and system controller.

1.1.1 Automotive Suspension System

A Suspension system is used to reduce the undesirable vibration of a moving automobile. With different control methods, suspension systems can be classified as passive, active and semi-active controls.

For a passive suspension system, it includes the suspension springs and shock absorbers. The shock absorbers normally are dampers, which is used to absorb vibration. In general, the mass of the vehicle body is usually called "sprung mass" and the mass of the gearbox and the other associated suspension components are called "unsprung mass". The passive suspension system can store the energy by the springs and dissipate the energy through the dampers. However, the parameters of the passive system are fixed and cannot be modulated in accordance with the operating condition of the vehicle. They are only synthesized through off-line design techniques and no on-line feedback actions are taken. Because of this limitation, the performance of the passive system may not be satisfactory for different operation conditions. Therefore, the passive system could not be effective to deal with road disturbances and various uncertainties.

Comparing to the passive system, the dampers between the sprung mass and unsprung mass are replaced by the force actuators in an active suspension system [1]-[9]. The actuators are installed in parallel to the suspension springs. Based on the on-line measurements from sensors, the operating conditions of the vehicle are monitored. The controller receives the signals from sensors, and then it will send suitable commands to the actuators based on the control algorithm. Then actuators can generate suitable forces or torques to suppress vibration of the vehicle body. The active control system can adapt for system variations and provide high performance in wide frequency range. Therefore, the active systems could be much more effective than the passive systems. However, active systems generally require high power so the cost may be increased. Moreover, the systems could be destabilized and the complexity of the systems could also be increased.

In order to reduce the shortcomings but still keep the benefits of active suspension system, the semi-active suspension has been proposed [7]-[17]. For a semi-active suspension system, the passive dampers in the passive suspension system are replaced with controllable devices. Similar to the active suspension system, sensors can measure the operating conditions of the vehicle. The controller will send suitable commands to the controllable devices based on the received signals and control algorithm. When the controllable devices received the commands, their properties will be changed so that suitable damping forces can suppress the vibration. The semi-active control can achieve a desirable system performance when comparing to passive system. In addition, it consumes less power, less complex and the system is more stable when comparing to the active system.

1.1.2 Controllable Devices

As mentioned in the previous sub-section, one kind of controllable semi-active device is that its properties of the device can be changed. Another semi-active device allows changing the size of the orifice, which the hydraulic fluid passes through. In order to change the size of the orifice, motor or other actuators are needed. For this kind of device, it is not so convenient to use since it needs an extra actuator adding into the system. It will also increase the weight and complexity of the system. Therefore, the devices with changeable properties could be better choices. There exist two well-known semi-active controllable devices. They are the so-called magnetorheological damper (MR damper) [24]-[34] and electrorheological damper (ER damper) [22], [35]. Their properties can be adapted such that the damping forces are controllable. However, there may exist some limitations. For example, ER dampers need very large input voltage, and both ER and MR dampers cannot produce arbitrary damping forces to the system so that the performances sometimes may not be as good as active control systems. In this study, the MR damper is considered. It is used in the suspension system to produce controllable damping force. The MR damper is controlled by input voltage. Through the current driver, the suitable current will pass to the coil to produce the electromagnetic field applying to the MR fluid such that the viscosity of the fluid can be controlled.

1.1.3 MR Fluid and Damper

The MR damper is the semi-active device, which contains some MR fluids inside the damper. The MR fluids are materials that respond to an applied magnetic field with a change in rheological behavior [24]. With this property, the MR fluid devices can be applied in vibration control systems and aerobic exercise equipments [30]. The modeling and the dynamic characterization of the MR damper have been developed by several researchers [31]-[34]. Different control methods for suspension systems with MR dampers have also been proposed [23], [39] and [40].

1.2 Vibration Control

In this section, a brief description of the development and the past related researches are presented. It covers active, semi-active and robust control of automotive suspension systems.

1.2.1 Active Control

Active control systems reduce vibration by using actuators to generate external forces. There are several active control algorithms to produce suitable control forces. For example, a new nonlinear backstepping design for the control of active suspension systems can improve the inherent tradeoff between ride quality and suspension travel [3].

Another active suspension control approach is to use a filtered feedback control scheme and a novel compressible fluid suspension strut for a quarter-vehicle suspension system [4]. An active suspension employing an electrohydraulic pressure control system with optimal parameters can improve both ride comfort and handling properties [5]. Taghirad and Esmailzadeh proposed LQG/LQR active control method for automobile suspension systems, which can retain both ride comfort and road handling characteristics [6]. Among these work, the active control method has been shown to be effective for vibration suppression.

1.2.2 Semi-active Control

Semi-active control can change the properties of semi-active devices so that suitable damping forces can be generated to suppress vibration. There are some alternative semi-active control methods. A computer controlled semi-active suspension system can improve skyhook control logic to provide better control of the suspension parameters as well as improve the trade-off between ride comfort and road handling [10]. A new adaptive skyhook control of vehicle semi-active suspensions can provide adequate damping for the wheel hop frequency and improve the performance compared with the system of the traditional skyhook controller [11]. A modified skyhook control for the semi-active Macpherson suspension system, which utilizes a filtered absolute velocity of the sprung mass and a filtered relative velocity of the sprung and unsprung masses, can achieve competitive performance [14]. Ahmadian performed a deep analysis for semiactive control of single and multiple degree of freedom systems [16] and [17].

1.2.3 Robust Control

To deal with uncertainties, several robust control algorithms are proposed. A robust control called sliding mode control has been developed. A sliding mode controller for active suspension system can adapt the change of load and road conditions and the performance of the active system is much better than the passive system especially around resonance frequency [18]. A sliding mode controller for vehicle active suspension systems with non-linearities can improve both the ride quality and handling performance. This sliding mode active suspension system also showed robust tracking performances even when suspension parameters changed suddenly [21]. A sliding mode controller for ER suspension system can provide a favorable control performance and effective vibration isolation subjected to parameter uncertainties and external disturbances [22].

1.3 Research Objective

The objective of this thesis is to develop an effective semi-active automotive suspension system. In order to achieve this goal, a parametric study on the 2DoF quarter car model for passive, skyhook, groundhook and hybrid suspension systems will be performed. Moreover, the influences of parameters on each system will be discussed. Based on these analyses, the optimal parameters and system will be found, and this optimal system will be selected as the reference model for the sliding mode controller. The simulation results for three kinds of excitation inputs will be used to evaluate the performance of those control systems.

1.4 Thesis Outline

Chapter 1: An introduction of the passive, active and semi-active suspension system with controllable devices and vibration controllers is presented. The comparison in advantages and limitations of these three suspension systems are discussed. The previous researches in the related areas have been discussed in the literature review. The objective of this thesis is also presented.

Chapter 2: A parametric study of four suspension systems is presented. Based on the concept of transmissibility, the characteristics of passive, skyhook, groundhook and hybrid suspension systems are studied. Moreover, the comparison between the ideal and non-ideal systems for skyhook, groundhook and hybrid semi-active control is discussed. The stability and optimization of the suspension system is investigated.

Chapter 3: The components of the controllable suspension systems are described. The formulation of the sliding mode controllers with different reference models and the damper controller are developed.

Chapter 4: The computer simulation results for three different excitation tests are presented in this chapter. Bump excitation, random excitation and road elevation profile results are analyzed and discussed.

Chapter 5: The results and conclusions from this study are summarized with some recommendations for the future development.

Chapter 2

PARAMETRIC STUDY OF SUSPENSION SYSTEMS

In order to develop an effective semi-active suspension system, one would like to study the characteristics of the system parameters. In this thesis, three semi-active control configurations are proposed. They are skyhook, groundhook and hybrid semi-active control systems. In order to know the properties of these systems, a parametric analysis for the passive and these three semi-active suspension systems is performed. The transmissibilities of those four systems are compared and the characteristics of each system are discussed. The differences between the ideal and non-ideal systems for three semi-active controls are also discussed. Finally, the stability for those four suspension systems and the parametric optimization of the hybrid system are investigated.

2.1 System Models and Transmissibility

A typical primary automotive suspension system can be modeled to a two degree-of-freedom (2DoF) system, which is so-called 2DoF quarter car model shown in Figure 1. For this model, the tire is considered as massless spring and both the sprung and the unsprung masses are considered. Since the damping of the tires is very small comparing to that of the suspension damper, it is relatively insignificant and assumed to be zero (see Figure 2).

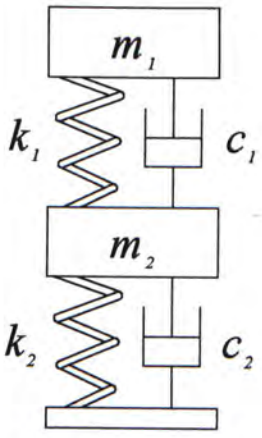

Figure 1 : 2DoF quarter car model

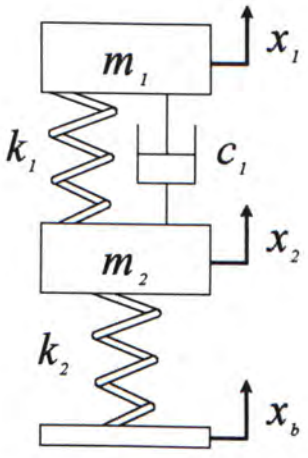

Figure 2 : 2DoF quarter car model (neglecting the tire damping $c_2 = 0$)

The three semi-active suspension systems can be classified by Ideal and Non-Ideal cases. For the Ideal cases, the semi-active devices in off-state will not generate any force to the system. However, for Non-Ideal cases, they will generate a minimum force when they are in off-state. The comparison between the Ideal and Non-Ideal cases will be discussed in the terms of transmissibility.

2.1.1 Passive Suspension System

With the reference to Figure 2, a quarter of the vehicle mass with passengers is represented by a sprung mass m_1 and the mass of wheels, tires and other components are represented by an unsprung mass m_2. The vertical motion of sprung mass and unsprung mass can be described by x_1 and x_2, respectively. The excitation due to the road disturbance is x_b. Moreover, the suspension spring constant is k_1 and the tire spring constant is k_2. The damping coefficient of the damper and the tire are c_1 and c_2, respectively.

By applying Newton's second law to the quarter car model, the equations of motion are:

$$\begin{cases} m_1\ddot{x}_1 + c_1(\dot{x}_1 - \dot{x}_2) + k_1(x_1 - x_2) = 0 \\ m_2\ddot{x}_2 + c_1(\dot{x}_2 - \dot{x}_1) + c_2(\dot{x}_2 - \dot{x}_b) + k_1(x_2 - x_1) + k_2(x_2 - x_b) = 0 \end{cases} \quad (1)$$

By Laplace transform, the equations become:

$$\begin{bmatrix} m_1s^2 + c_1s + k_1 & -(c_1s + k_1) \\ -(c_1s + k_1) & m_2s^2 + (c_1 + c_2)s + (k_1 + k_2) \end{bmatrix} \begin{bmatrix} X_1(s) \\ X_2(s) \end{bmatrix} = \begin{bmatrix} 0 \\ (c_2s + k_2)X_b(s) \end{bmatrix} \quad (2)$$

Then the equation (2) becomes

$$\begin{bmatrix} X_1(s) \\ X_2(s) \end{bmatrix} = \frac{1}{|A|} \begin{bmatrix} m_2s^2 + (c_1 + c_2)s + (k_1 + k_2) & (c_1s + k_1) \\ (c_1s + k_1) & m_1s^2 + c_1s + k_1 \end{bmatrix} \begin{bmatrix} 0 \\ (c_2s + k_2)X_b(s) \end{bmatrix}$$

$$= \frac{1}{|A|} \begin{bmatrix} (c_1s + k_1)(c_2s + k_2)X_b(s) \\ (m_1s^2 + c_1s + k_1)(c_2s + k_2)X_b(s) \end{bmatrix}$$

where

$$A = \begin{bmatrix} m_1s^2 + c_1s + k_1 & -(c_1s + k_1) \\ -(c_1s + k_1) & m_2s^2 + (c_1 + c_2)s + (k_1 + k_2) \end{bmatrix}$$

$$|A| = m_1m_2s^4 + [m_1(c_1 + c_2) + m_2c_1]s^3 + [m_1(k_1 + k_2) + m_2k_1 + c_1c_2]s^2 + (c_1k_2 + c_1k_1)s + k_1k_2$$

The displacement transmissibility is the magnitude ratio of the displacement output to the displacement input. The displacement transmissibility of sprung mass and unsprung mass are Td_1 and Td_2, respectively.

$$Td_1 = \left|\frac{X_1}{X_b}\right| = \sqrt{\frac{[(c_2\omega_b)^2 + (k_2)^2][(c_1\omega_b)^2 + (k_1)^2]}{a^2 + b^2}}$$
$$Td_2 = \left|\frac{X_2}{X_b}\right| = \sqrt{\frac{[(c_2\omega_b)^2 + (k_2)^2][(-m_1\omega_b{}^2 + k_1)^2 + (c_1\omega_b)^2]}{a^2 + b^2}} \quad (3)$$

where

$a = m_1 m_2 \omega_b{}^4 - [m_1(k_1 + k_2) + m_2 k_1 + c_1 c_2]\omega_b{}^2 + k_1 k_2$

$b = -[m_1(c_1 + c_2) + m_2 c_1]\omega_b{}^3 + (c_1 k_2 + c_1 k_1)\omega_b$

X_1 and X_2 is the amplitudes of the displacement of the sprung mass and unsprung mass

X_b is the amplitude of the displacement of the base

Let the mass ratio $m_r = m_1 / m_2$, spring ratio $k_r = k_1 / k_2$, damping ratio of the suspension damper $\zeta_1 = c_1 / 2\sqrt{m_1 k_1}$, the natural frequency $\omega_{n1} = \sqrt{k_1 / m_1}$, driving frequency ω_b, and frequency ratio $r = \omega_b / \omega_{n1}$. The damping of the tire is neglected so that $c_2 = 0$. Then the equation (3) becomes:

$$Td_1 = \left|\frac{X_1}{X_b}\right| = \sqrt{\frac{m_r{}^2(1 + (2\zeta_1 r)^2]}{[k_r r^4 - (k_r + m_r k_r + m_r)r^2 + m_r]^2 + [-(m_r + 1)2k_r\zeta_1 r^3 + 2\zeta_1 m_r r]^2}}$$
$$Td_2 = \left|\frac{X_2}{X_b}\right| = \sqrt{\frac{m_r{}^2[(1 - r^2)^2 + (2\zeta_1 r)^2]}{[k_r r^4 - (k_r + m_r k_r + m_r)r^2 + m_r]^2 + [-(m_r + 1)2k_r\zeta_1 r^3 + 2\zeta_1 m_r r]^2}} \quad (4)$$

Similarly, the acceleration transmissibility is the ratio of the acceleration amplitude of output to the amplitude of displacement input. The acceleration transmissibilies of sprung mass and unsprung mass are Ta_1 and Ta_2, respectively. The ratio representation of the acceleration transmissibilities are

$$Ta_1 = \left|\frac{\ddot{X}_1}{X_b}\right| = r^2\sqrt{\frac{m_r{}^2(1+(2\zeta_1 r)^2]}{[k_r r^4-(k_r+m_r k_r+m_r)r^2+m_r]^2+[-(m_r+1)2k_r\zeta_1 r^3+2\zeta_1 m_r r]^2}}$$
$$Ta_2 = \left|\frac{\ddot{X}_2}{X_b}\right| = r^2\sqrt{\frac{m_r{}^2[(1-r^2)^2+(2\zeta_1 r)^2]}{[k_r r^4-(k_r+m_r k_r+m_r)r^2+m_r]^2+[-(m_r+1)2k_r\zeta_1 r^3+2\zeta_1 m_r r]^2}} \quad (5)$$

With the reference to [42], the parameters of the quarter car model for a typical car are given in Table 1.

Table 1 : Parameters for a typical car

Parameter	Value
Sprung mass of quarter car (m_1)	454.5 kg
Unsprung mass of quarter car (m_2)	45.45 kg
Mass ratio (m_r)	10
Spring constant of suspension system (k_1)	22 kN/m
Spring constant of tire (k_2)	176 kN/m
Spring ratio (k_r)	0.125
Damping coefficient of tire (c_2)	0 N-s/m

Substitute the above parameters to the equation (4) and (5), the displacement and acceleration transmissibilities of the sprung mass and unsprung mass of the passive suspension system are shown in Figure 3.

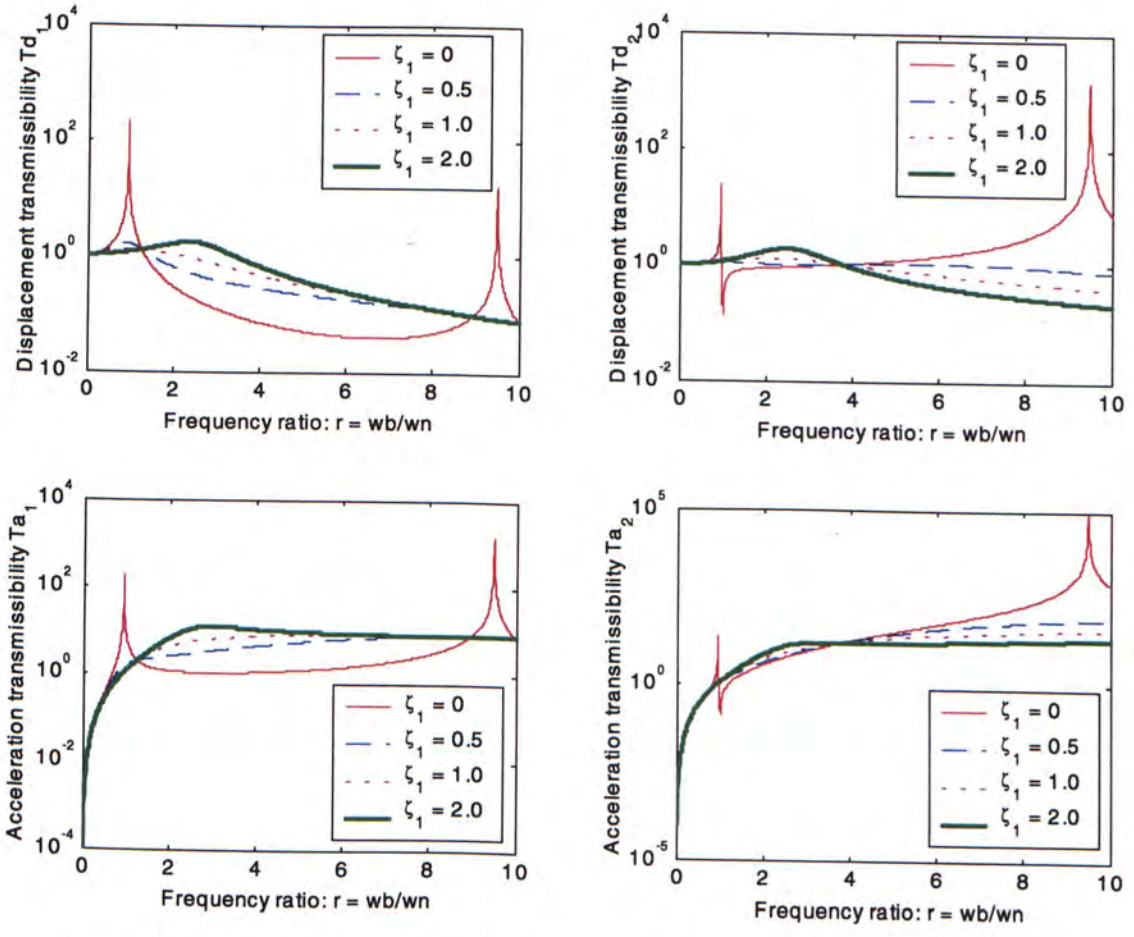

Figure 3 : The displacement and acceleration transmissibilities of the passive system

The transmissibilities of the passive suspension system for various damping ratios are shown in Figure 3. The resonances of this passive system occur around $r_1 = 1$ and $r_2 = 9.49$. For the extreme case $\zeta_1 = 0$, the system becomes mass-spring system. The transmissibilities at the natural frequencies are very large. For increasing the damping ratio ζ_1, the transmissibility at the first resonance will decrease and the peak of the transmissibility of the sprung mass will shift to higher frequency. Therefore, it is a tradeoff between the broadband frequency isolation and the resonance control in the passive suspension.

2.1.2 *Skyhook Suspension System*

The skyhook control policy for semi-active damper is used to switch the damper on or off in order to adjust the damping level to dissipate the energy due to vibration. The example in Figure 4 illustrates the on-off skyhook policy. The equations of the skyhook policy are

$$\begin{aligned} v_1 \times v_{12} > 0, \quad & c = c_{on} \\ v_1 \times v_{12} < 0, \quad & c = c_{off} \end{aligned} \tag{6}$$

where v_1 represents the absolute velocity of the sprung mass, $\dot{x}_1$

v_{12} represents the relative velocity across the damper, $\dot{x}_1 - \dot{x}_2$

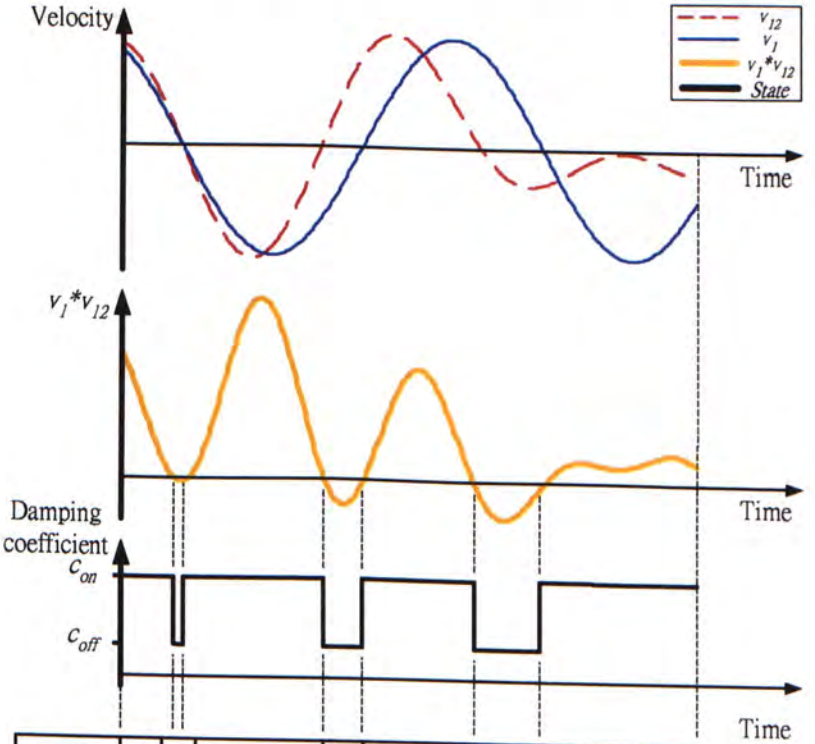

v_1	+	+	-	-	+	+	-
v_{12}	+	-	-	+	+	-	-
v_1*v_{12}	+	-	+	-	+	-	+
State	on	off	on	off	on	off	on

Figure 4 : Example for skyhook control policy

The skyhook suspension system can be classified to "Ideal skyhook system" and "Non-Ideal skyhook system". For Ideal skyhook system, the damping coefficient for the off-state is 0, i.e. $c_{off} = 0$. For Non-Ideal skyhook system, the damping coefficient for the off-state is positive number, i.e. $c_{off} > 0$. The Non-Ideal and Ideal skyhook configurations are also shown in Figure 5 and Figure 6.

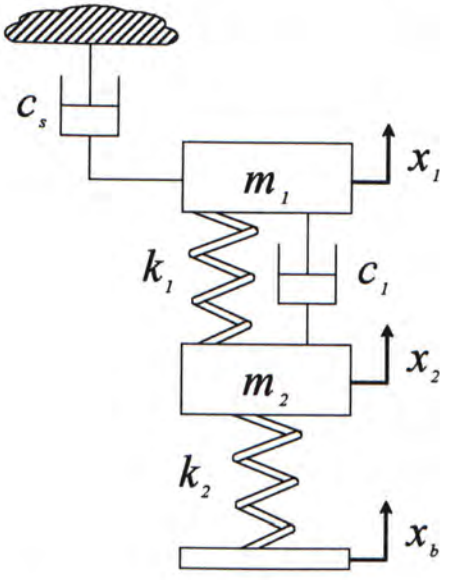

Figure 5 : Non-Ideal skyhook configuration

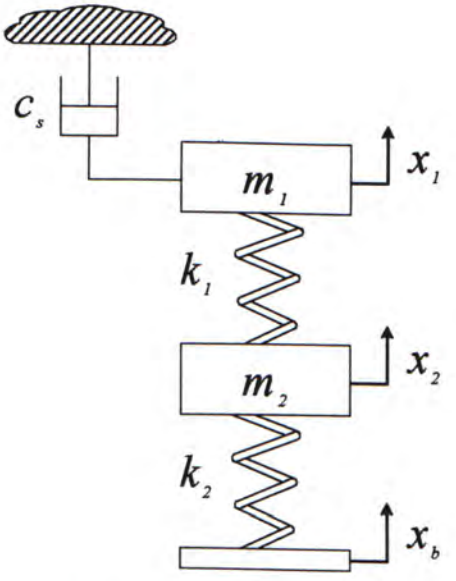

Figure 6: Ideal skyhook configuration

Based on the on-off skyhook policy, the damping coefficient of the Non-Ideal skyhook system is $c_{off} = c_1$ for off-state and $c_{on} = c_1 + c_s$ for on-state. Since for the Ideal case the damping coefficient for off-state should be equal to zero (i.e. $c_{off} = c_1 = 0$), the damping coefficient for on-state becomes $c_{on} = c_s$. Then the skyhook policies for Non-ideal and Ideal systems become

$$Non-Ideal: \begin{cases} v_1 \times v_{12} > 0, & c = c_{on} = c_1 + c_s \\ v_1 \times v_{12} < 0, & c = c_{off} = c_1 \end{cases} \quad (7)$$

$$Ideal: \begin{cases} v_1 \times v_{12} > 0, & c = c_{on} = c_s \\ v_1 \times v_{12} < 0, & c = c_{off} = 0 \end{cases} \quad (8)$$

The damping forces of the Non-Ideal and Ideal skyhook systems are illustrated in Figure 7 and Figure 8. It can be seen that there is the minimum level of the damping force in the Non-Ideal system when it is turned off. When the Ideal system is turned off, there is no damping force acting on the system. That is the difference between Non-Ideal and Ideal system.

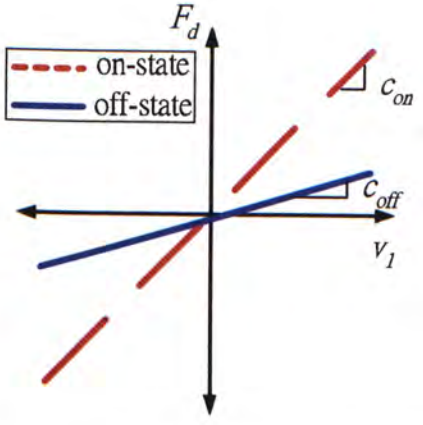

Figure 7 : Non-Ideal on-off skyhook system

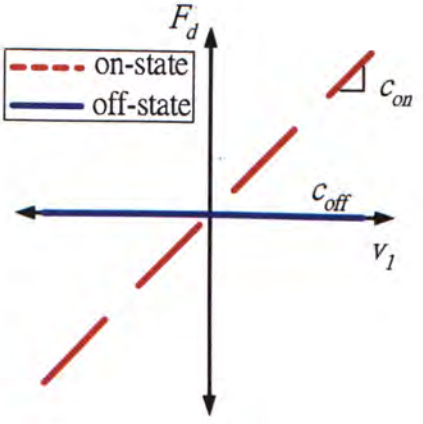

Figure 8 : Ideal on-off skyhook system

Note that when comparing the Non-Ideal and Ideal systems, the damping coefficient of on-state c_{on} should be equal. This is because the maximum damping coefficient of the semi-active damper is assumed to be the same for Non-Ideal and Ideal systems. The only difference is the damping coefficient for off-state c_{off}. Therefore the damping coefficient of Non-Ideal system for on-state, $c_{on} = c_1 + c_s$, is assumed to be equal to the damping ratio of Ideal system for on-state, $c_{on} = c_s$.

Before discussing the characteristics of the Non-Ideal and Ideal 2DoF skyhook systems, it would also be good to compare the Non-Ideal and Ideal Single Degree-of-Freedom (SDoF) skyhook systems.

The configuration of the Non-Ideal and Ideal SDoF skyhook systems [16] are similar to the 2DoF skyhook systems, as shown in Figure 9 and Figure 10. Based on the equation of motion, the transmissibility ratio can be found out (see Table 2). For the Ideal system, the damping ratio of on-state is $\zeta_{on} = c_s / 2\sqrt{m_1 k_1} = \zeta_s$ and the damping ratio of off-state is $\zeta_{off} = 0$. For the Non-Ideal system, the damping ratio of on-state is $\zeta_{on} = (c_s + c_1) / 2\sqrt{m_1 k_1} = \zeta_s + \zeta_1$ and the damping ratio of off-state is $\zeta_{off} = c_1 / 2\sqrt{m_1 k_1} = \zeta_1$.

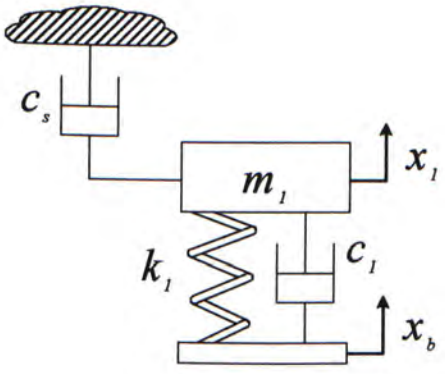

Figure 9 : Non-Ideal SDoF skyhook system

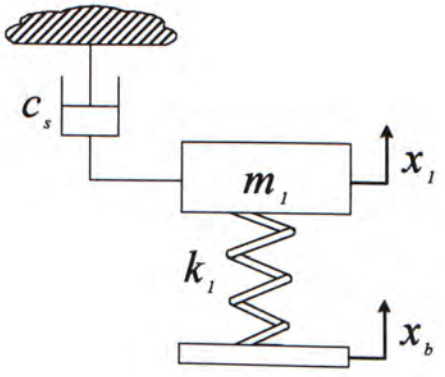

Figure 10 : Ideal SDoF skyhook system

Table 2 : Comparison between Non-Ideal and Ideal SDoF skyhook system

Ideal SDoF skyhook system	Non-Ideal SDoF skyhook system
$(Td_1)_I = \left\lvert\frac{X_1}{X_b}\right\rvert = \sqrt{\frac{1}{(1-r^2)^2 + (2\zeta_s r)^2}}$ $= \sqrt{\frac{1}{(1-r^2)^2 + (2\zeta_{on} r)^2}}$ $= \sqrt{\frac{1}{a}}$ *where* $a = (1-r^2)^2 + (2\zeta_{on} r)^2$	$(Td_1)_N = \left\lvert\frac{X_1}{X_b}\right\rvert = \sqrt{\frac{1+(2\zeta_1 r)^2}{(1-r^2)^2 + (2(\zeta_s + \zeta_1) r)^2}}$ $= \sqrt{\frac{1+(2\zeta_{off} r)^2}{(1-r^2)^2 + (2\zeta_{on} r)^2}}$ $= \sqrt{\frac{1+b}{a}}$ *where* $a = (1-r^2)^2 + (2\zeta_{on} r)^2$ $b = (2\zeta_{off} r)^2$

The comparison of the displacement transmissibility (in Table 2) shows that the displacement transmissibility of Ideal skyhook system, $(Td_1)_I$ is smaller than that of the Non-Ideal skyhook system, $(Td_1)_N$, $\forall\, r>0$, $\zeta_{on}>0$ and $\zeta_{off}>0$.

Since $\zeta_{off}>0$, $b>0$ for $r>0$.

Thus $(Td_1)_N=\sqrt{\frac{b}{a}+\frac{1}{a}}>\sqrt{\frac{1}{a}}=(Td_1)_I, \forall\, a>0 \text{ and } b>0.$

For the SDoF skyhook systems, the Ideal system (always with lower transmissibility) is better than the Non-Ideal system for vibration isolation. However, *is the 2DoF Ideal skyhook system better than the 2DoF Non-Ideal skyhook system?* Let's have a deep discussion.

Similar to the procedures for the passive system, the transmissibilities of the 2DoF skyhook system can be derived. The damping ratio of the "skyhook damper" is $\zeta_s=c_s/2\sqrt{m_1k_1}$ and damping ratio of the suspension damper is $\zeta_1=c_1/2\sqrt{m_1k_1}$.

For the Ideal skyhook system, the displacement and acceleration transmissibilities are:

$$Td_1=\left|\frac{X_1}{X_b}\right|=\sqrt{\frac{m_r^{\,2}}{[k_r r^4-(k_r+m_r k_r+m_r)r^2+m_r]^2+[-2k_r\zeta_s r^3+2(k_r+1)\zeta_s m_r r]^2}}$$

$$Td_2=\left|\frac{X_2}{X_b}\right|=\sqrt{\frac{m_r^{\,2}[(1-r^2)^2+(2\zeta_s r)^2]}{[k_r r^4-(k_r+m_r k_r+m_r)r^2+m_r]^2+[-2k_r\zeta_s r^3+2(k_r+1)\zeta_s m_r r]^2}} \quad (9)$$

$$Ta_1=\left|\frac{\ddot{X}_1}{X_b}\right|=r^2\sqrt{\frac{m_r^{\,2}}{[k_r r^4-(k_r+m_r k_r+m_r)r^2+m_r]^2+[-2k_r\zeta_s r^3+2(k_r+1)\zeta_s m_r r]^2}}$$

$$Ta_2=\left|\frac{\ddot{X}_2}{X_b}\right|=r^2\sqrt{\frac{m_r^{\,2}[(1-r^2)^2+(2\zeta_s r)^2]}{[k_r r^4-(k_r+m_r k_r+m_r)r^2+m_r]^2+[-2k_r\zeta_s r^3+2(k_r+1)\zeta_s m_r r]^2}} \quad (10)$$

Based on the above transmissibility equations with parameters in Table 1, displacement and acceleration transmissibilities of Ideal skyhook system for different damping ratios ζ_s are shown in Figure 11.

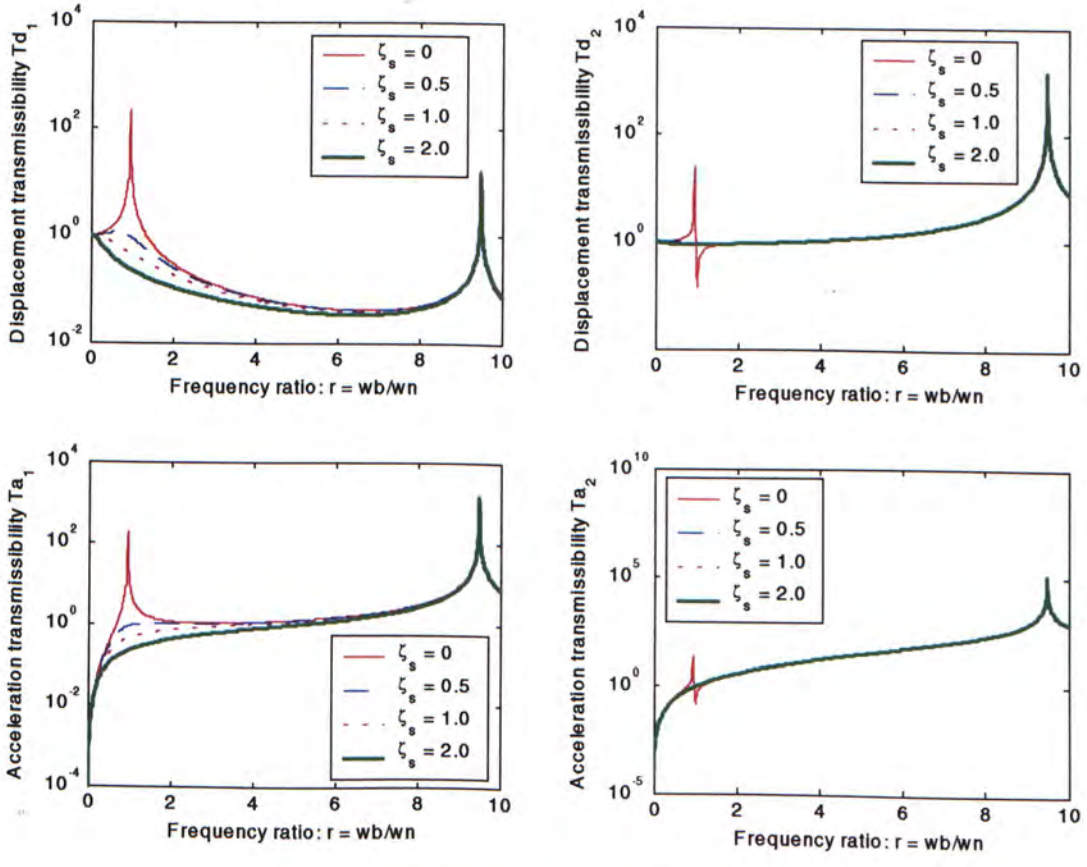

Figure 11 : Transmissibility of the Ideal skyhook system

In Figure 11, the displacement transmissibility of the sprung mass, Td_1, of the Ideal skyhook system around the second mode, r = 6 to 10, are similar for different damping ratios, ζ_s. Note that for $\zeta_s = 0$, it is the passive system with no damping effect, $\zeta_1 = 0$. Comparing to the passive system without damping effect, the behavior of the Ideal skyhook systems (for different damping ratios, ζ_s) around the second mode are very close because there are no damping effect between the sprung mass and unsprung

mass. If the excitation frequency to the Ideal skyhook system is near to the second mode, it will reach resonance like a spring-mass system. For the first mode shown in both displacement and acceleration transmissibilities of the sprung mass, Td_1 and Ta_1, the higher damping ratios, the lower transmissibilities will be.

For the Non-Ideal skyhook system, the displacement and acceleration transmissibilities are:

$$Td_1 = \left|\frac{X_1}{X_b}\right| = \sqrt{\frac{m_r^{\,2}[1+(2\zeta_1 r)^2]}{a_N^{\,2}+b_N^{\,2}}}$$
$$Td_2 = \left|\frac{X_2}{X_b}\right| = \sqrt{\frac{m_r^{\,2}[(1-r^2)^2+(2(\zeta_1+\zeta_s)r)^2]}{a_N^{\,2}+b_N^{\,2}}} \qquad (11)$$

$$Ta_1 = \left|\frac{\ddot{X}_1}{X_b}\right| = r^2\sqrt{\frac{m_r^{\,2}[1+(2\zeta_1 r)^2]}{a_N^{\,2}+b_N^{\,2}}}$$
$$Ta_2 = \left|\frac{\ddot{X}_2}{X_b}\right| = r^2\sqrt{\frac{m_r^{\,2}[(1-r^2)^2+(2(\zeta_1+\zeta_s)r)^2]}{a_N^{\,2}+b_N^{\,2}}} \qquad (12)$$

where

$$a_N = k_r r^4 - (k_r + m_r k_r + m_r + 4\zeta_1\zeta_s m_r k_r)r^2 + m_r$$
$$b_N = -[2\zeta_1 k_r(m_r+1) + 2k_r\zeta_s]r^3 + [2\zeta_1 m_r + 2(k_r+1)\zeta_s m_r]r$$

In order to compare to the Ideal skyhook system, parameters of the Non-Ideal skyhook system are the same as the Ideal skyhook system, which are shown in Table 1, while the damping ratios ζ_1 and ζ_s are varied. Similar to the SDoF case, the damping ratio of on-state is $\zeta_{on} = c_s / 2\sqrt{m_1 k_1} = \zeta_s$ and the damping ratio of off-state is $\zeta_{off} = 0$ for the Ideal system. The damping ratio of on-state is $\zeta_{on} = (c_s + c_1)/2\sqrt{m_1 k_1} = \zeta_s + \zeta_1$ and the damping ratio of off-state is $\zeta_{off} = c_1 / 2\sqrt{m_1 k_1} = \zeta_1$ for the Non-Ideal system.

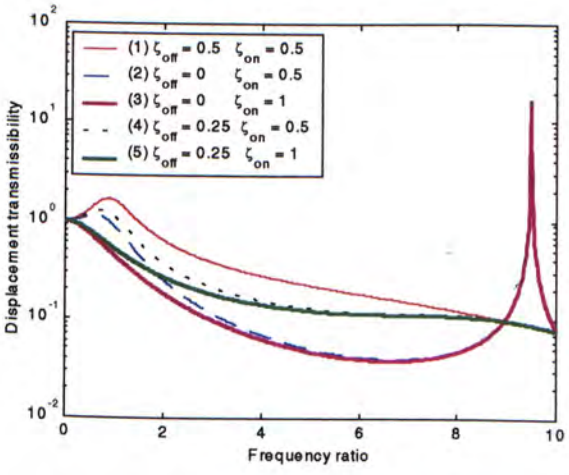

Figure 12 : Displacement transmissibility

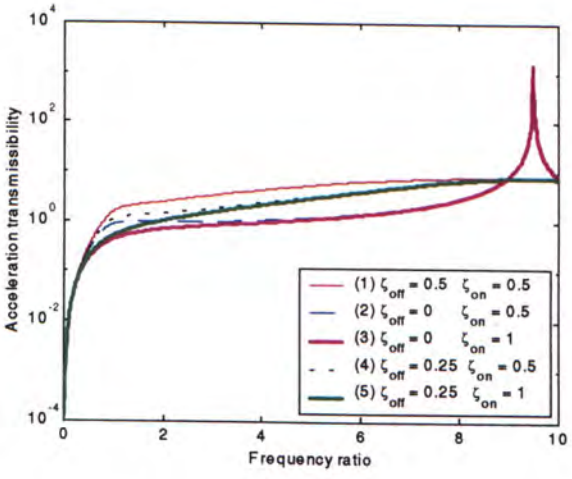

Figure 13 : Acceleration transmissibility

Based on Equations (9) - (12), the transmissibilities for Non-Ideal and Ideal skyhook systems are shown in Figure 12 and 13. Two systems are under the same conditions that we have mentioned (same parameters and same damping ratio at on-state). There are five cases in both two figures. Curve (1) is the passive system with the damping ratio $\zeta_{on} = \zeta_{off} = \zeta_1 = 0.5$. Curve (2) is the Ideal skyhook system with the damping ratio of "skyhook damper" $\zeta_{on} = \zeta_s = 0.5$. Curve (3) is the Ideal skyhook system with the damping ratio of "skyhook damper" $\zeta_{on} = \zeta_s = 1$. Curve (4) is the Non-Ideal skyhook system with the damping ratio of the suspension damper $\zeta_{off} = \zeta_1 = 0.25$ and the damping ratio of the "skyhook damper" $\zeta_s = \zeta_{on} - \zeta_1 = 0.5 - 0.25 = 0.25$. Curve (5) is the Non-Ideal skyhook system with the damping ratio of suspension damper $\zeta_{off} = \zeta_1 = 0.25$ and the damping ratio of "skyhook damper" $\zeta_s = \zeta_{on} - \zeta_1 = 0.75$. In these figures, it can be seen that the Ideal system is not always better than the Non-Ideal system especially around the second mode. So the situation in the 2DoF system is different from the SDoF system.

For the Curves (1), (2) and (4), the maximum damping ratios are the same ($\zeta_{on} = 0.5$). Around the first resonance r = 1, the displacement and acceleration transmissibilities of the passive system are the highest but the Ideal skyhook system has lower transmissibilities comparing with the Non-Ideal skyhook system. It is because the Ideal skyhook has no coupling effect between the sprung mass and unsprung mass. Around the first mode, less coupling effect between the sprung mass and unsprung mass, less transmissibilities will be. So Non-Ideal skyhook system (less coupling effect and transmissibility levels) is also better than the passive system. On the other hand, the Ideal skyhook system has the highest transmissibilities around the second resonance $r = 9.49$. However, the Non-Ideal skyhook system has similar transmissibilities to that of the passive system. Since both passive and Non-Ideal skyhook systems have damping capacities between sprung mass and unsprung mass, the transmissibilities around the second mode are much less than that of the Ideal skyhook system which has no damping effect around the second mode. The Ideal skyhook system behaves like a pure spring-mass system to reach the resonance in the second natural frequency. Comparing Curves (2) and (3), increasing the damping ratio ζ_{on} could decrease the transmissibilities for the Ideal skyhook system. Similarly, Curve (4) and (5) show that the transmissibilities of the Non-Ideal skyhook system with larger damping ratio ζ_{on} are lower. However, comparing the Non-Ideal system and Ideal system with same damping ratio ζ_{on} around first mode (see Curves (2) & (4) and Curves (3) & (5)), the transmissibilities of Non-Ideal skyhook system are still higher than those of the Ideal skyhook system. Therefore, the 2DoF Ideal skyhook system is *NOT* always better than the 2DoF Non-Ideal skyhook system.

2.1.3 *Groundhook Suspension System*

Similar to the skyhook control policy, the groundhook control policy is also used to switch the damper on or off. However, the objectives of them are different. The skyhook control is used to minimize the vertical motion of the sprung mass. The groundhook control is used to minimize the vertical motion of the unsprung mass. The example in Figure 4 illustrates the on-off groundhook policy. The equations of the groundhook policy are

$$\begin{aligned} -v_2 \times v_{12} > 0, \qquad & c = c_{on} \\ -v_2 \times v_{12} < 0, \qquad & c = c_{off} \end{aligned} \tag{13}$$

where v_2 represents the absolute velocity of the unsprung mass, $\dot{x}_2$

v_{12} represents the relative velocity across the damper, $\dot{x}_1 - \dot{x}_2$

When the relative velocity across the damper v_{12} and the absolute velocity v_2 of the unsprung mass are positive, the damping force F_d acting to the unsprung mass is pulling it up. The minimum damping is desired to reduce the pulling force acting on the unsprung mass. Similarly, if the v_{12} and v_2 are negative, the minimum damping is needed to reduce the damping force, which pushes the unsprung mass. When v_{12} changes to negative but v_2 is still positve, the damping force pushes the unsprung mass down. The maximum damping is desired to resist the unsprung mass moving upward. If v_{12} changes to positive and v_2 changes to negative, the maximum damping is also needed to pull the unsprung mass in order to maintain the original position.

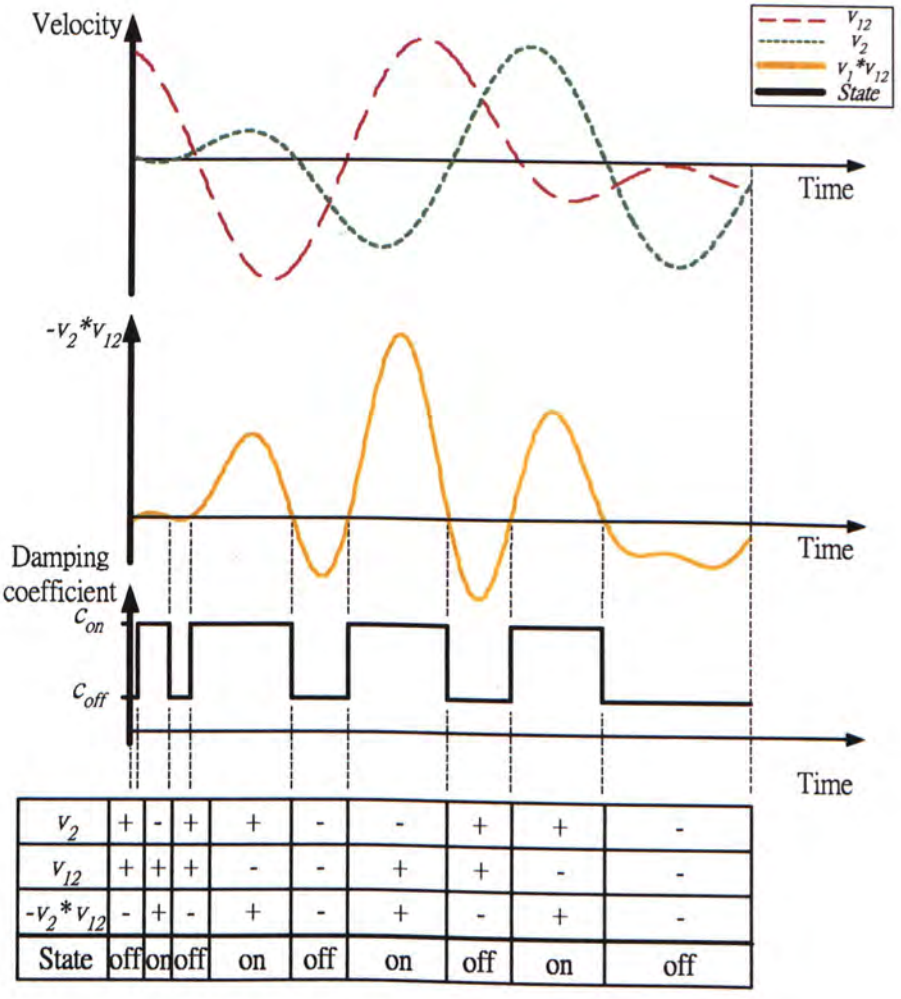

v_2	+	-	+	+	-	-	+	+	-
v_{12}	+	+	+	-	-	+	+	-	-
$-v_2*v_{12}$	-	+	-	+	-	+	-	+	-
State	off	on	off	on	off	on	off	on	off

Figure 14 : Example for groundhook control policy

The groundhook suspension systems are similar to the skyhook systems that can be classified to "Ideal groundhook systems" and "Non-Ideal systems". For the Ideal groundhook system, the damping coefficient for the off-state is 0, i.e. $c_{off} = 0$, and the damping coefficient for the on-state is $c_{on} = c_g$. For the Non-Ideal groundhook system, the damping coefficient for the off-state is positive number, i.e. $c_{off} = c_1 > 0$ and the damping coefficient for the on-state is $c_{on} = c_1 + c_g$. The Non-Ideal and Ideal groundhook configurations are shown in Figure 15 and Figure 16.

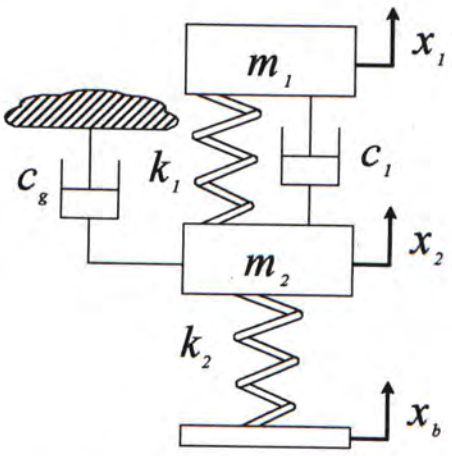

Figure 15 : Non-Ideal groundhook configuration

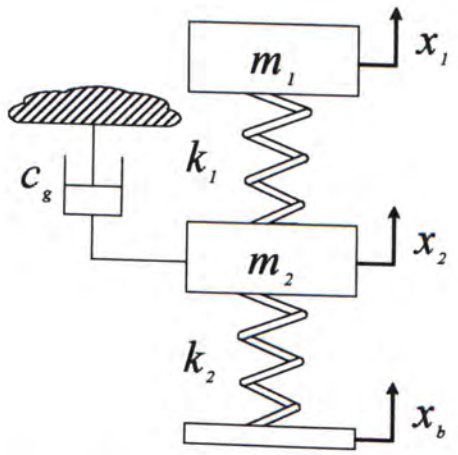

Figure 16 : Ideal groundhook configuration

The groundhook policies for the Non-Ideal and Ideal systems are similar to skyhook systems. The groundhook policies and the transmissibility equations are shown below:

Groundhook policies:

$$Non-Ideal:\begin{cases} -v_2 \times v_{12} > 0, & c = c_{on} = c_1 + c_g \\ -v_2 \times v_{12} < 0, & c = c_{off} = c_1 \end{cases} \tag{14}$$

$$Ideal:\begin{cases} -v_2 \times v_{12} > 0, & c = c_{on} = c_g \\ -v_2 \times v_{12} < 0, & c = c_{off} = 0 \end{cases} \tag{15}$$

For the Ideal groundhook system, the displacement and acceleration transmissibilities are:

$$Td_1 = \left|\frac{X_1}{X_b}\right| = \sqrt{\frac{m_r^{\,2}}{[k_r r^4 - (k_r + m_r k_r + m_r) r^2 + m_r]^2 + [-2k_r m_r \zeta_g r^3 + 2k_r \zeta_g m_r r]^2}}$$

$$Td_2 = \left|\frac{X_2}{X_b}\right| = \sqrt{\frac{m_r^{\,2}(1-r^2)^2}{[k_r r^4 - (k_r + m_r k_r + m_r) r^2 + m_r]^2 + [-2k_r m_r \zeta_g r^3 + 2k_r \zeta_g m_r r]^2}} \tag{16}$$

$$Ta_1 = \left|\frac{\ddot{X}_1}{X_b}\right| = r^2 \sqrt{\frac{m_r^{\,2}}{[k_r r^4 - (k_r + m_r k_r + m_r) r^2 + m_r]^2 + [-2k_r \zeta_s r^3 + 2(k_r + 1)\zeta_s m_r r]^2}}$$

$$Ta_2 = \left|\frac{\ddot{X}_2}{X_b}\right| = r^2 \sqrt{\frac{m_r^{\,2}[(1-r^2)^2 + (2\zeta_s r)^2]}{[k_r r^4 - (k_r + m_r k_r + m_r) r^2 + m_r]^2 + [-2k_r \zeta_s r^3 + 2(k_r + 1)\zeta_s m_r r]^2}} \tag{17}$$

Note that the damping ratio of the "groundhook damper" is $\zeta_g = c_g / 2\sqrt{m_1 k_1}$ and the damping ratio of the suspension damper is $\zeta_1 = c_1 / 2\sqrt{m_1 k_1}$. Based on above transmissibility equations with the same parameters shown in Table 1 and different damping ratios ζ_g, the transmissibilities of the Ideal groundhook systems are shown in Figure 17.

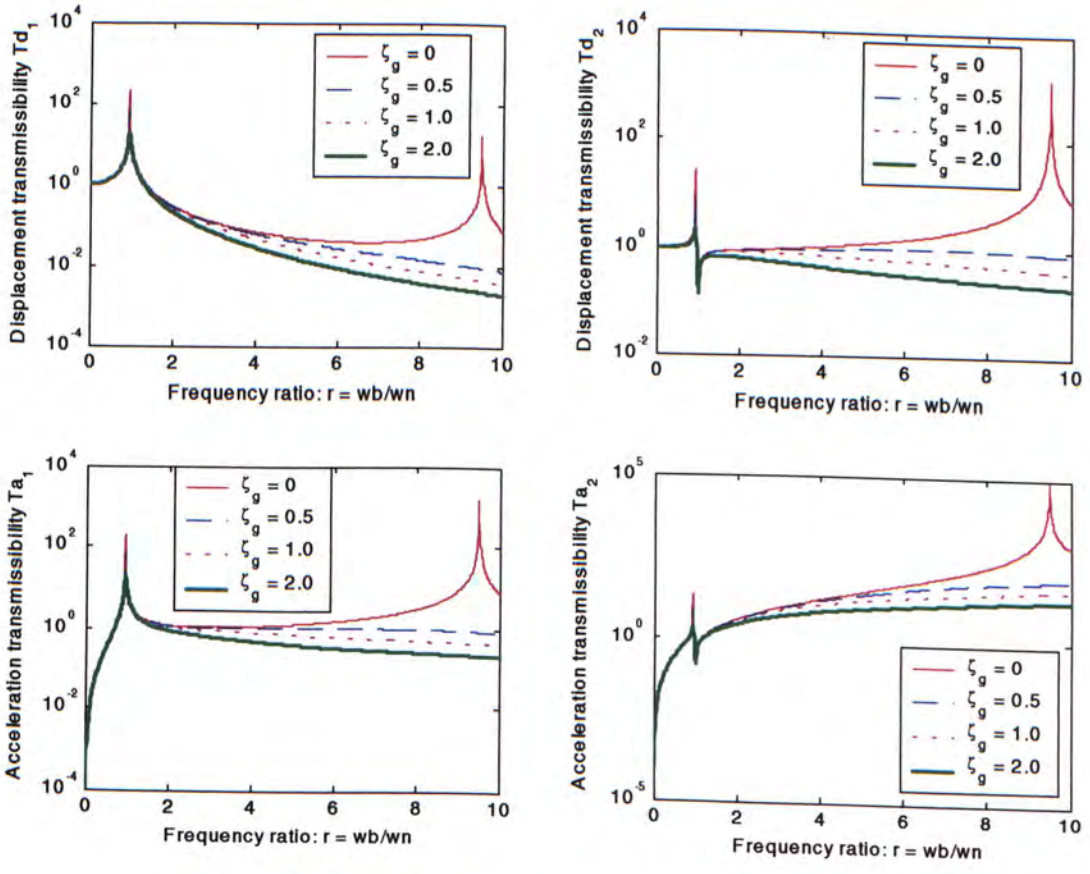

Figure 17 : Transmissibility of the Ideal groundhook system

In the Figure 17, the damping ratio $\zeta_g = 0$ means that it is the passive system without damping effect, i.e. $\zeta_1 = 0$. Note that the behaviors of the Ideal groundhook system (for different damping ratios, ζ_g) around the first natural frequency are similar to the passive system without damping effect. The reason is that there are also no damping effects to the sprung mass for those two systems. If the excitation frequency of the Ideal groundhook system is near to the first natural frequency, it will reach the resonance like the passive system without damping, which is a spring mass system. In both displacement and acceleration transmissibilities of the sprung mass around the second mode, Td_1 and Ta_1, system with larger damping ratio (ζ_g) will have lower transmissibilities (Td_1 and Ta_1).

For the Non-Ideal groundhook system, displacement and acceleration transmissibilities are:

$$Td_1 = \left|\frac{X_1}{X_b}\right| = \sqrt{\frac{m_r{}^2[1+(2\zeta_1 r)^2]}{a_N{}^2 + b_N{}^2}}$$
$$Td_2 = \left|\frac{X_2}{X_b}\right| = \sqrt{\frac{m_r{}^2[(1-r^2)^2+(2\zeta_1 r)^2]}{a_N{}^2 + b_N{}^2}} \qquad (18)$$

$$Ta_1 = \left|\frac{\ddot{X}_1}{X_b}\right| = r^2\sqrt{\frac{m_r{}^2[1+(2\zeta_1 r)^2]}{a_N{}^2 + b_N{}^2}}$$
$$Ta_2 = \left|\frac{\ddot{X}_2}{X_b}\right| = r^2\sqrt{\frac{m_r{}^2[(1-r^2)^2+(2\zeta_1 r)^2]}{a_N{}^2 + b_N{}^2}} \qquad (19)$$

where

$$a_N = k_r r^4 - (k_r + m_r k_r + m_r + 4\zeta_1\zeta_g m_r k_r)r^2 + m_r$$
$$b_N = -[2\zeta_1 k_r(m_r+1) + 2\zeta_g m_r k_r]r^3 + [2\zeta_1 m_r + 2\zeta_g m_r k_r]r$$

Using the same parameters shown in Table 1 and the varied damping ratios ζ_1 and ζ_g, the comparison between the Non-Ideal and Ideal groundhook system is shown in Figure 18 and Figure 19. Similar to the skyhook systems, the damping ratio of the Ideal system for on-state is $\zeta_{on} = c_g / 2\sqrt{m_1 k_1} = \zeta_g$ and the damping ratio for off-state is $\zeta_{off} = 0$. For the Non-Ideal system, $\zeta_{on} = (c_1 + c_g)/2\sqrt{m_1 k_1} = \zeta_1 + \zeta_g$ is the damping ratio for on-state and $\zeta_{off} = c_1 / 2\sqrt{m_1 k_1} = \zeta_1$ is the damping ratio for off-state.

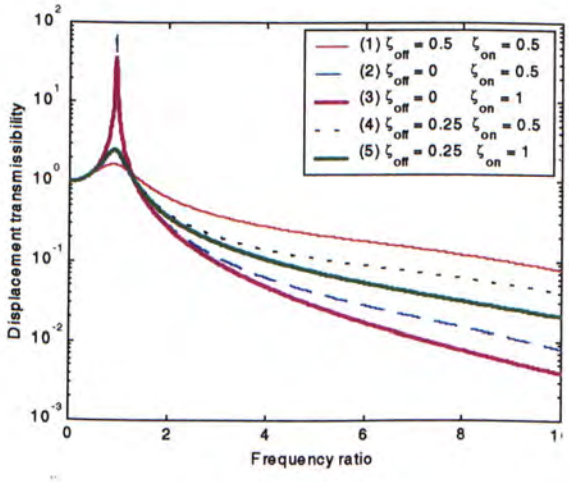

Figure 18 : Displacement transmissibility

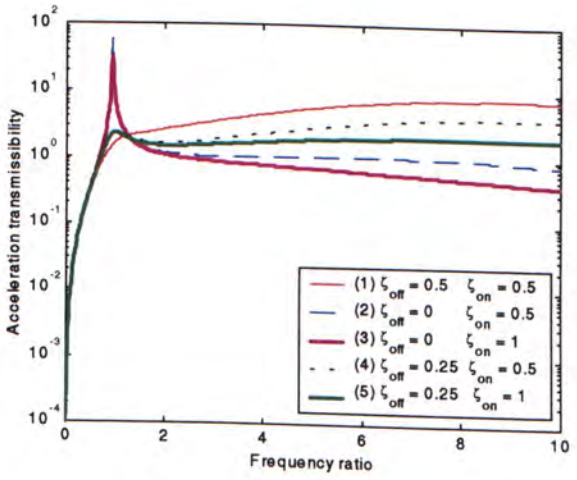

Figure 19 : Acceleration transmissibility

Figure 18 and Figure 19 show the comparison of the displacement and acceleration transmissibilities between the Non-Ideal and Ideal groundhook systems of the sprung mass. Both the Non-Ideal and Ideal system have the same parameters and same damping ratio of on-state. There are five cases in each figure. Curve (1) shows the transmissibilities of the passive system with damping ratio $\zeta_{on} = \zeta_{off} = \zeta_1 = 0.5$. Curve (2) shows the transmissibilities of the Ideal groundhook system with the damping ratio,

$\zeta_{on} = \zeta_g = 0.5$. Curve (3) shows the transmissibilities of the Ideal groundhook system with the damping ratio, $\zeta_{on} = \zeta_g = 1$. Curve (4) shows the transmissibilities of the Non-Ideal groundhook system with the damping ratio of suspension damper, $\zeta_{off} = \zeta_1 = 0.25$ and the damping ratio of "groundhook damper", $\zeta_g = \zeta_{on} - \zeta_1 = 0.5 - 0.25 = 0.25$. Curve (5) shows the transmissibilities of the Non-Ideal groundhook system with the damping ratio of suspension damper $\zeta_{off} = \zeta_1 = 0.25$ and the damping ratio of the "groundhook damper", $\zeta_g = \zeta_{on} - \zeta_1 = 1 - 0.25 = 0.75$. In these two figures, it can be shown that the Ideal system is also not always better than Non-Ideal system especially around the first natural frequency.

Comparing the Curve (1), (2) and (4), the maximum damping ratios are the same that means the damping ratio of the passive system is equal to the damping ratios of the Non-Ideal and Ideal groundhook system for on-state. (i.e. $\zeta_{on} = 0.5$). Around the first natural frequency r = 1, the displacement and acceleration transmissibilities of the Ideal groundhook system are the highest but the passive system has lower transmissibilities comparing with the Non-Ideal groundhook system. The reason is that the Ideal groundhook has no damping effect on the sprung mass so that the transmissibilities will be the highest. And also, the Non-Ideal groundhook has no enough damping effect on the sprung mass comparing to the passive system. Therefore, the passive system has lower transmissibilities than the groundhook system around the first natural frequency. However, the groundhook systems are better than passive system for other frequency range.

On the other hand, the Ideal groundhook system has the lowest transmissibilities around the second natural frequency $r = 7.75$. Moreover, the transmissibilities of the Non-Ideal skyhook system are lower than the passive system. Since the Ideal groundhook system has largest damping effect to the unsprung mass (but no coupling effect between sprung mass and unsprung mass), the transmissibilities around the second mode are much less than that of the Non-Ideal groundhook system. The passive system has larger coupling effect between the sprung mass and unsprung mass so the transmissibilities of the sprung mass around second mode is higher. Therefore, the Ideal groundhook system is better than the Non-Ideal groundbook system and passive system around the second natural frequency.

Comparing for the Ideal groundhook cases, Curve (2) and (3), increasing the damping ratio ζ_{on} can decrease the transmissibilities for the Ideal groundhook system. Similarly, Curve (4) and (5) show that the transmissibilities of the Non-Ideal groundhook system with larger damping ratio ζ_{on} are lower. However, comparing to the Non-Ideal and Ideal system with same damping ratio ζ_{on} around second mode (refer to the Curve (2) & (4) and Curve (3) & (5)), the transmissibilities of the Non-Ideal groundhook systems are still higher than that of the Ideal groundhook system. It can be shown that the Ideal groundhook system has good ability for vibration suppression around the second mode (larger damping ratio is better) but it has resonance around the first mode. Although the Non-Ideal groundhook system is not as good as Ideal groundhook system around the second mode, it has a good performance in a wide frequency range (especially for both first and second mode).

2.1.4 *Hybrid Suspension System*

The hybrid system can combine skyhook and groundhook systems to take advantage of the benefits of both of them. The hybrid system can allow user to specify the controller how close to the skyhook or groundhook system so that it can be used to provide proper control on both sprung mass and unsprung mass depending on different applications. The hybrid policy is the linear combination of the equation (6) and (13) and it is shown below:

$$\begin{aligned} &\alpha v_1 \times v_{12} - (1-\alpha) v_2 \times v_{12} > 0, \qquad c = c_{on} \\ &\alpha v_1 \times v_{12} - (1-\alpha) v_2 \times v_{12} < 0, \qquad c = c_{off} \end{aligned} \tag{20}$$

where v_1 represents the absolute velocity of the sprung mass, $\dot{x}_1$

v_2 represents the absolute velocity of the unsprung mass, $\dot{x}_2$

v_{12} represents the relative velocity across the damper, $\dot{x}_1 - \dot{x}_2$

α represents the hybrid gain to specify the controller how close to the skyhook or groundhook system

The damping coefficient is also the linear combination of the damping coefficients of the skyhook and groundhook systems, i.e.

$$\begin{cases} c_{on} = \alpha(c_1 + c_s) + (1-\alpha)(c_1 + c_g) \\ c_{off} = \alpha c_1 + (1-\alpha) c_1 \end{cases}$$
$$\begin{cases} c_{on} = \alpha c_s + c_1 + c_g - \alpha c_g \\ c_{off} = c_1 \end{cases} \tag{21}$$

Let $c_s = c_g = c_h$, then combine the equation (20) and (21) that becomes:

$$\begin{aligned} &\alpha v_1 \times v_{12} - (1-\alpha) v_2 \times v_{12} > 0, \qquad c = c_{on} = c_1 + c_h \\ &\alpha v_1 \times v_{12} - (1-\alpha) v_2 \times v_{12} < 0, \qquad c = c_{off} = c_1 \end{aligned} \tag{22}$$

Figure 20 shows the example for hybrid control policy with the hybrid gain, $\alpha = 0.5$. When the linear combination of the skyhook policy and ground policy is positive (i.e. $\alpha v_1 \times v_{12} - (1-\alpha) v_2 \times v_{12} > 0$), the maximum damping is desired to balance the motion between the sprung mass and unsprung mass. Similarly, if the combination of the skyhook policy and ground policy is negative (i.e. $\alpha v_1 \times v_{12} - (1-\alpha) v_2 \times v_{12} < 0$), the minimum damping is desired so that no extra damping effect to increase the vibration.

The hybrid gain α is used to adjust the weight between skyhook and groundhook policy. If the hybrid gain equal to zero (i.e. $\alpha = 0$), the hybrid policy becomes the same as the grounhook policy. If the hybrid gain equal to one (i.e. $\alpha = 1$), then it becomes to skyhook policy. The hybrid gain, α, can be adjusted to provide the proper compromise between the motion control of sprung mass and the motion control of unsprung mass.

For the example showing in the Figure 20, $\alpha = 0.5$ is selected. Note that this hybrid system tries to balance the weight between skyhook and groundhook (same degree of importance). One question could be asked: *What is the suitable value for the hybrid gain?* In the following section, we will try to answer this question with some analyses.

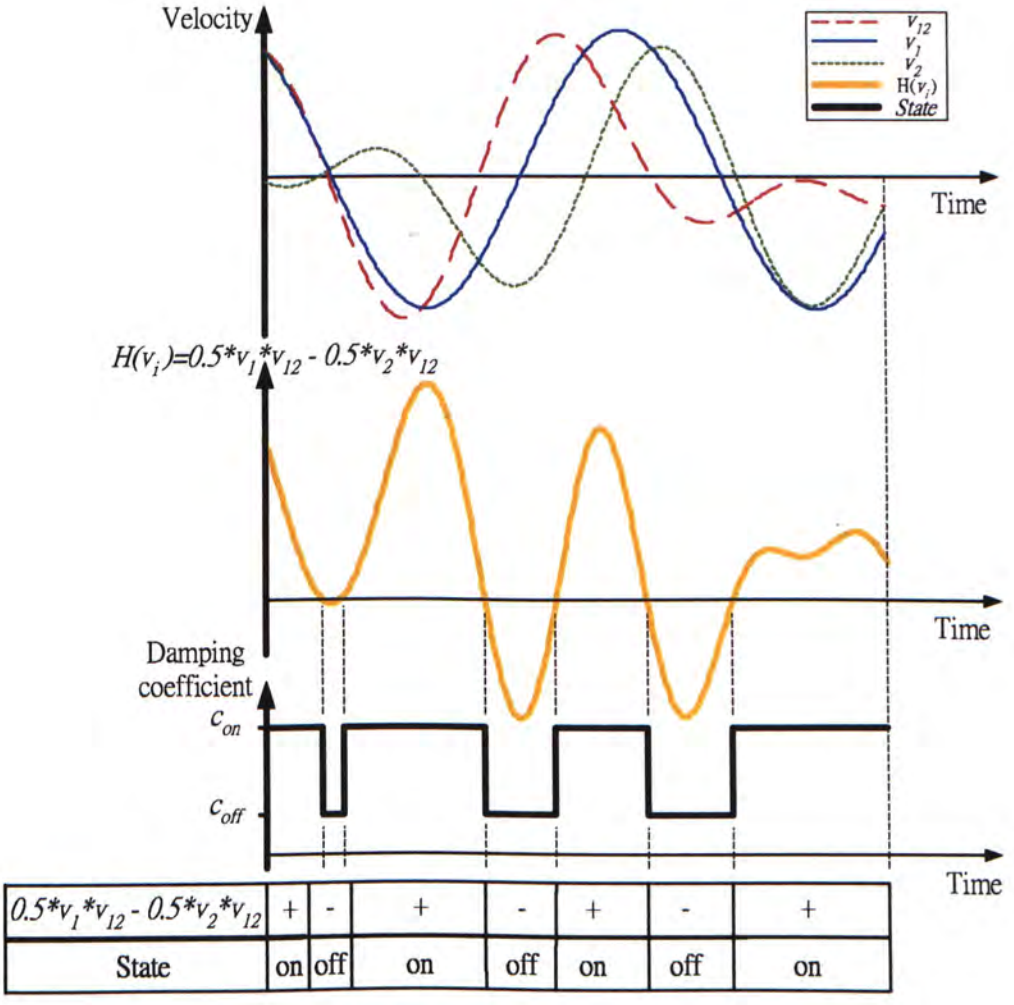

Figure 20 : Example of Hybrid control policy

The hybrid suspension system is similar to the skyhook and groundhook system that can also be classified to "Ideal hybrid system" and "Non-Ideal system". For the Ideal hybrid system, the damping coefficient for the off-state is 0, i.e. $c_{off} = 0$, and the damping coefficient for the on-state is $c_{on} = c_h$. For the Non-Ideal hybrid system, the damping coefficient for the off-state is positive number, i.e. $c_{off} = c_1 > 0$ and the damping coefficient for the on-state is $c_{on} = c_1 + c_h$. The Non-Ideal and Ideal hybrid configurations are also shown in Figure 21 and Figure 22.

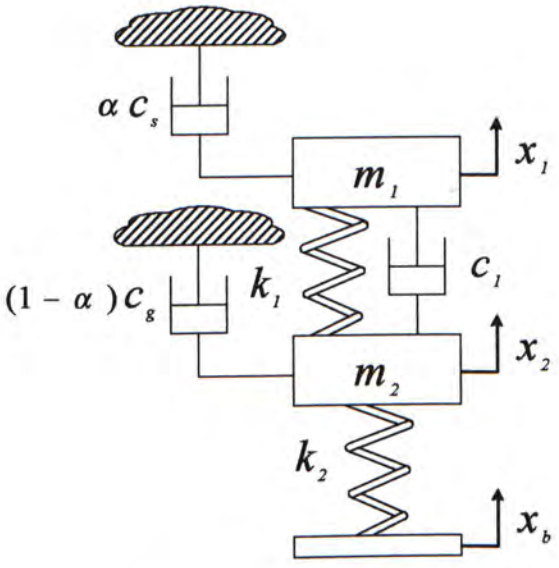

Figure 21 : Non-Ideal hybrid configuration

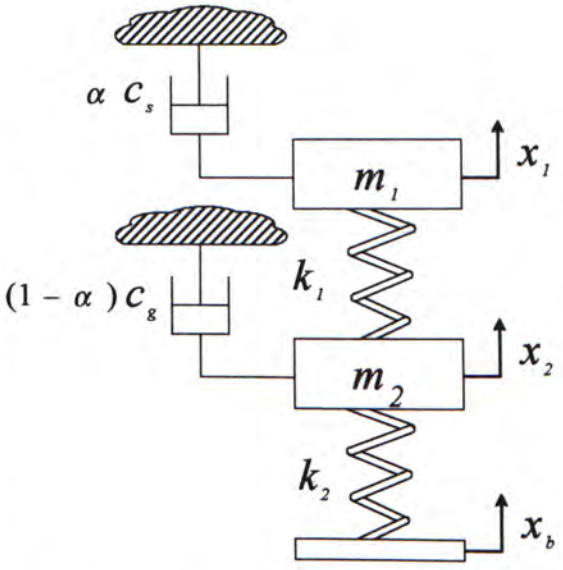

Figure 22 : Ideal hybrid configuration

It was mentioned that the hybrid policies for Non-Ideal and Ideal system are similar to the skyhook and groundhook systems because it is the linear combination of the skyhook and groudhook policies. Then, the hybrid policies for the Non-Ideal and Ideal systems are shown below:

Hybrid policies:

$$Non-Ideal: \begin{cases} \alpha v_1 \times v_{12} - (1-\alpha) v_2 \times v_{12} > 0, & c = c_{on} = c_1 + c_h \\ \alpha v_1 \times v_{12} - (1-\alpha) v_2 \times v_{12} < 0, & c = c_{off} = c_1 \end{cases} \quad (23)$$

$$Ideal: \begin{cases} \alpha v_1 \times v_{12} - (1-\alpha) v_2 \times v_{12} > 0, & c = c_{on} = c_h \\ \alpha v_1 \times v_{12} - (1-\alpha) v_2 \times v_{12} < 0, & c = c_{off} = 0 \end{cases} \quad (24)$$

For the Ideal hybrid system, the displacement and acceleration transmissibilities are:

$$Td_1 = \left|\frac{X_1}{X_b}\right| = \sqrt{\frac{m_r^{\,2}}{a_I^{\,2} + b_I^{\,2}}}$$
$$Td_2 = \left|\frac{X_2}{X_b}\right| = \sqrt{\frac{m_r^{\,2}[(1-r^2)^2 + (2\alpha\zeta_h r)^2]}{a_I^{\,2} + b_I^{\,2}}} \tag{25}$$

$$Ta_1 = \left|\frac{\ddot{X}_1}{X_b}\right| = r^2\sqrt{\frac{m_r^{\,2}}{a_I^{\,2} + b_I^{\,2}}}$$
$$Ta_2 = \left|\frac{\ddot{X}_2}{X_b}\right| = r^2\sqrt{\frac{m_r^{\,2}[(1-r^2)^2 + (2\alpha\zeta_h r)^2]}{a_I^{\,2} + b_I^{\,2}}} \tag{26}$$

where

$$a_I = k_r r^4 - (k_r + m_r k_r + m_r + 4m_r k_r \alpha(1-\alpha)\zeta_h^{\,2})r^2 + m_r$$
$$b_I = -[2k_r\zeta_h((1-\alpha)m_r + \alpha)]r^3 + 2m_r(\alpha + k_r)\zeta_h]r$$

Note that the damping ratio of the "skyhook damper" $\zeta_s = c_s / 2\sqrt{m_1 k_1}$ is equal to the damping ratio of the "groundhook damper" $\zeta_g = c_g / 2\sqrt{m_1 k_1}$. Since $c_s = c_g = c_h$, the damping coefficient of combining "skyhook damper" and "groundkhook damper" is $\alpha c_s + (1-\alpha)c_g = \alpha c_h + c_h - \alpha c_h = c_h$. Therefore the damping ratio of the combined dampers of hybrid system then becomes $\zeta_h = c_h / 2\sqrt{m_1 k_1}$ and damping ratio of the suspension damper is $\zeta_1 = 0$. Based on above transmissibility equations with the same parameters shown in Table 1, different hybrid gain α and the constant damping ratio $\zeta_h = 1$, the displacement and acceleration transmissibilities of the Ideal hybrid system are shown in Figure 23.

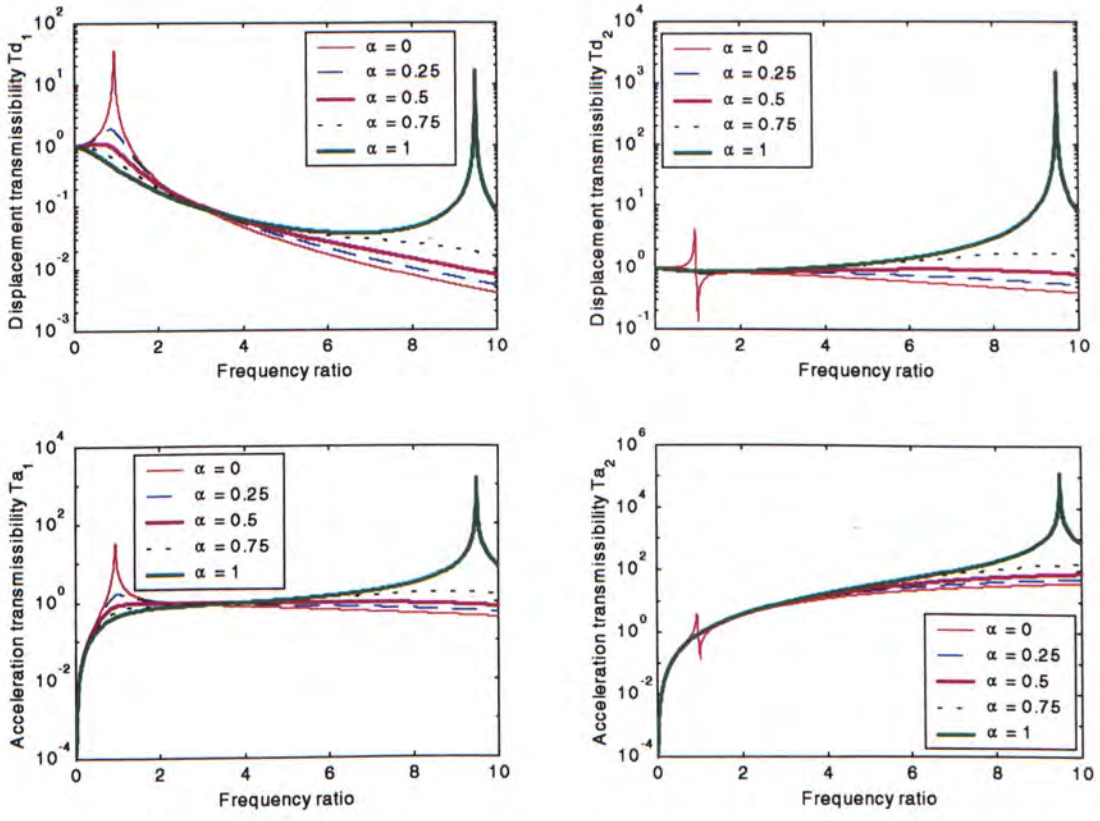

Figure 23 : Transmissibility of the Ideal hybrid system

In the Figure 23, the hybrid gain $\alpha = 0$ means that it is the Ideal grounhook system with damping ratio $\zeta_g = \zeta_h = 1$ (refer to Figure 17). On the other hand, the hybrid gain $\alpha = 1$ means that it is the Ideal skyhook system with damping ratio $\zeta_s = \zeta_h = 1$ (refer to Figure 11). For the hybrid gain between 0 and 1 (i.e. $0 < \alpha < 1$), the hybrid system has the compromised behaviors of the skyhook and groundhook systems. As the previous discussion, the skyhook system can reduce the transmissibilities around the first mode and the groundhook system can also reduce the transmissibilities around the second mode. With the hybrid effect (i.e. $0 < \alpha < 1$), the transmissibilities around both first and second mode can be compromised (refer to Figure 23 for α = 0.25, 0.5,

and 0.75). If the hybrid gain is smaller (e.g. $\alpha = 0.25$), the performance is much similar to the groundhook system. The transmissibilities around first mode are higher but around the second mode are lower. If the hybrid gain is larger (e.g. $\alpha = 0.75$), the performance is much similar to the skyhook system. The transmissibilities around first mode are lower but around the second mode are higher. When the hybrid gain set to be equal weight for skyhook and groundhook (i.e. $\alpha = 0.5$), it seems that the transmissibilities around the both first mode and second mode can be balanced such that the transmissibilities around the whole frequency range can be under a low level. But now it cannot be said that $\alpha = 0.5$ is good enough or not. Therefore, the next following section will try to find the optimum value of the hybrid gain.

Now back to the transmissibilities of hybrid system. For the Non-Ideal hybrid system, the displacement and the acceleration transmissibilities are:

$$Td_1 = \left|\frac{X_1}{X_b}\right| = \sqrt{\frac{m_r{}^2[1+(2\zeta_1 r)^2]}{a_N{}^2 + b_N{}^2}}$$
$$Td_2 = \left|\frac{X_2}{X_b}\right| = \sqrt{\frac{m_r{}^2[(1-r^2)^2+(2(\zeta_1+\alpha\zeta_h)r)^2]}{a_N{}^2 + b_N{}^2}} \qquad (27)$$

$$Ta_1 = \left|\frac{\ddot{X}_1}{X_b}\right| = r^2\sqrt{\frac{m_r{}^2[1+(2\zeta_1 r)^2]}{a_N{}^2 + b_N{}^2}}$$
$$Ta_2 = \left|\frac{\ddot{X}_2}{X_b}\right| = r^2\sqrt{\frac{m_r{}^2[(1-r^2)^2+(2(\zeta_1+\alpha\zeta_h)r)^2]}{a_N{}^2 + b_N{}^2}} \qquad (28)$$

where

$$a_N = k_r r^4 - (k_r + m_r k_r + m_r + 4m_r k_r(\zeta_1\zeta_h + \alpha(1-\alpha)\zeta_h{}^2))r^2 + m_r$$
$$b_N = -[2k_r(m_r(\zeta_1+\zeta_h)+\zeta_1 - \alpha\zeta_h(m_r-1))]r^3 + 2m_r[\zeta_1 + (\alpha + k_r)\zeta_h]r$$

Using the same parameters shown in Table 1 with $\alpha = 0.5$ and the varied damping ratios ζ_1 and ζ_h, the comparison of the Non-Ideal and Ideal hybrid system is shown in Figure 24 and Figure 25. In the previous discussion, the damping ratio of the Ideal hybrid system for on-state is $\zeta_{on} = c_h / 2\sqrt{m_1 k_1} = \zeta_h$ and the damping ratio for off-state is $\zeta_{off} = 0$. The damping ratios of the Non-Ideal hybrid system for on-state and off-state are $\zeta_{on} = (c_1 + c_h)/2\sqrt{m_1 k_1} = \zeta_1 + \zeta_h$ and $\zeta_{off} = c_1 / 2\sqrt{m_1 k_1} = \zeta_1$, respectively.

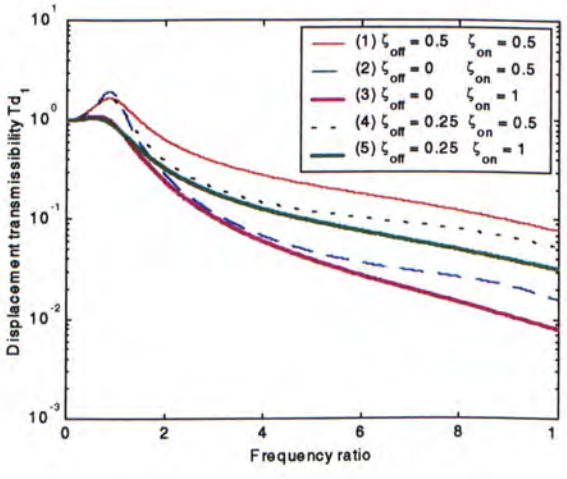

Figure 24 : Displacement transmissibility

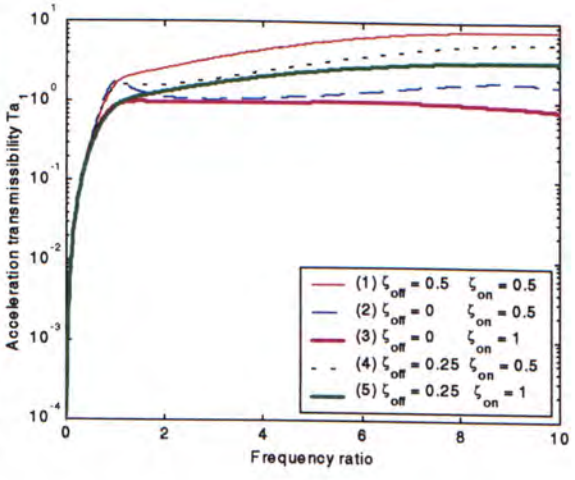

Figure 25 : Acceleration transmissibility

In the Figure 24 and Figure 25, the comparisons of the displacement and acceleration transmissibilities between the Non-Ideal and Ideal hybrid systems of the sprung mass are shown. There are five cases in each figure. Curve (1) shows the transmissibilities of the passive system with the damping ratio, $\zeta_{off} = \zeta_1 = 0.5$. It is the baseline, which is used to be a reference. Comparing to the Ideal hybrid case, Curve (2) and the Non-Ideal hybrid case, Curve (3), the transmissibilities of the Ideal case are higher around the first mode but they are lower than Non-Ideal and passive cases for higher frequency ration, $r > 1.5$.

For the Non-Ideal cases, the transmissibilities are similar to the passive case, Curve (1), around the first mode (see Curve 2 and Curve 4). For $r > 1.5$, the transmissibilities of the Non-Ideal cases are lower than the passive case but higher than the Ideal cases.

Comparing for the Ideal hybrid cases, Curve (2) and (3), increasing the damping ratio ζ_{on} can decrease the transmissibilities for the Ideal hybrid system for all frequency range. Similarly, the transmissibilities for the Non-Ideal hybrid cases (see Curve (4) and (5)) are lower with larger damping ratio ζ_{on}. Comparing the Non-Ideal and Ideal systems with the same damping ratio ζ_{on} around second mode (refer to Curve (2) & (4) and Curve (3) & (5)), the transmissibilities of the Non-Ideal hybrid system are little bit higher than the Ideal hybrid system. However, the transmissibilities of the Non-Ideal hybrid system are little bit lower than the Ideal hybrid system around the first mode. It can be shown that the hybrid systems somehow are similar to the groundhook systems but the transmissibilies of the hybrid systems have not the larger resonance peak as groundhook case. Although the transmissibilities of the Ideal hybrid system is a little bit higher comparing to the Non-Ideal hybrid system around the first mode, it has a good performance in a wide frequency range (except for $r < 1.5$).

2.1.5 *Comparison among four suspension systems*

In the previous sub-sections, a deep discussion about the passive suspension system and the three semi-active suspension systems (skyhook, groundhook and hybrid for the Ideal and Non-Ideal cases) has been presented individually. Now, we try to compare the properties of those systems in the terms of transmissibility. The displacement and acceleration transmissibilities of the sprung mass and unsprung mass of the passive system and the Ideal semi-active systems are shown in the Figure 26.

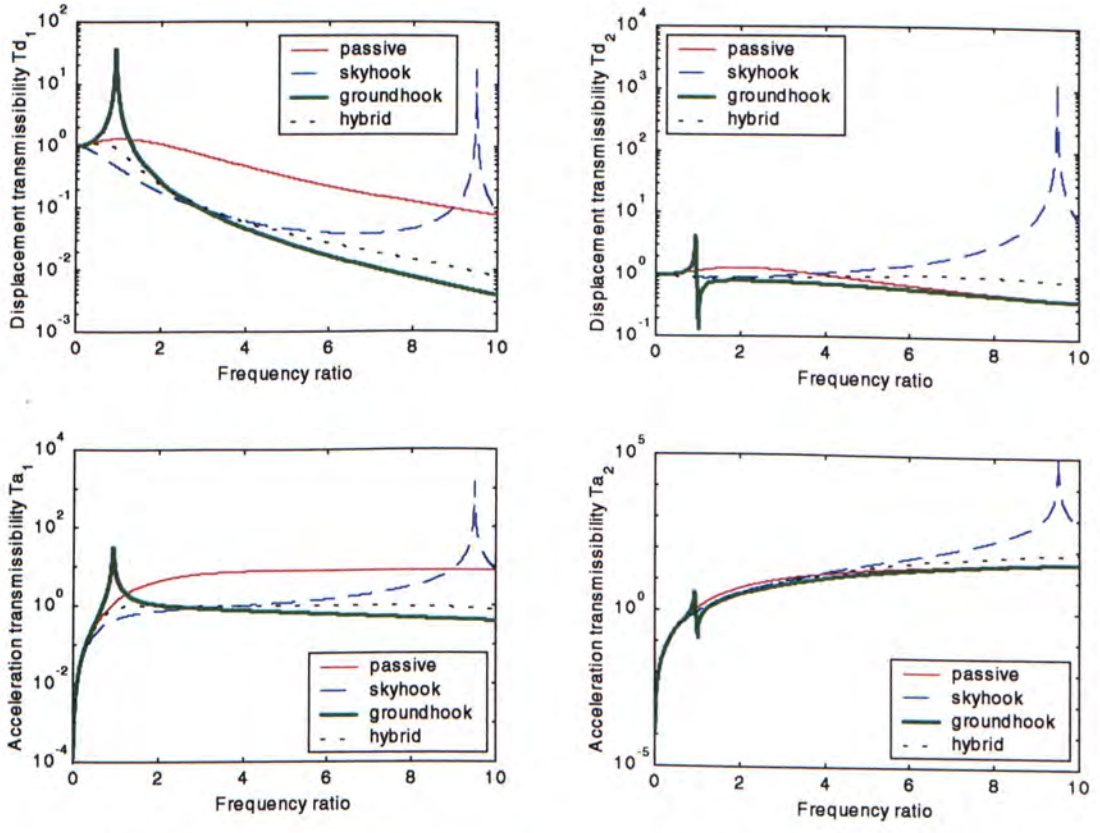

Figure 26 : Comparison of passive and three Ideal semi-active suspension systems

The parameters are the same as previous sub-sections. For the system parameters, it is shown in Table 1. The damping coefficient of the passive system is $\zeta_1 = 1$. For the three semi-active systems, the damping coefficient of the on-state is $\zeta_{on} = 1$ and off-state is $\zeta_{off} = 0$. For the hybrid system, the hybrid gain is $\alpha = 0.5$. That means the weight of the skyhook and groundhook behaviors are the same.

The passive system is chosen to be a baseline that is used to compare those three semi-active systems. Under same situation (same system parameters and same maximum damping ratios), the groundhook system has a resonance around the first natural frequency but the skyhook system has a resonance around the second natural frequency so that their transmissibilities around their resonance frequency ranges are higher than the passive system. There is an intersection point around the frequency ratio $r = 3$ in each transmissibility figure of the sprung mass (Td_1 and Ta_1). Before this intersection point, the skyhook system has lowest transmissibility level but the groundhook system has lowest transmissibility level for the frequency larger than this point. The curves of the transmissibilities of the hybrid system seem also across this intersection points but in the section 2.4.3 will show that it is not true. For all frequency range, the transmissibilities of the hybrid system are lower than passive system. Since the hybrid system doesn't have any peak around the natural frequencies, the effective frequency range of the Ideal hybrid system is wider than the Ideal skyhook and Ideal groundhook system. Note that the acceleration transmissibility of the hybrid is decreasing for increasing the frequency ratio. It seems that the maximum point is around the frequency range $1 \le r \le 3$.

Is the maximum point at the intersection point? If the answer is YES, *can we use this information to find the optimum parameters of the Ideal hybrid system?* This is an interesting issue. We will try to find the answer in the next section. Now, let's discuss the comparison between the passive system and the Non-Ideal semi-active systems. Again, the parameters are the same as Ideal cases except the damping coefficient of the off-state. For the system parameters, it is shown in Table 1. The damping coefficient of the passive system is $\zeta_1 = 1$. For the three semi-active systems, the damping coefficient of the on-state is $\zeta_{on} = 1$ and but the off-state is $\zeta_{off} = 0.5$. For the hybrid system, the hybrid gain is also $\alpha = 0.5$.

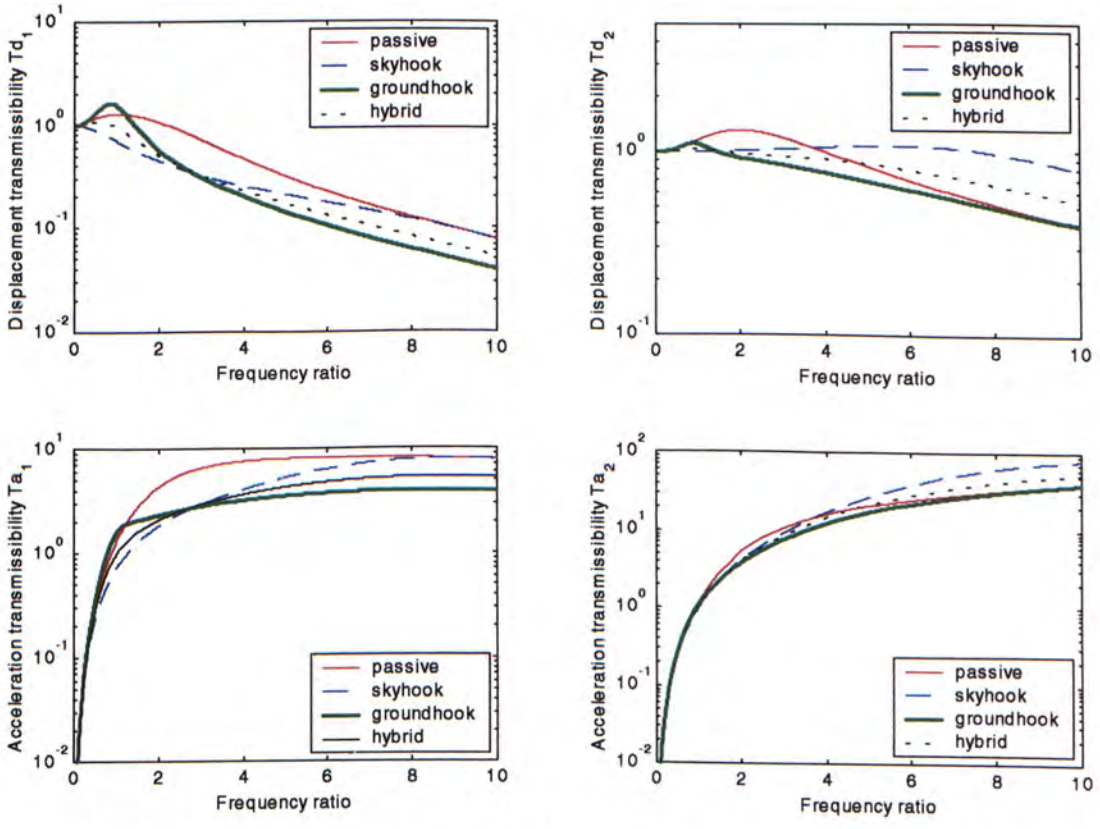

Figure 27 : Comparison of passive and 3 Non-Ideal semi-active suspension systems

Same as the Ideal systems comparison, the passive system is chosen to be a baseline that is used to compare those three Non-Ideal semi-active systems. Under same situation (same system parameters and same maximum damping ratios), the differences of the transmissibilities level between all suspension systems are less than the Ideal case. The groundhook system still has a peak (lower peak compare to the Ideal system) around the first natural frequency and it is a little bit higher than the passive system. Moreover, the skyhook system also has a small peak around the second natural frequency. Actually, the transmissibility level of this peak is similar to passive system.

Similar to the Ideal case, there is an intersection point around the frequency ratio $r = 3$ in each transmissibility figure of sprung mass (Td_1 and Ta_1). Before this intersection point, the skyhook system has the lowest transmissibility level but the groundhook system has the lowest transmissibility level when the frequency is larger than that point. On average, the displacement transmissibility of the hybrid system is relatively low for the whole frequency range. The curves of the transmissibilities of the hybrid system seem also across this intersection points. Actually, we have already discussed in the sub-section of hybrid suspension system that the Ideal hybrid system is better than the Non-Ideal hybrid system for overall frequency range. Now comparing Figure 26 and Figure 27, the transmissibilities level of the hybrid system are relatively low for both Ideal and Non-Ideal cases. In addition, the transmissibilities level of the Ideal hybrid system is lower than the Non-Ideal hybrid system. Therefore, we can say that the Ideal hybrid system has the best performance for vibration suppression from this particular set of the system parameters.

2.2 *Characteristics analysis*

The previous section has shown the transmissibility equations of the passive and three semi-active suspension systems with Ideal and Non-Ideal models. The transmissibility equations are the functions of multiple variables. In this section, we aim to study the characteristics of the transmissibility by changing different parameteres and setup design guidelines for selecting suitable parameters for suspension systems.

2.2.1 Passive Suspension System

Since the acceleration of the sprung mass is the major consideration factor, the trend of the acceleration transmissibility of the sprung mass will be discussed in this section. However, the acceleration transmissibility equation is the function of mass ratio m_r, sprung ratio k_r, damping ratio ζ, and frequency ratio r. It is necessary to specify the range of those parameters. In this study, the frequency ratio r is $0:0.01:10$, the mass ratio m_r and spring ratio k_r are selected to be 0.1, 1 and 10 and the damping ratio ζ is selected to be 0, 0.5 and 5 (see Table 3).

Table 3 : Range of the parameters of the acceleration transmissibility equation

Mass ratio, m_r	0.1, 1 and 10
Spring ratio, k_r	0.1, 1 and 10
Damping ratio, ζ	0, 0.5 and 5
Frequency ratio, r	0 : 0.01 : 10

In Figure 28, there are 9 graphs. For the column 1, the mass ratio is kept constant i.e. $m_r = 0.1$ and the spring ratio is varied (0.1, 1 and 10 from top to bottom). Similarly, for the column 2 and 3, the mass ratio $m_r = 1$ and $m_r = 10$ respectively and the spring ratio is also varied from top to bottom ($k_r = 0.1$, 1 and 10). For each graph, there are three curves, which are respected to three damping ratios $\zeta = 0, 0.5$ and 5.

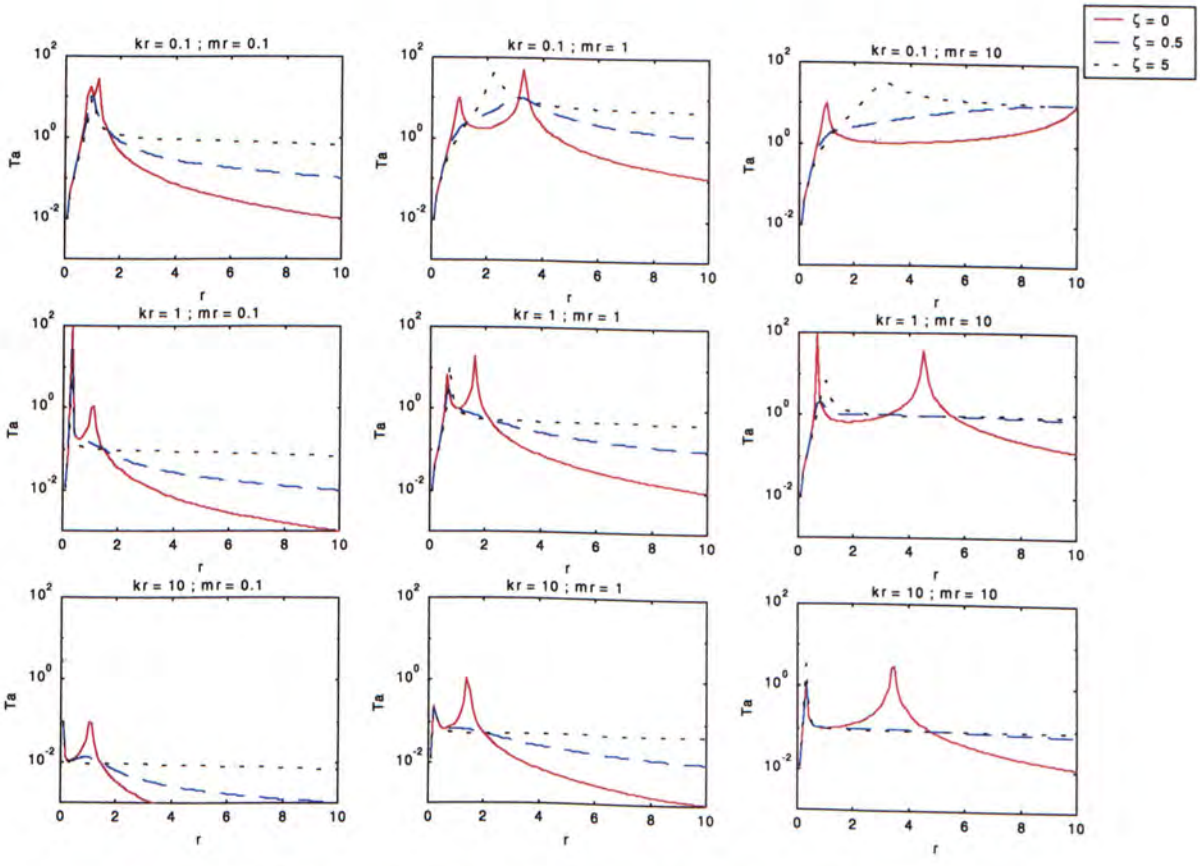

Figure 28 : Acceleration transmissibility of passive system with varied parameters

It can be seen that there are two peaks of the acceleration transmissibilities (where one peak for the case ($m_r = 10$ and $k_r = 0.1$) is out of frequency range shown) for the damping ratio is zero (i.e. $\zeta = 0$). The difference between two natural frequencies of the acceleration transmissibilities Ta is increased when the mass ratio m_r is increased. It

is more obvious when the spring ratio is small (refer to the first row of Figure 28). Moreover, the transmissibility level is decreased for decreasing the mass ratio and increasing the spring ratio. For the damping ratio is not equal to zero ($\zeta = 0.5$ and 5), there are only one peak of the acceleration transmissibility. For the damping ratio $\zeta = 0.5$, the transmissibility level is the lowest comparing to $\zeta = 0$ and 5. It implies that the optimum damping ratio exist in this range. With suitable damping ratio, the lower transmissibility level will be obtained. About how to find the optimum damping ratio, it will be discussed on next section. Table 4 shows the effect of the transmissibility level by changing different parameters. This is useful for the suspension system design. Definitely, there are many constraints for designing a suspension system (e.g. tire deflection limit, weight of the suspension system, weight of the vehicle etc.) so it is not so straightforward to apply. However, it is a good reference for design consideration.

Table 4 : Effect of parameters to transmissibility level for passive system

Transmissibility level	Mass ratio	Spring ratio	Damping ratio
HIGH	LARGE	SMALL	LARGE or SMALL
LOW	SMALL	LARGE	OPTIMIZED

2.2.2 Skyhook Suspension System

With the same parameters (shown in Table 3), the acceleration transmissibilities of skyhook system are shown in Figure 29. There are also 9 graphs in Figure 29. The pattern is similar to passive system but there are five curves for each graph, which are respected to five damping ratio pairs. For $\zeta_{on} = 0$ and $\zeta_{off} = 0$, it is the undamped passive system. For $\zeta_{off} = 0$, they are the Ideal skyhook cases and for $\zeta_{off} > 0$, they are Non-Ideal skyhook cases.

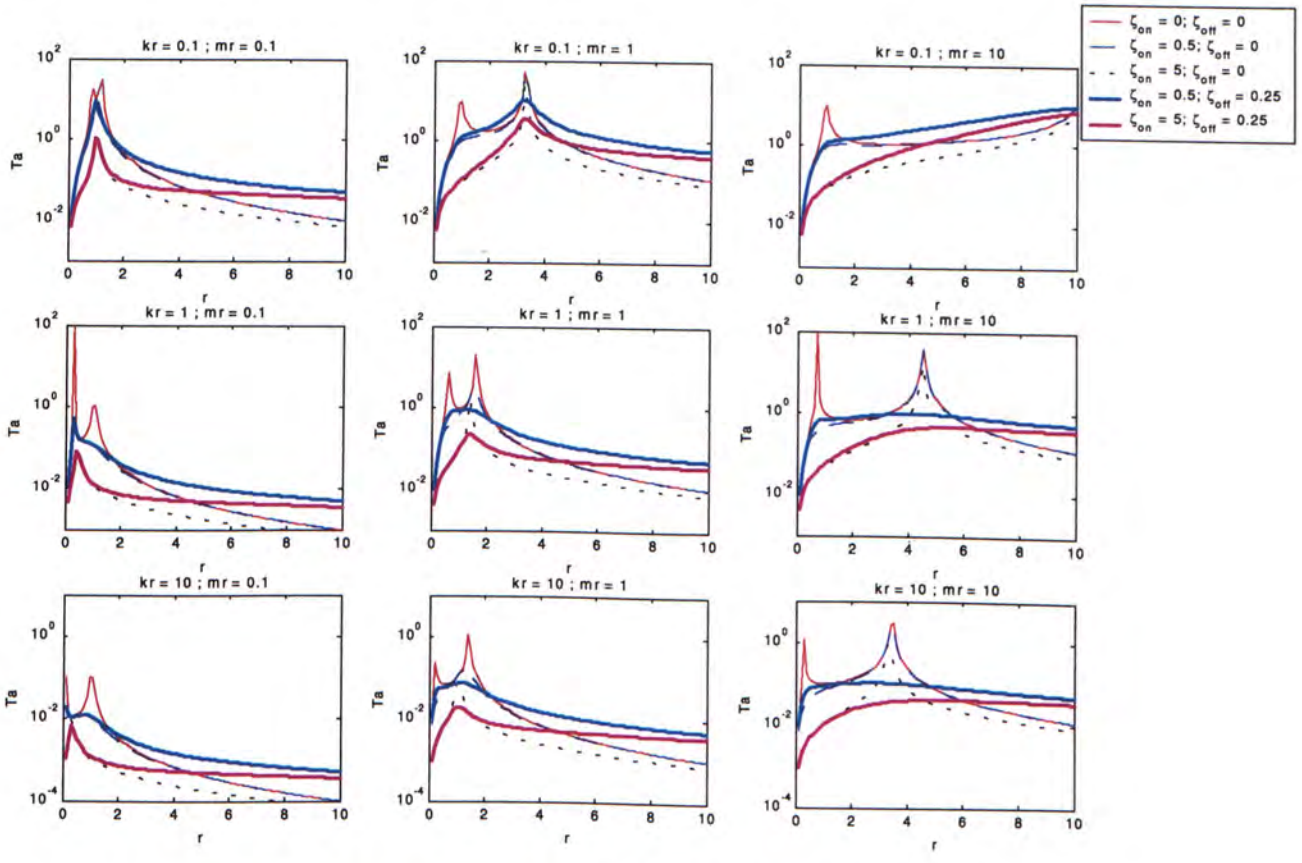

Figure 29 : Acceleration transmissibility of skyhook system with varied parameters

In the section 2.1.2, the comparison between the Ideal skyhook system and the Non-Ideal skyhook system has been discussed. This section will focus on the effect of different parameters to the acceleration transmissibility of both Ideal and Non-Ideal skyhook systems. For the case of passive system without damping $\zeta_{on} = 0$ and $\zeta_{off} = 0$, it is the base line and used to compare the skyhook systems. It can be seen that there is only one peak of the acceleration transmissibility for the Ideal skyhook system. When the smaller mass ratio and larger spring ratio are selected, the transmissibility level is decreased. Moreover, the peak of the acceleration transmissibility is shift to left such that the natural frequency will be smaller. In addition, the lower transmissibility level will be obtained when a larger damping ratio is selected.

On the other hand, there is also only one peak of the acceleration transmissibility for the Non-Ideal skyhook system with small mass ratio. If the mass ratio is larger (e.g. $m_r = 10$), the peak will disappear. It is because the damping for off-state can reduce the transmissibility level around the second natural frequency. Similar to the Ideal skyhook case, the transmissibility level is reduced and the peak is shift to left when the smaller mass ratio and larger spring ratio are given. By increasing the damping ratio of the on-state the transmissibility level will also be reduced.

Table 5 shows the effect of the transmissibility level by changing different parameters (for both Ideal and Non-Ideal system). Normally, people use the skyhook control policy to control the vibrating system. It is not necessary to know the characteristics of different parameters. However, there are some people to use the skyhook model to act as a reference model. Then this characteristics analysis is useful. This characteristics analysis shows the relationship between the transmissibility and the different parameters. It can provide enough information to design a good reference model. It can become a reference for the control method selection. Moreover, it can help engineer to understand this control method (Not just use only).

Table 5 : Effect of parameters to transmissibility level for skyhook system

	Transmissibility level	Mass ratio	Spring ratio	Damping ratio
Non-Ideal system	HIGH	LARGE	SMALL	SMALL
	LOW	SMALL	LARGE	LARGE
Ideal system	HIGH	LARGE	SMALL	SMALL
	LOW	SMALL	LARGE	LARGE

2.2.3 *Groundhook Suspension System*

Again use the same range of parameters (shown in Table 3), the acceleration transmissibility of groundhook system is shown in Figure 30. The arrangement is the same as the skyhook system. All together 9 graphs are shown in Figure 30. There are five curves to respect five damping ratio pairs for each graph. For $\zeta_{on} = 0$ and $\zeta_{off} = 0$, it is the passive case without damping. For $\zeta_{off} = 0$, they are Ideal groundhook cases and for $\zeta_{off} > 0$, they are Non-Ideal groundhook cases.

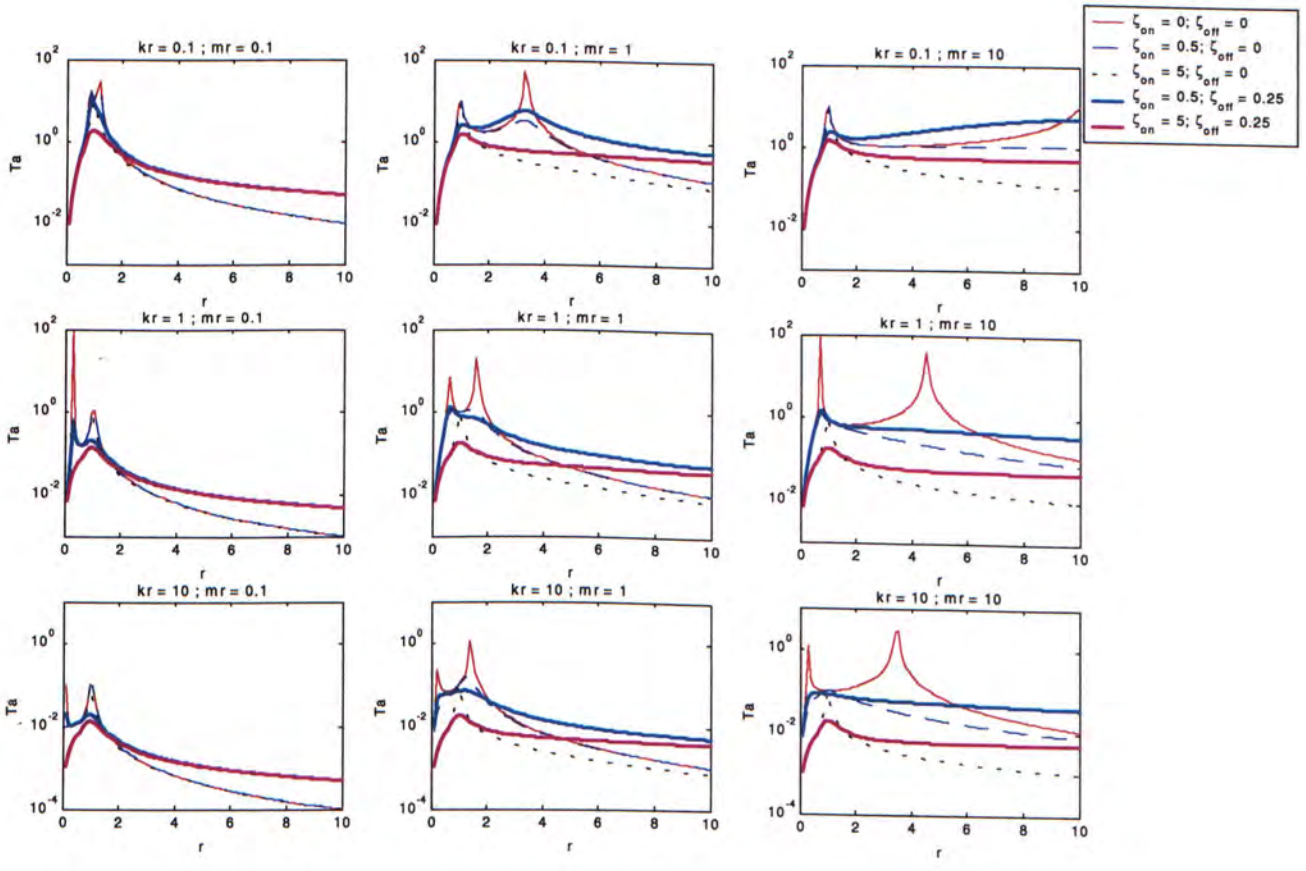

Figure 30: Acceleration transmissibility of groundhook system with varied parameters

The characteristics of the groundhook system are similar to the skyhook system. When the smaller mass ratio and larger spring ratio are selected, the transmissibility level is small and the peak of the acceleration transmissibility is shift to left. When a larger damping ratio is given, the lower transmissibility level will be obtained.

However, there are some special points worth to discuss. First of all, there is only one peak (for both Ideal and Non-Ideal groundhook system) if the mass ratio is large (e.g. $m_r = 10$). The peak is around the first natural frequency, which is different to the skyhook system. If the damping ratio is small ($\zeta_{on} = 0.5$), the spring ratio is small ($k_r \leq 1$) and the mass ratio is equal to 1, there are two peaks around the two natural frequencies for both Ideal and Non-Ideal groundhook cases. Different to the skyhook case, the peak of the transmissibility will not be shift to left.

Table 6 shows the effect of the transmissibility level by changing different parameters for groundhook system. The characteristics of the parameters are very similar to the skyhook system.

Table 6 : Effect of parameters to transmissibility level for groundhook system

	Transmissibility level	Mass ratio	Spring ratio	Damping ratio
Non-Ideal system	HIGH	LARGE	SMALL	SMALL
	LOW	SMALL	LARGE	LARGE
Ideal system	HIGH	LARGE	SMALL	SMALL
	LOW	SMALL	LARGE	LARGE

2.2.4 *Hybrid Suspension System*

Again to use the same range of parameters (shown in Table 3), the acceleration transmissibility of hybrid system is shown in Figure 31. The arrangement is the same as the skyhook and groundhook systems. All together 9 graphs are shown in Figure 31 where $\alpha = 0.5$ for all cases. There are five curves to respect five damping ratio pairs for each graph. For $\zeta_{on} = 0$ and $\zeta_{off} = 0$, it is the passive case without damping. For $\zeta_{off} = 0$, they are Ideal hybrid cases. For $\zeta_{off} > 0$, they are Non-Ideal hybrid cases.

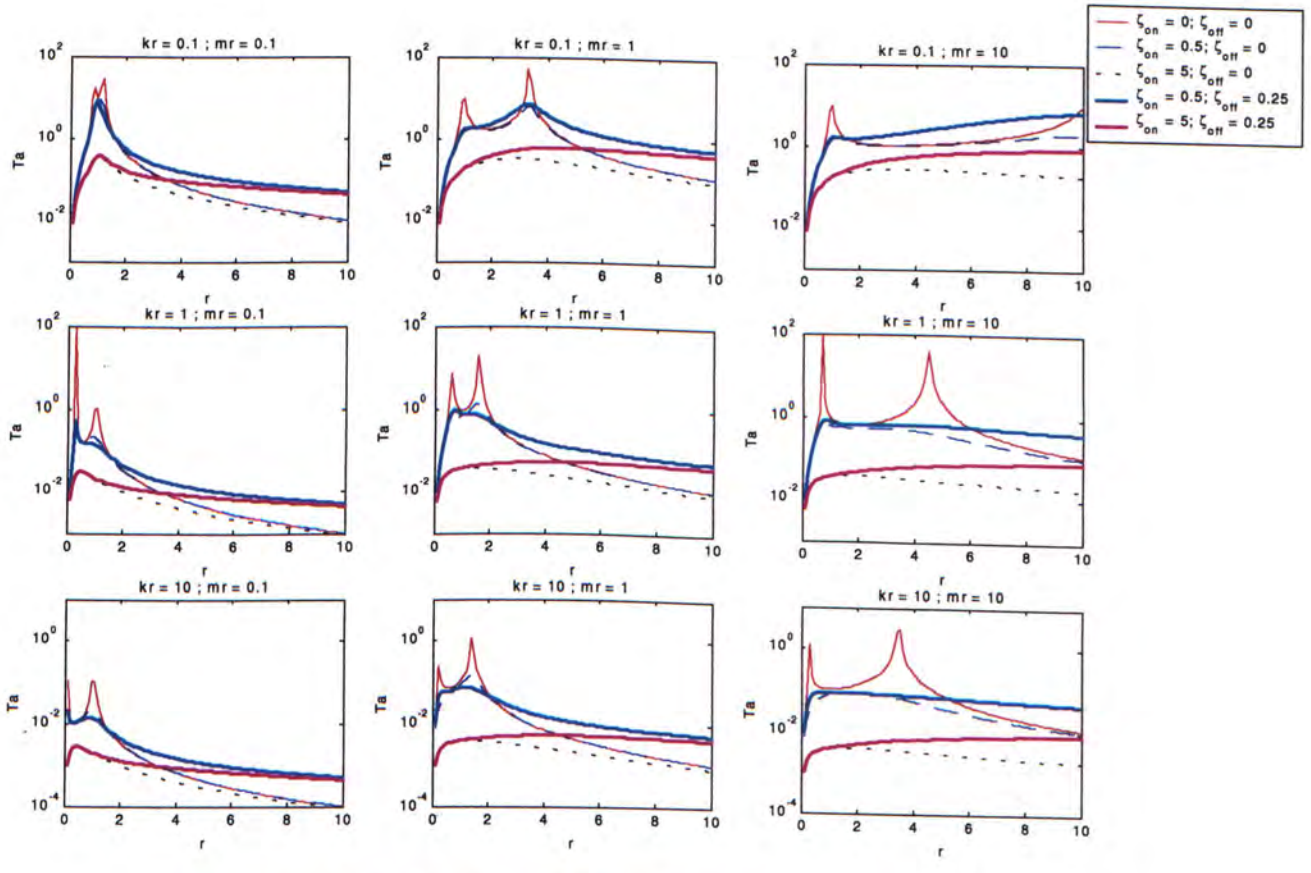

Figure 31 : Acceleration transmissibility of hybrid system with varied parameters

In the section 2.1.4, the effect of the transmissibility by changing the hybrid gain α has been discussed. This section will focus on other parameters (e.g. mass ratio, spring ratio and damping ratio) and choose a constant hybrid gain $\alpha = 0.5$. The characteristics of the hybrid system are similar to the skyhook and groundhook system.

It has been shown in the section 2.1.5 that the comparison between the skyhook, groundhook and hybrid systems. Actually, the characteristics of the parameters of three semi-active systems are similar especially for the effect of mass ratio and spring ratio. However, the reduction of the transmissibility level by increasing the damping ratio for hybrid system is much obvious than the skyhook and groundhook systems. The reason is that there are resonance frequencies for skyhook and groundhook system but hybrid system can compensate the shortcomings of skyhook and groundhook systems such that there is no higher peak in the whole frequency range. Table 6 shows the effect of the transmissibility level by changing different parameters for hybrid system (still keep the hybrid gain $\alpha = 0.5$). The characteristics of the parameters are similar to the skyhook and groundhook system.

Table 7 : Effect of parameters to transmissibility level for hybrid system

	Transmissibility level	Mass ratio	Spring ratio	Damping ratio	Hybrid gain, α
Non-Ideal system	HIGH	LARGE	SMALL	SMALL	LARGE or SMALL
	LOW	SMALL	LARGE	LARGE	OPTIMIZED
Ideal system	HIGH	LARGE	SMALL	SMALL	LARGE or SMALL
	LOW	SMALL	LARGE	LARGE	OPTIMIZED

2.3 *Stability*

A concept of stability due to Lyapunov is that the output and all the internal variables never become unbounded and go to zero as time goes to infinity for sufficiently small initial conditions. This concept is very important for the engineering practice. Since the initial conditions and the excitation function are always only approximately known, the systems need to allow only small changes in the behavior of the system from small disturbances. In this section, this stability concept will be introduced and the stability of the four suspension systems will also be discussed.

2.3.1 *Stability in the Sense of Lyapunov for Suspension Systems*

The linear time-invariant homogeneous vibrating system,

$$\dot{x}(t) = Ax(t), \qquad x(0) = x_0 \tag{29}$$

is called stable in the sense of Lyapunov at the equilibrium state $x = 0$ if for every positive $R > 0$ there exits a positive number $r > 0$ such that for all initial conditions is bounded by

$$\|x(0)\| < r \tag{30}$$

the corresponding trajectories $x(t)$ remain bounded for all $t \geq 0$ by R:

$$\|x\| < R, \qquad \forall t \geq 0 \tag{31}$$

Thus the definition of the stability can be written as:

$$\forall R > 0, \quad \exists r > 0, \quad \|x(0)\| < r \quad \Rightarrow \quad \forall t \geq 0, \|x(t)\| < R \tag{32}$$

Conversely, an equilibrium point is unstable if the initial condition within the boundary r (for every $r > 0$) and eventually leave the boundary R for $t \to \infty$. If the equilibrium point $x = 0$ is unstable, the vibrating system is not stable.

For vibration suppression, only Lyapunov stability is not enough. What we need is Lyapunov stability but also require that the attitude gradually go back to its equilibrium point.

The definition of the asymptotically stable is that an equilibrium point $x = 0$ is asymptotically stable if it is stable, and if in addition there exists some $r > 0$ such that $\|x(0)\| < r$ implies that $x(t) \to 0$ as $t \to \infty$. The vibrating system is called asymptotically stable if it is stable and if, for every bounded initial condition, the corresponding trajectory tends to the equilibrium point $x = 0$ as $t \to \infty$,

$$\lim_{t \to \infty} x(t) = 0 \tag{33}$$

Since an asymptotically stable system could also be termed stable, it is desirable to adopt the following convention. A vibrating system will be called marginally stable if it is stable, but not asymptotically stable.

The geometrical implications of the concepts of stability are illustrated in Figure 32 for a 2DoF suspension system. It has been shown that the system is called stable means that the system trajectory can be kept arbitrarily close to the origin by starting sufficiently close to it.

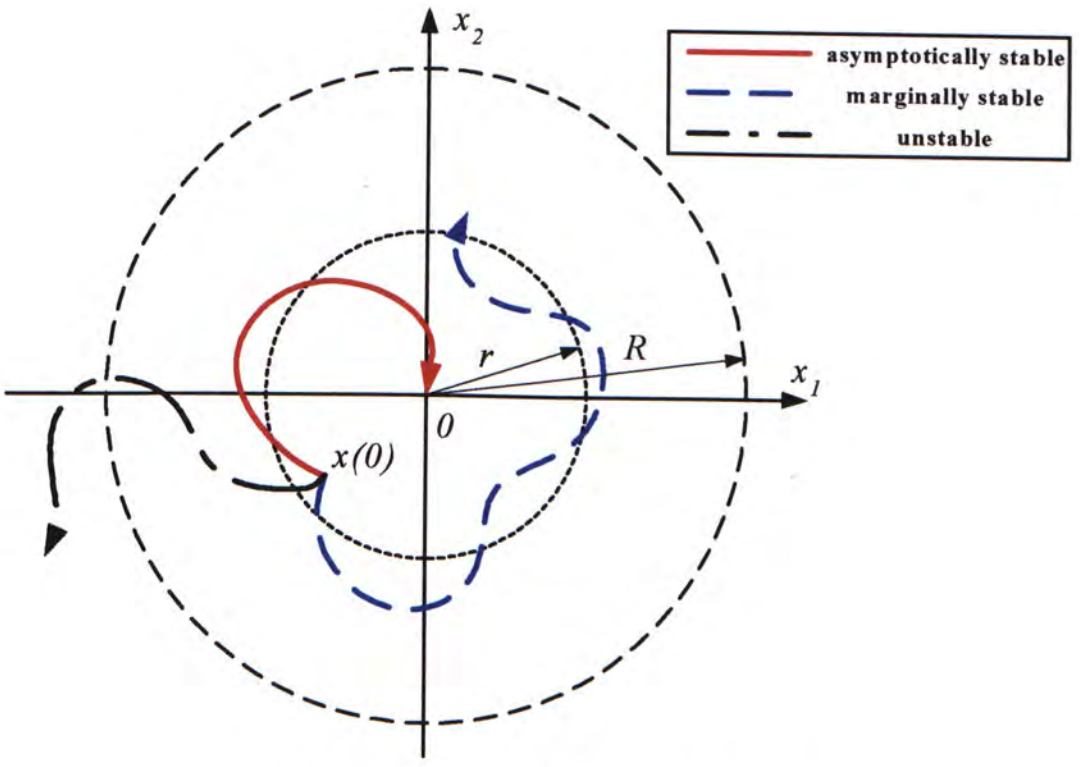

Figure 32 : Illustration of the concepts of stability

The stability definitions can be applied to a linear system (29) then it can characterize its stability behavior simply be means of the eigenvalues λ_i. The linear time-invariant homogeneous system $\dot{x}(t) = Ax(t)$ is:

Asymptotically stable if and only if all eigenvalues of A have negative real parts,

$$\mathrm{Re}\,\lambda_i < 0, \qquad i = 1:n \tag{34}$$

Marginally stable if there are on eigenvalues of A with positive real parts and there exists at least one eigenvalue with a vanishing real part, moreover the multiplicity v_j of each eigenvalue with a vanishing real part equals the nullity d_j of the corresponding characteristic matrix $(\lambda_j I - A)$:

$$\mathrm{Re}\lambda_i \le 0, \quad i = 1:n, \quad \mathrm{Re}\lambda_j = 0 : d_j = v_j \tag{35}$$

Unstable if at least one eigenvalue of A has a positive real part or there exists at least one multiple eigenvalue with a vanishing real part whose multiplicity v_j exceeds the nullity d_j of its characteristic matrix $(\lambda_j I - A)$:

$$\mathrm{Re}\lambda_i > 0 \text{ for one } i \text{ or } \mathrm{Re}\lambda_j = 0, v_j > d_j \text{ for one } j \tag{36}$$

2.3.2 Stability for four Suspension Systems

In the above sub-section, the concepts of stability have been introduced. Now this sub-section bases on those concepts to find out the stability of the passive, skyhook, groundhook and hybrid suspension system. The stability of the system will be discussed by means of eigenvalues. The characteristic equation will also be derived. By solving the characteristic equation, the eigenvalues will be obtained. Based on the stability concepts (34), (35) and (36), the stability of the systems will be identified.

First of all, the stability of the 2DoF passive suspension system will be discussed. From the equation of motion in equation (1), the state space equation of the 2DoF passive suspension system is

$$\dot{x} = \begin{bmatrix} \dot{x}_1 \\ \dot{x}_2 \\ \ddot{x}_1 \\ \ddot{x}_2 \end{bmatrix} = \begin{bmatrix} 0 & 0 & 1 & 0 \\ 0 & 0 & 0 & 1 \\ -\frac{k_1}{m_1} & \frac{k_1}{m_1} & -\frac{c_1}{m_1} & \frac{c_1}{m_1} \\ \frac{k_1}{m_2} & -(\frac{k_1+k_2}{m_2}) & \frac{c_1}{m_2} & -(\frac{c_1}{m_2}) \end{bmatrix} \begin{bmatrix} x_1 \\ x_2 \\ \dot{x}_1 \\ \dot{x}_2 \end{bmatrix} + \begin{bmatrix} 0 & 0 \\ 0 & 0 \\ 0 & 0 \\ \frac{k_2}{m_2} & 0 \end{bmatrix} \begin{bmatrix} y \\ \dot{y} \end{bmatrix}$$

$$\text{where } A_p = \begin{bmatrix} 0 & 0 & 1 & 0 \\ 0 & 0 & 0 & 1 \\ -\frac{k_1}{m_1} & \frac{k_1}{m_1} & -\frac{c_1}{m_1} & \frac{c_1}{m_1} \\ \frac{k_1}{m_2} & -(\frac{k_1+k_2}{m_2}) & \frac{c_1}{m_2} & -(\frac{c_1}{m_2}) \end{bmatrix} \tag{37}$$

The characteristic equation of the equation (37) is $p_p(\lambda) = \det(\lambda I - A_p)$, i.e.

$$p_p(\lambda) = \lambda^4 + (\frac{c_1}{m_1} + \frac{c_1}{m_2})\lambda^3 + (\frac{k_1}{m_1} + \frac{k_1}{m_2} + \frac{k_2}{m_2})\lambda^2 + (\frac{c_1 k_2}{m_1 m_2})\lambda + \frac{k_1 k_2}{m_1 m_2} \tag{38}$$

By solving the characteristic equation $p_p(\lambda)$, the eigenvalues λ_i will be obtained. Then use the stability concepts (34), (35) and (36), the stability of the passive suspension system can be identified. Then follow the same procedure, the characteristic equations of the skyhook, groundhook and hybrid system will be obtained as follows:

Since the Ideal case is the subset of the Non-Ideal case, the derivation of the characteristic equation of skyhook system will be shown for Non-Ideal case. From the equation of motion of Non-Ideal skyhook system, the state space equation is

$$\dot{x} = \begin{bmatrix} \dot{x}_1 \\ \dot{x}_2 \\ \ddot{x}_1 \\ \ddot{x}_2 \end{bmatrix} = \begin{bmatrix} 0 & 0 & 1 & 0 \\ 0 & 0 & 0 & 1 \\ -\frac{k_1}{m_1} & \frac{k_1}{m_1} & -\frac{c_s + c_1}{m_1} & \frac{c_1}{m_1} \\ \frac{k_1}{m_2} & -(\frac{k_1 + k_2}{m_2}) & \frac{c_1}{m_2} & -(\frac{c_1}{m_2}) \end{bmatrix} \begin{bmatrix} x_1 \\ x_2 \\ \dot{x}_1 \\ \dot{x}_2 \end{bmatrix} + \begin{bmatrix} 0 & 0 \\ 0 & 0 \\ 0 & 0 \\ \frac{k_2}{m_2} & 0 \end{bmatrix} \begin{bmatrix} y \\ \dot{y} \end{bmatrix}$$

$$\text{where } A_s = \begin{bmatrix} 0 & 0 & 1 & 0 \\ 0 & 0 & 0 & 1 \\ -\frac{k_1}{m_1} & \frac{k_1}{m_1} & -\frac{c_s + c_1}{m_1} & \frac{c_1}{m_1} \\ \frac{k_1}{m_2} & -(\frac{k_1 + k_2}{m_2}) & \frac{c_1}{m_2} & -(\frac{c_1}{m_2}) \end{bmatrix} \tag{39}$$

The characteristic equation of the equation (39) is $p_s(\lambda) = \det(\lambda I - A_s)$, i.e.

$$p_s(\lambda) = \lambda^4 + (\frac{c_1}{m_1} + \frac{c_s}{m_1} + \frac{c_1}{m_2})\lambda^3 + (\frac{c_s c_1}{m_1 m_2} + \frac{k_1}{m_1} + \frac{(k_1 + k_2)}{m_2})\lambda^2 + (\frac{c_s k_1}{m_1 m_2} + \frac{c_s k_2}{m_1 m_2} + \frac{c_1 k_2}{m_1 m_2})\lambda + \frac{k_1 k_2}{m_1 m_2} \tag{40}$$

In order to compare the systems easily, let the damping coefficient of on-state be $c_{on} = c_s + c_1$ and off-state be $c_{off} = c_1$. Then the characteristic equation becomes:

$$p_s(\lambda) = \lambda^4 + (\frac{c_{on}}{m_1} + \frac{c_{off}}{m_2})\lambda^3 + (\frac{(c_{on} - c_{off})c_{off}}{m_1 m_2} + \frac{k_1}{m_1} + \frac{(k_1 + k_2)}{m_2})\lambda^2 + (\frac{(c_{on} - c_{off})k_1}{m_1 m_2} + \frac{c_{on} k_2}{m_1 m_2})\lambda + \frac{k_1 k_2}{m_1 m_2} \tag{41}$$

From the equation of motion of the Non-Ideal groundhook suspension system, the state space equation is

$$\dot{x} = \begin{bmatrix} \dot{x}_1 \\ \dot{x}_2 \\ \ddot{x}_1 \\ \ddot{x}_2 \end{bmatrix} = \begin{bmatrix} 0 & 0 & 1 & 0 \\ 0 & 0 & 0 & 1 \\ -\frac{k_1}{m_1} & \frac{k_1}{m_1} & -\frac{c_1}{m_1} & \frac{c_1}{m_1} \\ \frac{k_1}{m_2} & -(\frac{k_1+k_2}{m_2}) & \frac{c_1}{m_2} & -(\frac{c_g+c_1}{m_2}) \end{bmatrix} \begin{bmatrix} x_1 \\ x_2 \\ \dot{x}_1 \\ \dot{x}_2 \end{bmatrix} + \begin{bmatrix} 0 & 0 \\ 0 & 0 \\ 0 & 0 \\ \frac{k_2}{m_2} & 0 \end{bmatrix} \begin{bmatrix} y \\ \dot{y} \end{bmatrix}$$

where $A_g = \begin{bmatrix} 0 & 0 & 1 & 0 \\ 0 & 0 & 0 & 1 \\ -\frac{k_1}{m_1} & \frac{k_1}{m_1} & -\frac{c_1}{m_1} & \frac{c_1}{m_1} \\ \frac{k_1}{m_2} & -(\frac{k_1+k_2}{m_2}) & \frac{c_1}{m_2} & -(\frac{c_g+c_1}{m_2}) \end{bmatrix}$ (42)

The characteristic equation of the equation (42) is $p_g(\lambda) = \det(\lambda I - A_g)$, i.e.

$$p_g(\lambda) = \lambda^4 + (\frac{c_1}{m_1} + \frac{c_g}{m_2} + \frac{c_1}{m_2})\lambda^3 + (\frac{c_g c_1}{m_1 m_2} + \frac{k_1}{m_1} + \frac{(k_1+k_2)}{m_2})\lambda^2 + (\frac{c_g k_1}{m_1 m_2} + \frac{c_1 k_2}{m_1 m_2})\lambda + \frac{k_1 k_2}{m_1 m_2} \quad (43)$$

Similar to skyhook case, let the damping coefficient of on-state be $c_{on} = c_g + c_1$ and off-state be $c_{off} = c_1$. Then the characteristic equation becomes:

$$p_g(\lambda) = \lambda^4 + (\frac{c_{off}}{m_1} + \frac{c_{on}}{m_2})\lambda^3 + (\frac{(c_{on} - c_{off})c_{off}}{m_1 m_2} + \frac{k_1}{m_1} + \frac{(k_1+k_2)}{m_2})\lambda^2 + (\frac{(c_{on} - c_{off})k_1}{m_1 m_2} + \frac{c_{off} k_2}{m_1 m_2})\lambda + \frac{k_1 k_2}{m_1 m_2} \quad (44)$$

From the equation of motion of the Non-Ideal hybrid suspension system, the state space equation is

$$\dot{x} = \begin{bmatrix} \dot{x}_1 \\ \dot{x}_2 \\ \ddot{x}_1 \\ \ddot{x}_2 \end{bmatrix} = \begin{bmatrix} 0 & 0 & 1 & 0 \\ 0 & 0 & 0 & 1 \\ -\frac{k_1}{m_1} & \frac{k_1}{m_1} & -\frac{c_s + c_1}{m_1} & \frac{c_1}{m_1} \\ \frac{k_1}{m_2} & -(\frac{k_1 + k_2}{m_2}) & \frac{c_1}{m_2} & -(\frac{c_g + c_1}{m_2}) \end{bmatrix} \begin{bmatrix} x_1 \\ x_2 \\ \dot{x}_1 \\ \dot{x}_2 \end{bmatrix} + \begin{bmatrix} 0 & 0 \\ 0 & 0 \\ 0 & 0 \\ \frac{k_2}{m_2} & 0 \end{bmatrix} \begin{bmatrix} y \\ \dot{y} \end{bmatrix}$$

where $A_h = \begin{bmatrix} 0 & 0 & 1 & 0 \\ 0 & 0 & 0 & 1 \\ -\frac{k_1}{m_1} & \frac{k_1}{m_1} & -\frac{c_s + c_1}{m_1} & \frac{c_1}{m_1} \\ \frac{k_1}{m_2} & -(\frac{k_1 + k_2}{m_2}) & \frac{c_1}{m_2} & -(\frac{c_g + c_1}{m_2}) \end{bmatrix}$ (45)

The characteristic equation of the equation (45) is $p_h(\lambda) = \det(\lambda I - A_h)$, i.e.

$$p_h(\lambda) = \lambda^4 + (\frac{c_1}{m_1} + \frac{c_s}{m_1} + \frac{c_g}{m_2} + \frac{c_1}{m_2})\lambda^3 + (\frac{c_s c_g + c_s c_1 + c_g c_1}{m_1 m_2} + \frac{k_1}{m_1} + \frac{(k_1 + k_2)}{m_2})\lambda^2 + (\frac{c_s k_1}{m_1 m_2} + \frac{c_s k_2}{m_1 m_2} + \frac{c_g k_1}{m_1 m_2} + \frac{c_1 k_2}{m_1 m_2})\lambda + \frac{k_1 k_2}{m_1 m_2} \quad (46)$$

Similar to skyhook case, let the damping coefficient of on-state be $c_{on} = c_g + c_1$ and off-state be $c_{off} = c_1$. Then the characteristic equation becomes:

$$p_h(\lambda) = \lambda^4 + (\frac{c_{off}}{m_1} + \frac{c_{on}}{m_2} + \alpha(c_{on} - c_{off})(\frac{1}{m_1} - \frac{1}{m_2}))\lambda^3 + (\frac{\alpha(1-\alpha)(c_{on} - c_{off})^2 + (c_{on} - c_{off})c_{off}}{m_1 m_2} + \frac{k_1}{m_1} + \frac{(k_1 + k_2)}{m_2})\lambda^2 + (\frac{(c_{on} - c_{off})k_1}{m_1 m_2} + \frac{c_{off} k_2}{m_1 m_2} + \frac{\alpha(c_{on} - c_{off})k_2}{m_1 m_2})\lambda + \frac{k_1 k_2}{m_1 m_2} \quad (47)$$

The parameters shown in Table 8 are the same as the Table 1 except the values of damping coefficients: $c_1 = \sqrt{m_1 k_1} = 6324$ N - s/m , $c_{on} = 2\sqrt{m_1 k_1} = 6324$ N - s/m , $c_{off} = \sqrt{m_1 k_1} = 3162$ N - s/m for Non-Ideal systems and $c_{off} = 0$ N - s/m for Ideal systems. Substitute those parameters shown in Table 8 to the characteristic equation, the eigenvalues λ_i of systems will be obtained and the stabilities of the four suspension systems can also be identified (refer to the Table 9).

Table 8 : Parameters of the suspension systems

Parameter	Value
Sprung mass of quarter car (m_1)	454.5 kg
Unsprung mass of quarter car (m_2)	45.45 kg
Spring constant of suspension system (k_1)	22000 N/m
Spring constant of tire (k_2)	176000 N/m
Damping coefficient of suspension damper (c_1)	6324 N-s/m
Damping coefficient for on-state (c_{on})	6324 N-s/m
Damping coefficient for off-state (c_{off})	3162 N-s/m
Damping coefficient of tire (c_2)	0 N-s/m

Table 9 : Eigenvalues and stabilities of the four suspension systems

		Non-Ideal			Ideal		
λ_i	Passive	Skyhook	Groundhook	Hybrid	Skyhook	Groundhook	Hybrid
λ_1	-13.7946 + 9.7138i	-34.7868 +51.5972i	-2.9611 + 6.1606i	-4.9377 + 4.8335i	-0.0084 +66.0427i	-0.0842 + 6.5727i	-3.5221 + 5.5337i
λ_2	-13.7946 - 9.7138i	-34.7868 - 51.5972i	-2.9611 - 6.1606i	-4.9377 - 4.8335i	-0.0084 - 66.0427i	-0.0842 - 6.5727i	-3.5221 - 5.5337i
λ_3	-5.4883	-6.9574	-40.0779	-52.4606 +34.2625i	-4.6440	-47.3411	-34.7434 +56.1185i
λ_4	-119.9845	-6.9574	-100.1044	-52.4606 -34.2625i	-9.2540	-91.6376	-34.7434 -56.1185i
Re λ_i	All negative	All negative	All negative	All negative	All negative	All negative	All negative
	Asymptotically stable	Asymptotically stable	Asymptotically stable	Asymptotically stable	Asymptotically stable	Asymptotically stable	Asymptotically stable

2.4 *Optimization*

The parameters determining the behavior of the suspension systems, such as spring constants and damping coefficients, often don't have fixed values. The parameters can be varied within a certain range. Therefore, it can be attempted to choose the suitable parameters within these ranges so that the system becomes asymptotically stable and exhibits an optimum behavior in the working range. Based on the section 2.2, it can be known that the trend of vary parameters for the performance (in the sense of acceleration transmissibility). In the section, the main objective is to find a good way to choose a good hybrid gain for the hybrid system because the hybrid system has better performance comparing to the other suspension systems. One method proposed by [43]. The author tried to find the optimal damping coefficient of the passive suspension systems. Based on this method, the new idea for choosing a hybrid gain can be developed. Before discuss this idea, let's have an introduction of the optimization of the damping coefficient of the passive systems first.

2.4.1 *Single-Degree-of-Freedom Passive System*

As shown in typical vibration books (e.g. [42]-[46]), the equation of motion and the displacement transmissibility equation of the SDoF quarter car model are:

$$m_1\ddot{x}+c_1(\dot{x}-\dot{y})+k_1(x-x_b)=0 \tag{48}$$

$$Td=\left|\frac{X}{X_b}\right|=\sqrt{\frac{{k_1}^2+(c_1\omega_b)^2}{(k_1-m_1{\omega_b}^2)^2+(c_1\omega_b)^2}}=\sqrt{\frac{1+(2\zeta_1 r)^2}{(1-r^2)^2+(2\zeta_1 r)^2}} \tag{49}$$

The acceleration transmissibility of the SDoF passive suspension system is:

$$Ta = r^2\left|\frac{X}{X_b}\right| = r^2\sqrt{\frac{1+(2\zeta_1 r)^2}{(1-r^2)^2+(2\zeta_1 r)^2}} \tag{50}$$

In the Figure 33 and Figure 34, there are the displacement transmissibility and acceleration transmissibility of the SDoF passive suspension system. There are intersection points at $r=\sqrt{2}$ in the both figures. In order to obtain a good performance for riding comfort, the acceleration of the sprung mass has to be kept to a minimum. By differentiating the acceleration transmissibility Ta and let the equation of the derivative equal to zero at $r=\sqrt{2}$, the optimal damping ratio is:

$$\frac{d}{dr}Ta\Big|_{r=\sqrt{2}} = 0 \quad \Rightarrow \quad \zeta_{op} = \frac{1}{2\sqrt{2}} \text{ or } -\frac{1}{2\sqrt{2}} \text{ (rejected)} \tag{51}$$

Then the displacement and acceleration transmissibility become:

$$Td = \left|\frac{X}{X_b}\right| = \sqrt{\frac{2+r^2}{2r^4-3r^2+2}} \text{ and } Ta = r^2\left|\frac{X}{X_b}\right| = r^2\sqrt{\frac{2+r^2}{2r^4-3r^2+2}} \tag{52}$$

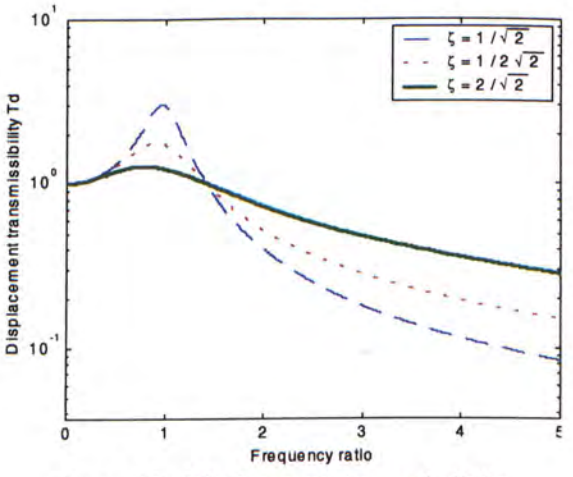

Figure 33 : Displacement transmissibility

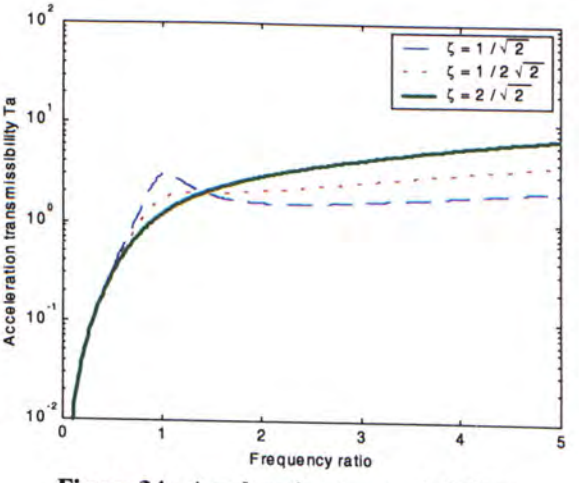

Figure 34 : Acceleration transmissibility

2.4.2 *Two-Degree-of-Freedom Passive System*

Recall the acceleration transmissibility of sprung mass of the 2DoF passive suspension system (equation (5)):

$$Ta_1 = \left|\frac{\ddot{X}_1}{X_b}\right| = r^2 \sqrt{\frac{m_r{}^2(1+(2\zeta_1 r)^2]}{[k_r r^4 - (k_r + m_r k_r + m_r)r^2 + m_r]^2 + [-(m_r+1)2k_r\zeta_1 r^3 + 2\zeta_1 m_r r]^2}} \quad (53)$$

In the Figure 35, there are the displacement transmissibility and acceleration transmissibility of the 2DoF passive suspension system. The first intersection points at $r = \sqrt{31-\sqrt{881}}$ are shown in Figure 35. By differentiating the acceleration transmissibility Ta_1 and let the equation of the derivative equal to zero at $r = \sqrt{31-\sqrt{881}}$, such that:

$$\frac{d}{dr} Ta_1 \Big|_{r=\sqrt{31-\sqrt{881}}} = 0 \quad (54)$$

Since the solution of the equation (54) is very complicate and not easily to use, it can be simplified by approximation such that the optimum damping ratio is:

$$\zeta_{op} \approx \frac{\sqrt{1+2k_r}}{2\sqrt{2}} \quad (55)$$

Then the displacement and acceleration transmissibility become:

$$Td_1 = \sqrt{\frac{m_r^2[2+(1+2k_r)r^2]}{2[k_r r^4 - (k_r + m_r k_r + m_r)r^2 + m_r]^2 + [-(m_r+1)k_r\sqrt{1+2k_r}\,r^3 + m_r\sqrt{1+2k_r}\,r]^2}}$$

$$Ta_1 = r^2\sqrt{\frac{m_r^2[2+(1+2k_r)r^2]}{2[k_r r^4 - (k_r + m_r k_r + m_r)r^2 + m_r]^2 + [-(m_r+1)k_r\sqrt{1+2k_r}\,r^3 + m_r\sqrt{1+2k_r}\,r]^2}} \quad (56)$$

By using the parameters, k_r and m_r in Table 1 and substitute those parameters into the equation (56), then the displacement and acceleration transmissibility of passive systems with different damping rations are shown below:

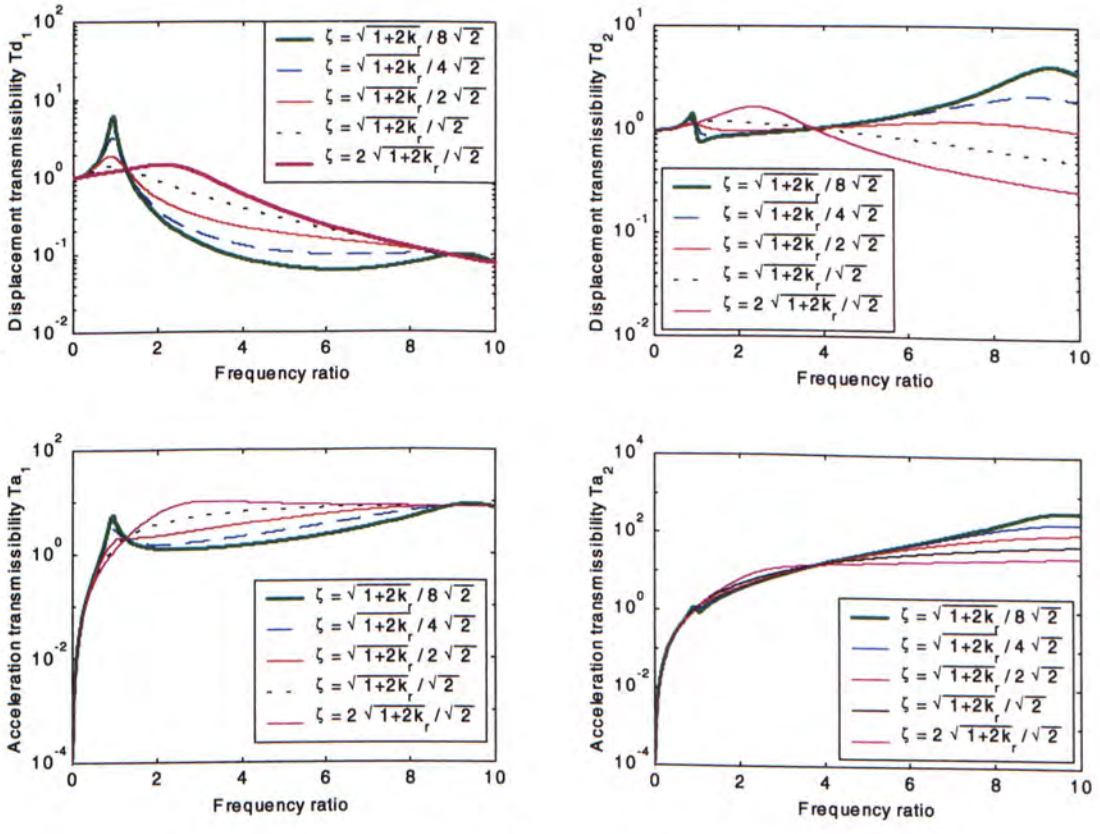

Figure 35 : Transmissibility of the optimized 2DoF passive system

2.4.3 *Hybrid Suspension System*

From the above two passive systems, this optimization method is to find a intersection point for all different damping ratios and then differentiate the acceleration transmissibility and let the equation of the derivative equal to zero at that intersection point in order to find the suitable damping ratio with minimum slope. However, there is no intersection point in the acceleration transmissibility of the hybrid suspension for all different hybrid gain. Figure 36 shows the acceleration transmissibility of the Ideal hybrid system, which has been shown in the Figure 23. It seems that there is a intersection point around the frequency ratio $r = 3$. However, it can be seen that there is no unique intersection point for all hybrid gains when we zoom in to the frequency range $r = 2.5$ to 3.5 (see Figure 37). Therefore the previous method cannot be applied on this situation directly.

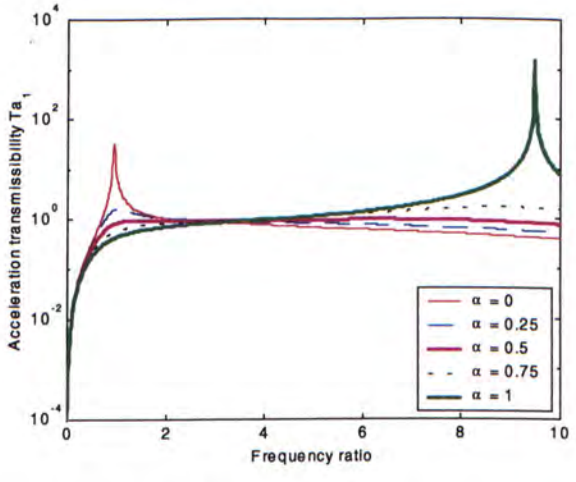

Figure 36 : Acceleration transmissibility

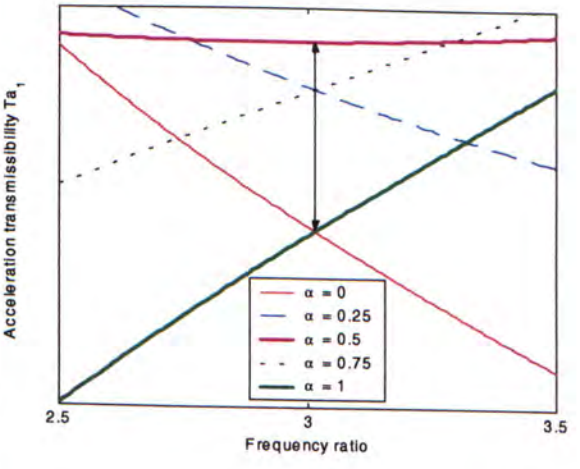

Figure 37 : Acceleration transmissibility (r=2.5:3.5)

Although there is no unique intersection point for all hybrid gains, the intersection points seem that lie on the same frequency ratio, which is shown in Figure 37 (the arrows point to the intersection points). However, it seems that the intersection points need to be created by the curves of α and $(1-\alpha)$. In order to prove this phenomenon, recall the acceleration transmissibility equation (equation (26)):

$$Ta_1 = \left|\frac{\ddot{X}_1}{X_b}\right| = r^2\sqrt{\frac{m_r^{\,2}}{a_I^{\,2}+b_I^{\,2}}} \tag{57}$$

where

$$a_I = k_r r^4 - (k_r + m_r k_r + m_r + 4m_r k_r \alpha(1-\alpha)\zeta_h^{\,2})r^2 + m_r$$
$$b_I = -[2k_r\zeta_h((1-\alpha)m_r + \alpha)]r^3 + 2m_r(\alpha + k_r)\zeta_h]r$$

Let $\alpha = h_1$ and $\alpha = h_2 = (1-h_1)$, substitute into equation (57), then

$$Ta_1' = Ta_1\big|_{\alpha=h_1} = r^2\sqrt{\frac{m_r^{\,2}}{a_1^{\,2}+b_1^{\,2}}} \tag{58}$$

where

$$a_I = k_r r^4 - (k_r + m_r k_r + m_r + 4m_r k_r h_1(1-h_1)\zeta_h^{\,2})r^2 + m_r$$
$$b_I = -[2k_r\zeta_h((1-h_1)m_r + h_1)]r^3 + 2m_r(h_1 + k_r)\zeta_h]r$$

$$Ta_1'' = Ta_1\big|_{\alpha=h_2=(1-h_1)} = r^2\sqrt{\frac{m_r^{\,2}}{a_2^{\,2}+b_2^{\,2}}} \tag{59}$$

where

$$a_I = k_r r^4 - (k_r + m_r k_r + m_r + 4m_r k_r h_1(1-h_1)\zeta_h^{\,2})r^2 + m_r$$
$$b_I = -[2k_r\zeta_h(h_1 m_r + \alpha)]r^3 + 2m_r((1-h_1) + k_r)\zeta_h]r$$

Assume Ta_1' and Ta_1'' are intersected, we have

$$Ta_1' - Ta_1'' = 0 \tag{60}$$

Solve the equation (60), then

$$r = \sqrt{(2+\frac{1}{k_r})(\frac{m_r}{1+m_r})}\Bigg|_{k_r=0.125 \text{ and } m_r=10} \cong 3.02 \tag{61}$$

For all Ta_1' and Ta_1'' with $\alpha = h_1$ and $\alpha = h_2 = (1-h_1)$ respectively, they have to intersect at $r = \sqrt{(2+\frac{1}{k_r})(\frac{m_r}{1+m_r})}$ for any $0 \le h_1 \le 1$ and $0 \le h_2 \le 1$. From the Figure 37, the transmissibility value at the intersection point is smaller which implies that the peaks of the transmissibility are higher. For example, transmissibility at the intersection point of $\alpha = 0$ and $\alpha = 1$ is the lowest but the peaks of transmissibility of them are highest. Therefore, the higher transmissibility at the intersection point will have lower transmissibility level around the frequency range. According to Figure 37, the h_1 increase and h_2 decrease will cause the intersection point moving upward. When $Ta_1' = Ta_1''$ at $r = \sqrt{(2+\frac{1}{k_r})(\frac{m_r}{1+m_r})}$, the intersection point will be maximum. Thus,

$$Ta_1' - Ta_1'' = 0 \quad \Rightarrow \quad \alpha = 0.5 \tag{62}$$

Therefore, based on the above result, the hybrid suspension system will have a good performance by choosing the hybrid gain $\alpha = 0.5$.

The other optimization method can be based on the concept of section 2.4.1 and 2.4.2, it is possible to find a hybrid gain, which the slope of the acceleration transmissibility at the frequency of the intersection point is equal to zero.

Recall the equation (61), the frequency ratio of the intersection point is:

$$r = \sqrt{(2+\frac{1}{k_r})(\frac{m_r}{1+m_r})}\Bigg|_{k_r=0.125 \text{ and } m_r=10} \cong 3.02$$

By differentiating the acceleration transmissibility Ta_1 and let the equation of the derivative equal to zero at $r \cong 3.02$, such that:

$$\frac{d}{dr} Ta_1 \Big|_{r\cong 3.02} = 0 \quad \Rightarrow \quad \alpha = 0.4992 \cong 0.5 \tag{63}$$

Therefore, this result is very close to that shown in the previous optimization method ($\alpha = 0.5$). However, this method needs further development because the solution of the equation (63) with general r is complicated.

Chapter 3

SUSPENSION SYSTEM WITH VIBRATION CONTROLLER

In Chapter 1, the controllable automotive suspension systems have been introduced. There are three main parts for the systems. They are suspension system model, controllable device and controller. MR damper (controllable semi-active device) has been selected in this study. The vibration controller includes two parts. They are system controller and damper controller. The details of the system model, the model of the MR damper and the derivation of the vibration controller will be discussed in this chapter.

3.1 Two-Degree-of-Freedom Quarter Car Model

The model of a car suspension can be represented by multi-degree-of-freedom system, which is shown in Figure 38. A quarter car model can be considered as a two degree-of-freedom suspension system as shown in Figure 39. The vehicle mass with passenger is represented by a sprung mass m_1 and the mass of wheels and associated components are represented by an unsprung mass m_2. The vertical motion of the system can be described by the displacement x_1 and x_2. The excitation due to road disturbance is x_b. The suspension spring constant is ks_1 and the tire spring constant is ks_2. Moreover, the damping force for the MR damper and damping coefficient of the tire are f_d and c_2, respectively.

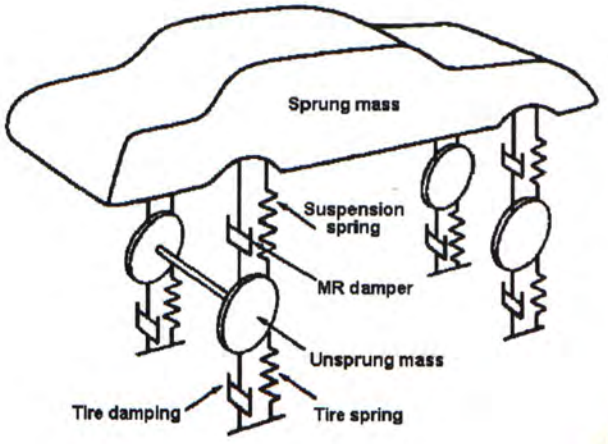

Figure 38 : A car model

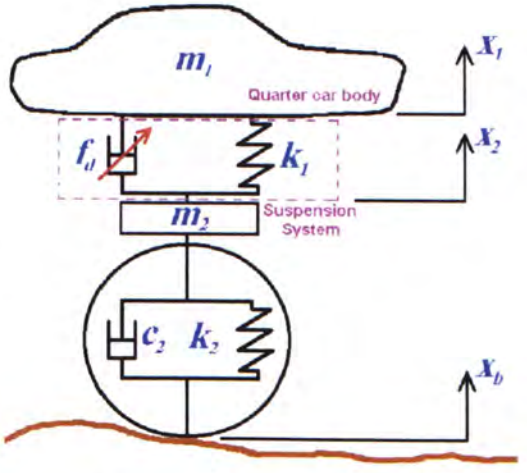

Figure 39 : A quarter car model

By applying Newton's second law to the quarter car model, the equations of motion for m_1 and m_2 are:

$$\begin{cases} m_1\ddot{x}_1 + k_1(x_1 - x_2) + f_d = 0 \\ m_2\ddot{x}_2 - c_2(\dot{x}_b - \dot{x}_2) - k_1(x_1 - x_2) - k_2(x_b - x_2) - f_d = 0 \end{cases} \tag{64}$$

The car suspension system can be represented in the state space form as follows:

$$\dot{x} = \begin{bmatrix} \dot{x}_1 \\ \dot{x}_2 \\ \ddot{x}_1 \\ \ddot{x}_2 \end{bmatrix} = \begin{bmatrix} 0 & 0 & 1 & 0 \\ 0 & 0 & 0 & 1 \\ -\frac{k_1}{m_1} & \frac{k_1}{m_1} & 0 & 0 \\ \frac{k_1}{m_2} & -(\frac{k_1+k_2}{m_2}) & 0 & -\frac{c_2}{m_2} \end{bmatrix} \begin{bmatrix} x_1 \\ x_2 \\ \dot{x}_1 \\ \dot{x}_2 \end{bmatrix} + \begin{bmatrix} 0 & 0 & 0 \\ 0 & 0 & 0 \\ -\frac{1}{m_1} & 0 & 0 \\ \frac{1}{m_2} & \frac{k_2}{m_2} & \frac{c_2}{m_2} \end{bmatrix} \begin{bmatrix} f_d \\ x_b \\ \dot{x}_b \end{bmatrix} \tag{65}$$

3.2 MR Damper

A prototype of MR damper (RD-1005-1 manufactured by Load Corporation) is used in this study. The length of the damper is 20.83 cm in its extended position. The mathematical model of the MR damper proposed by Spencer et al [31]. Figure 40 is adopted in this study. The hysteretic behavior in the damper is described by the Bouc-Wen model.

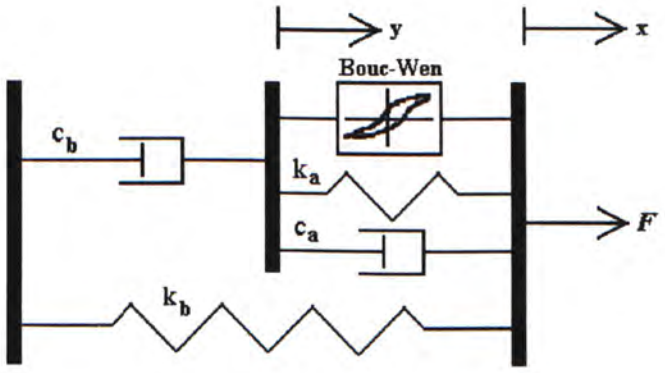

Figure 40 : Model of the MR damper

The model of the MR damper is shown in Figure 40. To obtain the governing equations for this model, consider only the upper part of the model. The resultant force on the rigid bar is zero.

$$\dot{y} = \frac{1}{(c_a + c_b)}\left[\alpha z + k_a(x - y) + c_a\dot{x}\right] \tag{66}$$

where z is given by

$$\dot{z} = -\gamma|\dot{x} - \dot{y}||z|^{n-1} z - \mu(\dot{x} - \dot{y})|z|^n + A(\dot{x} - \dot{y}) \tag{67}$$

The resultant force generated by the system is then found by the summation of the forces in the upper and lower sections of the system in Figure 40, yielding

$$F = c_b \dot{y} + k_b (x - x_0) \tag{68}$$

x_0 is used to account for the effect of the accumulator in the MR damper, α is a scaling value for the Bouc-Wen model and the parameters γ, μ, A and n are used to control the scale and shape of the hysteresis loop. Until now, only the case for the constant power input is considered. In order to adapt to the environment, a model with changing input voltage should be considered. To determine a model including the fluctuation of the magnetic fields, the dependence of the parameters on the applied current must be determined. Therefore, the following linear relations have been proposed [31]:

$$\alpha = \alpha(u) = \alpha_a + \alpha_b u \tag{69}$$

$$c_b = c_b(u) = c_{ba} + c_{bb} u \tag{70}$$

$$c_a = c_a(u) = c_{aa} + c_{ab} u \tag{71}$$

u is given by the following dynamic equation:

$$\dot{u} = -\eta(u - v) \tag{72}$$

where v is the voltage applied to the current driver. Equation (72) models the reaching rheological equilibrium of the MR fluid due to the change of magnetic field. The rate of reaching equilibrium is governed by η. This model can accurately predict the behaviour of the damper. Lai and Liao [39] determined the optimized parameters for the MR damper model by fitting the model to the experimental data. The resulting parameters are given in Table 1 [39].

Table 1: Parameters for the MR damper model

Parameter	Value	Parameter	Value
c_{aa}	784 Ns/m	α_a	12441 N/m
c_{ab}	1803 Ns/Vm	α_b	38430 N/Vm
k_a	3610 N/m	γ	136320 /m^2
c_{ba}	14649 Ns/m	μ	2059020 /m^2
c_{bb}	34622 Ns/Vm	A	58
k_b	840 N/m	n	2
x_0	0.0908 m	η	190 /s

3.3 Vibration Controller

In this study, a semi-active control system is proposed. The block diagram is shown in Figure 41. The plant is the two degree-of-freedom suspension system excluding the MR damper. The vibration controller consists of two controllers. The system controller generates the desired controlled force while the damper controller adjusts the voltage level to track the desired force. In the block diagram, the plant is represented by the state space equation (65) and the MR damper has been modeled and given in section 3.2. The damping force of the MR damper is f_d and the desired damping force generated by system controller is f_c.

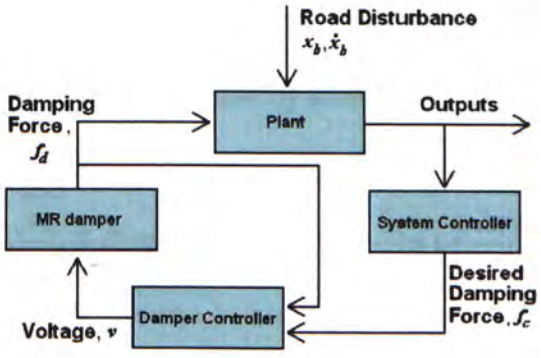

Figure 41 : Block diagram of the semi-active control system

3.3.1 System Controller: Sliding Mode Control

Sliding mode control is used as the system controller for the suspension system. The advantages of employing this control technique are that, the system can be designed to be robust with respect to modeling imprecision. And also, it can be synthesized for the nonlinear semi-active system adequately. In this study, the model-reference design approach is chosen. Therefore, the good reference is necessary to be considered.

In practice, the mass of the vehicle varies by the loading conditions such as the number of riding persons and payloads. Therefore, we consider that parameter perturbations of the sprung mass exist in the system. Assume the possible boundary of the sprung mass as follows:

$$m_1 = m_0 + \Delta m_1 \text{ and } |\Delta m_1| \leq 0.2 m_0 \tag{73}$$

where m_0 represents the nominal mass and Δm_1 is uncertain part. The mass uncertainty, which is 20% of nominal mass, is chosen here for the purpose of discussion.

The difference between the value of estimated nominal mass and the value of the real sprung mass is assumed to be bounded by known β:

$$\frac{1}{\beta} \le \frac{\frac{1}{m_0}}{\frac{1}{m_1}} \le \beta \Rightarrow \frac{1}{\beta} \le \frac{m_1}{m_0} \le \beta \Rightarrow \frac{1}{\beta} \le 1 + \frac{\Delta m_1}{m_0} \le \beta \tag{74}$$

where $1 + \frac{\Delta m_1}{m_0}$ is $\begin{cases} \text{maximum for } \Delta m_1 = 0.2\, m_0 \\ \text{minimum for } \Delta m_1 = -0.2\, m_0 \end{cases}$. So β can be chosen to be 1.25

The objective of the model-reference approach is to develop a control algorithm, which forces the plant dynamics to follow the dynamics of an ideal model. The controller can force the error between the plant and the model states to zero as time tends to infinity. This will ensure that the plant output follows the model output faithfully. Therefore, the design of the reference model is very important. In the following sub-sections, the design of the sliding control algorithm and different reference models will be discussed.

3.3.1.1 Reference models

In the previous sections, it has been mentioned that the best suspension model will be selected as the reference model. Thus, the Ideal hybrid system should be selected. Since the Ideal hybrid system is the linear combination of the Ideal skyhook system and Ideal groundhook system, we still want to compare the performance of those systems. Therefore, these three suspension systems will be selected as the reference models.

For the Ideal skyhook reference model (in Figure 6), the equation of motion is:

$$\begin{cases} m_{ref1}\ddot{x}_{ref1} + c_s\dot{x}_{ref1} + ks_{ref1}(x_{ref1} - x_{ref2}) = 0 \\ m_{ref2}\ddot{x}_{ref2} + ks_{ref1}(x_{ref2} - x_{ref1}) + ks_{ref2}(x_{ref2} - x_b) = 0 \end{cases} \tag{75}$$

And the state space equation is:

$$\dot{x} = \begin{bmatrix} \dot{x}_{ref1} \\ \dot{x}_{ref2} \\ \ddot{x}_{ref1} \\ \ddot{x}_{ref2} \end{bmatrix} = \begin{bmatrix} 0 & 0 & 1 & 0 \\ 0 & 0 & 0 & 1 \\ -\dfrac{ks_{ref1}}{m_{ref1}} & \dfrac{ks_{ref1}}{m_{ref1}} & -\dfrac{c_s}{m_{ref1}} & 0 \\ \dfrac{ks_{ref1}}{m_{ref2}} & -(\dfrac{ks_{ref1}+ks_{ref2}}{m_{ref2}}) & 0 & 0 \end{bmatrix} \begin{bmatrix} x_{ref1} \\ x_{ref2} \\ \dot{x}_{ref1} \\ \dot{x}_{ref2} \end{bmatrix} + \begin{bmatrix} 0 & 0 \\ 0 & 0 \\ 0 & 0 \\ \dfrac{ks_{ref2}}{m_{ref2}} & 0 \end{bmatrix} \begin{bmatrix} x_b \\ \dot{x}_b \end{bmatrix}$$

$$y = \begin{bmatrix} x_{ref1} \\ \dot{x}_{ref1} \\ \ddot{x}_{ref1} \end{bmatrix} = \begin{bmatrix} 1 & 0 & 0 & 0 \\ 0 & 0 & 1 & 0 \\ -\dfrac{ks_{ref1}}{m_{ref1}} & \dfrac{ks_{ref1}}{m_{ref1}} & -\dfrac{c_s}{m_{ref1}} & 0 \end{bmatrix} \begin{bmatrix} x_{ref1} \\ x_{ref2} \\ \dot{x}_{ref1} \\ \dot{x}_{ref2} \end{bmatrix} + \begin{bmatrix} 0 & 0 \\ 0 & 0 \\ 0 & 0 \end{bmatrix} \begin{bmatrix} x_b \\ \dot{x}_b \end{bmatrix} \tag{76}$$

For the Ideal groundyhook reference model (in Figure 16), the equation of motion is:

$$\begin{cases} m_{ref1}\ddot{x}_{ref1} + ks_{ref1}(x_{ref1} - x_{ref2}) = 0 \\ m_{ref2}\ddot{x}_{ref2} + c_g\dot{x}_{ref2} + ks_{ref1}(x_{ref2} - x_{ref1}) + ks_{ref2}(x_{ref2} - x_b) = 0 \end{cases} \tag{77}$$

And the state space equation is:

$$\dot{x} = \begin{bmatrix} \dot{x}_{ref1} \\ \dot{x}_{ref2} \\ \ddot{x}_{ref1} \\ \ddot{x}_{ref2} \end{bmatrix} = \begin{bmatrix} 0 & 0 & 1 & 0 \\ 0 & 0 & 0 & 1 \\ -\dfrac{ks_{ref1}}{m_{ref1}} & \dfrac{ks_{ref1}}{m_{ref1}} & 0 & 0 \\ \dfrac{ks_{ref1}}{m_{ref2}} & -(\dfrac{ks_{ref1}+ks_{ref2}}{m_{ref2}}) & 0 & -\dfrac{c_g}{m_{ref2}} \end{bmatrix} \begin{bmatrix} x_{ref1} \\ x_{ref2} \\ \dot{x}_{ref1} \\ \dot{x}_{ref2} \end{bmatrix} + \begin{bmatrix} 0 & 0 \\ 0 & 0 \\ 0 & 0 \\ \dfrac{ks_{ref2}}{m_{ref2}} & 0 \end{bmatrix} \begin{bmatrix} x_b \\ \dot{x}_b \end{bmatrix}$$

$$y = \begin{bmatrix} x_{ref1} \\ \dot{x}_{ref1} \\ \ddot{x}_{ref1} \end{bmatrix} = \begin{bmatrix} 1 & 0 & 0 & 0 \\ 0 & 0 & 1 & 0 \\ -\dfrac{ks_{ref1}}{m_{ref1}} & \dfrac{ks_{ref1}}{m_{ref1}} & 0 & 0 \end{bmatrix} \begin{bmatrix} x_{ref1} \\ x_{ref2} \\ \dot{x}_{ref1} \\ \dot{x}_{ref2} \end{bmatrix} + \begin{bmatrix} 0 & 0 \\ 0 & 0 \\ 0 & 0 \end{bmatrix} \begin{bmatrix} x_b \\ \dot{x}_b \end{bmatrix} \tag{78}$$

For the Ideal hybrid reference model (in Figure 22), the equation of motion is:

$$\begin{cases} m_{ref1}\ddot{x}_{ref1} + \alpha c_s \dot{x}_{ref1} + ks_{ref1}(x_{ref1} - x_{ref2}) = 0 \\ m_{ref2}\ddot{x}_{ref2} + (1-\alpha)c_g \dot{x}_{ref2} + ks_{ref1}(x_{ref2} - x_{ref1}) + ks_{ref2}(x_{ref2} - x_b) = 0 \end{cases} \tag{79}$$

And the state space equation is:

$$\dot{x} = \begin{bmatrix} \dot{x}_{ref1} \\ \dot{x}_{ref2} \\ \ddot{x}_{ref1} \\ \ddot{x}_{ref2} \end{bmatrix} = \begin{bmatrix} 0 & 0 & 1 & 0 \\ 0 & 0 & 0 & 1 \\ -\frac{ks_{ref1}}{m_{ref1}} & \frac{ks_{ref1}}{m_{ref1}} & -\frac{\alpha c_s}{m_{ref1}} & 0 \\ \frac{ks_{ref1}}{m_{ref2}} & -(\frac{ks_{ref1}+ks_{ref2}}{m_{ref2}}) & 0 & -\frac{(1-\alpha)c_g}{m_{ref2}} \end{bmatrix} \begin{bmatrix} x_{ref1} \\ x_{ref2} \\ \dot{x}_{ref1} \\ \dot{x}_{ref2} \end{bmatrix} + \begin{bmatrix} 0 & 0 \\ 0 & 0 \\ 0 & 0 \\ \frac{ks_{ref2}}{m_{ref2}} & 0 \end{bmatrix} \begin{bmatrix} x_b \\ \dot{x}_b \end{bmatrix} \tag{80}$$

$$y = \begin{bmatrix} x_{ref1} \\ \dot{x}_{ref1} \\ \ddot{x}_{ref1} \end{bmatrix} = \begin{bmatrix} 1 & 0 & 0 & 0 \\ 0 & 0 & 1 & 0 \\ -\frac{ks_{ref1}}{m_{ref1}} & \frac{ks_{ref1}}{m_{ref1}} & -\frac{\alpha c_s}{m_{ref1}} & 0 \end{bmatrix} \begin{bmatrix} x_{ref1} \\ x_{ref2} \\ \dot{x}_{ref1} \\ \dot{x}_{ref2} \end{bmatrix} + \begin{bmatrix} 0 & 0 \\ 0 & 0 \\ 0 & 0 \end{bmatrix} \begin{bmatrix} x_b \\ \dot{x}_b \end{bmatrix}$$

3.3.1.2 Sliding mode control algorithm

The sliding mode controller is designed to force the sprung mass motion of the system to track the sprung mass motion of the reference model. With the same road disturbance x_b, the responses of the reference model (x_{ref}, $\dot{x}_{ref}$ and $\ddot{x}_{ref}$) can be transferred to the sliding mode surface such that:

The sliding surface is defined as:

$$S = \dot{e} + \lambda e \tag{81}$$

where $e = x_1 - x_{ref1}$ and $\dot{e} = \dot{x}_1 - \dot{x}_{ref1}$

The sliding condition must be defined to ensure that the state will move toward and reach the sliding surface. The proposed sliding condition is

$$\frac{1}{2}\frac{d}{dt}S^2 \le -\varphi|S| \Rightarrow S\dot{S} \le -\varphi|S| \tag{82}$$

where φ is a positive constant.

From system model equations (64) and reference model equations (75,77 or 79),

$$\begin{aligned}\dot{S} &= \ddot{e} + \lambda\dot{e} \\ &= -\frac{k_1}{m_1}(x_1 - x_2) - \frac{f_d}{m_1} - \ddot{x}_{ref1} + \lambda\dot{e}\end{aligned} \tag{83}$$

The best approximation for the f_c, a control law should achieve $\dot{S} = 0$, thus

$$f_{d0} = m_0\left(-\frac{k_1}{m_0}(x_1 - x_2) - \ddot{x}_{ref1} + \lambda\dot{e}\right) \tag{84}$$

In order to satisfy sliding condition despite mass uncertainty, a term discontinuous across the surface is added to the f_{d0}. The desired control force f_c can be expressed as

$$f_c = f_{d0} - K\,\mathrm{sgn}(S) \tag{85}$$

where sgn is the sign function.

To avoid the chattering problem in the sliding surface, a saturation function could be applied on the equation (85). Then the equation (86) becomes

$$f_c = \begin{cases} f_{d0} - KS & \text{if } |S| < \Phi \\ f_{d0} - K\,\mathrm{sgn}(S) & \text{if } |S| > \Phi \end{cases} \tag{86}$$

where Φ is chosen to be 1.

Now, the switching gain K can be determined. Equation (83) can be interpreted as

$$\begin{cases} \dot{S} \le -\varphi & \text{when } S > 0 \\ \dot{S} > \varphi & \text{when } S < 0 \end{cases} \tag{87}$$

When $S > 0$, $\dot{S} \le -\varphi$ so the equation (86) becomes

$$\begin{cases} K' \ge \frac{1}{S}[(1-\frac{m_1}{m_0})(\ddot{x}_{ref1} - \lambda\dot{e}) + \frac{m_1}{m_0}\varphi] & \text{if } |S| < \Phi \\ K' \ge [(1-\frac{m_1}{m_0})(\ddot{x}_{ref1} - \lambda\dot{e}) + \frac{m_1}{m_0}\varphi] & \text{if } |S| > \Phi \end{cases} \tag{88}$$

where $K' = -\frac{K}{m_0}$

Similarly, when $S < 0$, $\dot{S} > \varphi$

$$\begin{cases} K' > \frac{1}{S}[(1-\frac{m_1}{m_0})(\ddot{x}_{ref1} - \lambda\dot{e}) - \frac{m_1}{m_0}\varphi] & \text{if } |S| < \Phi \\ K' > -[(1-\frac{m_1}{m_0})(\ddot{x}_{ref1} - \lambda\dot{e}) - \frac{m_1}{m_0}\varphi] & \text{if } |S| > \Phi \end{cases} \tag{89}$$

Combining two cases from Equations (88) and (89),

$$K' \geq \left| \left(1 - \frac{m_1}{m_0} \right) \left(\ddot{x}_{ref1} - \lambda \dot{e} \right) \right| + \frac{m_1}{m_0} \varphi$$

$$= \left| 1 - \frac{m_1}{m_0} \right| \left| \ddot{x}_{ref1} - \lambda \dot{e} \right| + \frac{m_1}{m_0} \varphi$$

$$\Rightarrow K' \geq (\beta - 1) \left| -\frac{f_{d0}}{m_0} - \frac{k_1}{m_0} x_1 + \frac{k_1}{m_0} x_2 \right| + \beta \varphi \tag{90}$$

In the simulation, K' should be bounded by Equation (74) so it can be chosen to be:

$$K' = (\beta - 1) \left[\frac{1}{m_0} |f_{d0}| + \frac{k_1}{m_0} |x_1| + \frac{k_1}{m_0} |x_2| \right] + \beta \varphi \tag{91}$$

Based on the above control algorithm, the desired control force f_c can be calculated. Figure 42 shows the algorithm of the sliding mode controller of the automotive suspension system.

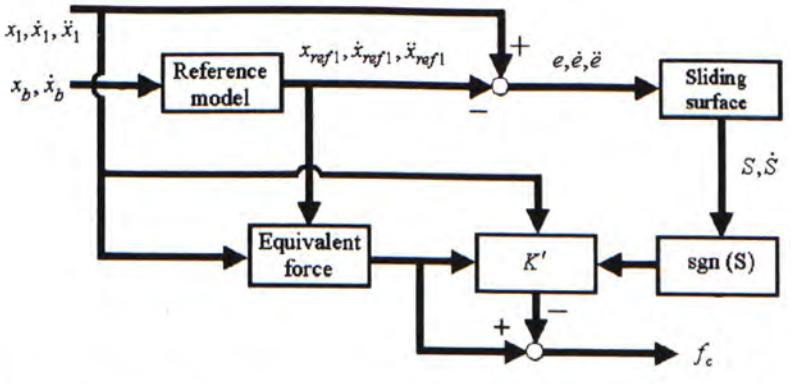

Figure 42 : Sliding mode control algorithm for automotive suspension system

3.3.2 *Damper Controller: Continuous-state Control*

Using the above controller, the desired control force can be found out. However, MR damper is a semi-active device so it cannot generate arbitrary force like an active actuator. The damping force of the MR damper depends on the relative displacement and velocity at the point of the attachment. Therefore, it is necessary to "turn off" the damper when the desired force is to add energy to the system. The damping force of the MR damper cannot be commanded directly even the desired force is dissipating energy. The MR damper needs to be controlled by input voltage command signal. This section will introduce a damper controller called continuous-state control, which is used to find the suitable input voltage command to the MR damper such that the damping force of the MR damper can achieve the desired control force.

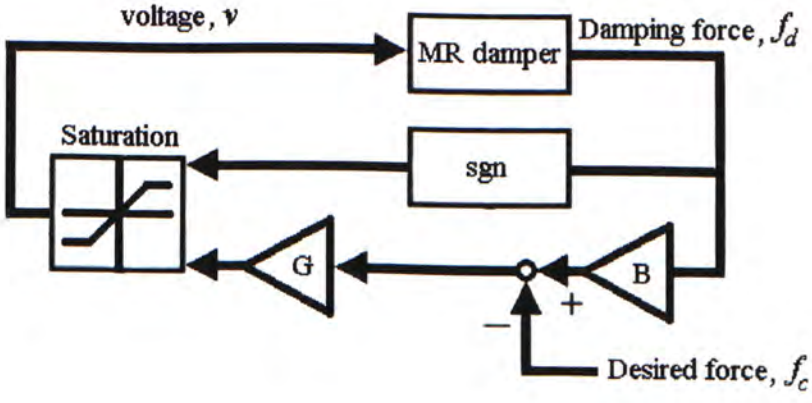

Figure 43 : Block diagram of continuous-state control

For the continuous-state control algorithm, it was a feedback control strategy that can linerize the response of the MR damper [35]. The block diagram has been shown in Figure 43. The damping force of MR damper is fed back with a feedback gain B and compared to the desired force. The resultant error is scaled by a gain G. To ensure the damper cannot generate energy to the system, the controller function is enabled only when the direction of damping force and the error having the same direction. Thus, it is necessary to have the sign correction. If they have different sign, the input voltage needs to set to be zero. The suitable control signal is then varied between the maximum and minimum voltages. The continuous-state algorithm for selecting the input voltage can be stated as

$$\begin{aligned} &\text{if} \quad G(f_c - Bf_d)\text{sgn}(f_d) > V_{\max} \\ &\qquad v = V_{\max} \\ &\text{elseif} \quad G(f_c - Bf_d)\text{sgn}(f_d) < V_{\min} \\ &\qquad v = V_{\min} \\ &\text{else} \\ &\qquad v = G(f_c - Bf_d)\text{sgn}(f_d) \end{aligned} \tag{92}$$

where V_{max} is the maximum voltage to the MR damper

V_{min} is the minimum voltage to the MR damper (i.e. 0 volt)

f_c is the desired control force calculated by the system controller

f_d is the damping force of the MR damper

G is the scaling factor

B is the feedback gain

Chapter 4

SIMULATION RESULTS

To evaluate the performance of the suspension system, the displacement and acceleration of the car body are considered. In this simulation, the sliding mode controller with continuous state damper control is used to control the suspension system. The values of G and B for the damper controller are determined by a trial-and-error method. The simulation parameters of the suspension system and the reference models used in this study are summarized in Table 10. In this study, the mass uncertainty (20% of the original sprung mass) Δm_1 = 90.9 kg is used. Note that the parameters of the quarter model refer to [42].

Table 10 : Simulation Parameters

Parameter	Value
Nominal sprung mass of quarter car (m_0)	454.5 kg
Mass uncertainty (Δm_1)	90.9 kg
Sprung mass of quarter car (m_1)	545.4 kg
Unsprung mass of quarter car (m_2)	45.45 kg
Spring constant of suspension system (k_1)	22000 N/m
Spring constant of tire (k_2)	176000 N/m
Damping coefficient of tire (c_2)	~0 N-s/m
Reference sprung mass (m_{ref1})	454.5 kg
Reference unsprung mass (m_{ref2})	45.45 kg
Spring constant of reference system (k_{ref1})	22000 N/m
Spring constant of reference tire (k_{ref2})	176000 N/m
Skyhook damping coefficient (c_s)	126480 N-s/m
Groundhook damping coefficient (c_g)	126480 N-s/m
Hybrid damping coefficient (c_h)	126480 N-s/m
Hybrid gain (α)	0.5
Reference damping coefficients (c_{ref1} and c_{ref2})	(for both) 0 N-s/m
Sliding mode control gain, (β)	1.25
Sliding mode control gain, (Φ)	1
Sliding mode control gain, (φ)	1
Damper control gain, (G)	0.0038
Damper control gain, (B)	1

All the simulation results include the passive cases (passive off: 0 V and passive on: 2 V) and controlled cases (sliding mode controller with skyhook, groundhook and hybrid reference models). In this section, it includes two parts. The first part is the transmissibility analysis. By using sinusoidal excitation with different frequencies, it can be measured the peak-to-peak values to get the input-output ratios. The second part is three simulation tests. There are three different excitations, which are bump excitation, random excitation (white noise) and road elevation profile. Based on these three tests, the performance of the controlled suspension system can be evaluated.

4.1 Transmissibility analysis

The characteristics of the two-degree-of-freedom MR suspension system are evaluated through transmissibility analysis. By applying sinusoidal excitation to the suspension system with different frequencies, the peak-to-peak value of both displacement and acceleration are measured such that the transmissibilities can be obtained. Figure 44 and Figure 45 show the displacement and acceleration transmissibilities of the sprung mass of the suspension system for 0 V input voltage, 2 V input voltage and controllers with skyhook, groundhook and hybrid reference models. The frequency range is from 0.2 Hz to 12 Hz. The displacement transmissibility is the ratio of the peak-to-peak values of sprung mass displacement and peak-to-peak values of sinusoidal excitation. The acceleration transmissibility is the ratio of the peak-to-peak values of sprung mass acceleration and the peak-to-peak values of sinusoidal excitation. The figures of the transmissibilities of unsprung mass will be shown in appendix A.1.

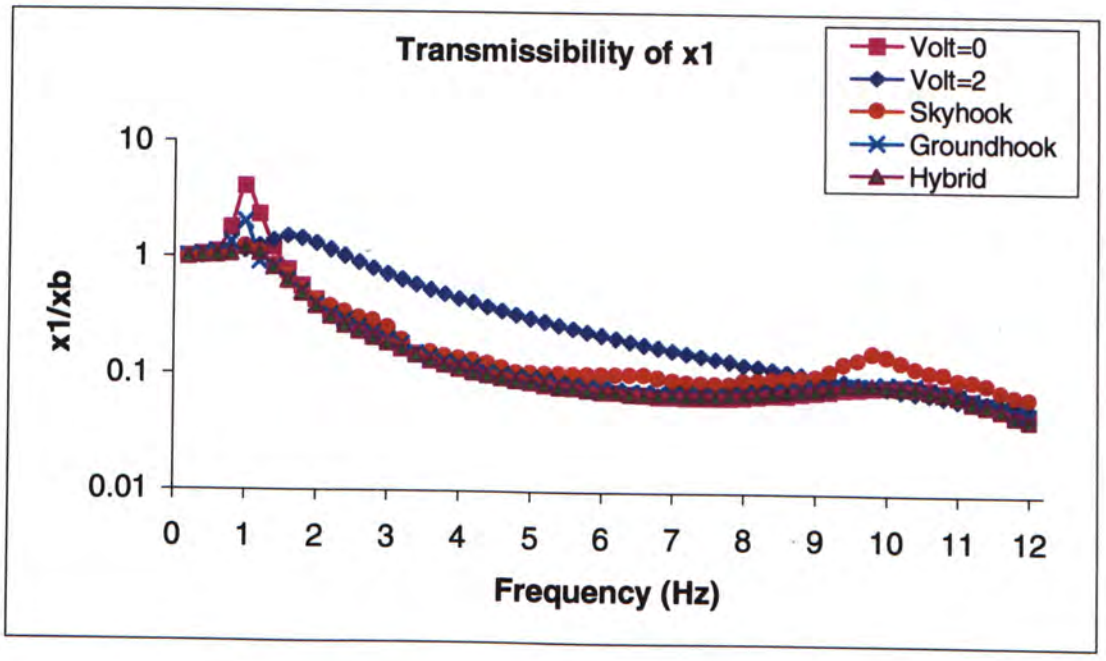

Figure 44: Displacement transmissibility of the sprung mass

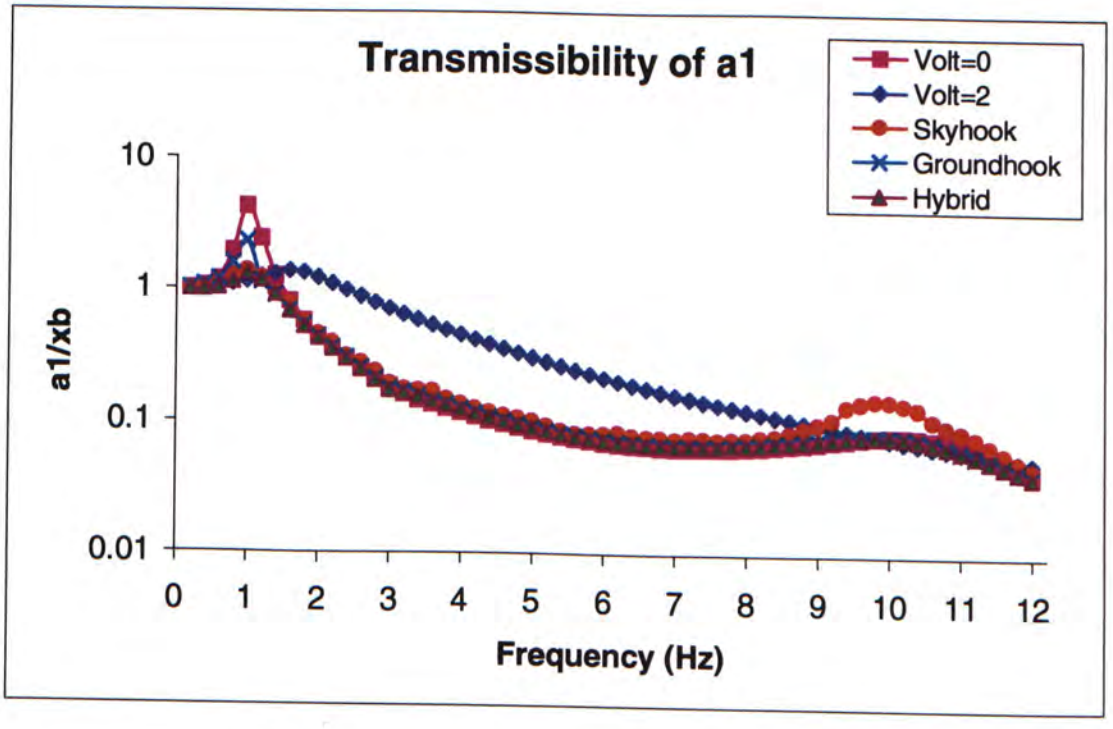

Figure 45 : Acceleration transmissibility of the sprung mass

For 0 V case, the frequencies of the peak amplitudes are 1 Hz and 9.8 Hz. It should be noted that the first peak frequency shifts to 1.8 Hz and the second peak frequency disappeared for 2 V input voltage. This is due to the change in system stiffness while applying constant voltage to the MR damper. The system changed from underdamped case to overdamped case. Moreover, the system with groundhook reference model controller has the peak amplitude at the frequency 1 Hz but the system with skyhook reference model controller has the peak amplitude at the frequency 9.8 Hz. For systems with hybrid reference model controller, there are no obvious peaks along the whole frequency range. It is because hybrid system has good vibration isolation performance around the resonance frequencies. Observing the figures, the displacement and acceleration transmissibilities of controlled systems with sliding mode controllers (included three different reference models) are always lower than those of the 0 V case within the frequency range. These results show that the controlled MR suspension systems can significantly reduce the vibration around the resonance corresponding to the sprung mass. Compared to the 2 V case, the displacement and acceleration transmissibilities of the system controllers with skyhook and groundhook reference model are higher around their resonances because the natural frequencies have been changed for the 2 V case. However, except the resonance frequencies, the transmissibilities of the system with constant 2 V are significantly higher than other systmes. Along the whole frequency range, the transmissibilities of the system with hybrid reference models are always the lowest comparing to the other four systems. According to the section 2.1, the hybrid system has a good performance for vibration suppression along whole frequency range.

4.2 Simulation

The performances of the suspension system under bump excitation, random excitation and road elevation profile are evaluated through computer simulation. The responses of the bump excitation will be shown in time domain from 0 second to 5 second. And also, the responses of the random excitation will be used the power spectral density to analysis (frequency domain). The root mean square values of each response will be calculated and then compare to the passive case (voltage = 0 V). In addition, the responses of the road elevation profile will also be shown in time domain. By calculating the root mean square value, the performances of controlled suspension systems can be evaluated.

4.2.1 Test by Bump Excitation

The bump input with amplitude 0.01m is shown in the Figure 46. For bump excitation, the time range of all responses is 0 second to 5 second.

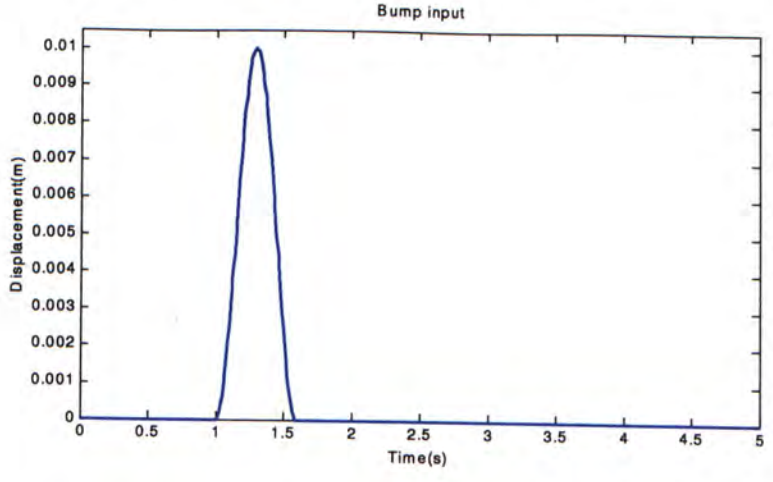

Figure 46 : Bump input

The responses of the suspension system due to the bump excitation are shown in the Figure 47. By comparing the controlled systems (including the controller with skyhook, groundhook and hybrid reference model) to the passive systems (0 V and 2 V), it can be seen that the displacement is reduced. In addition, the acceleration decays with faster time. Moreover, the rise times are slower and the settling times are faster comparing to the passive systems. With better performance in acceleration reduction, the controlled voltage applied to MR damper is less than 1.5 V. That means the power consumption of the controlled systems are much less than constant 2 V input. Although the performance of three controlled systems for bump excitation are similar, the hybrid case for voltage input is much more appropriate.

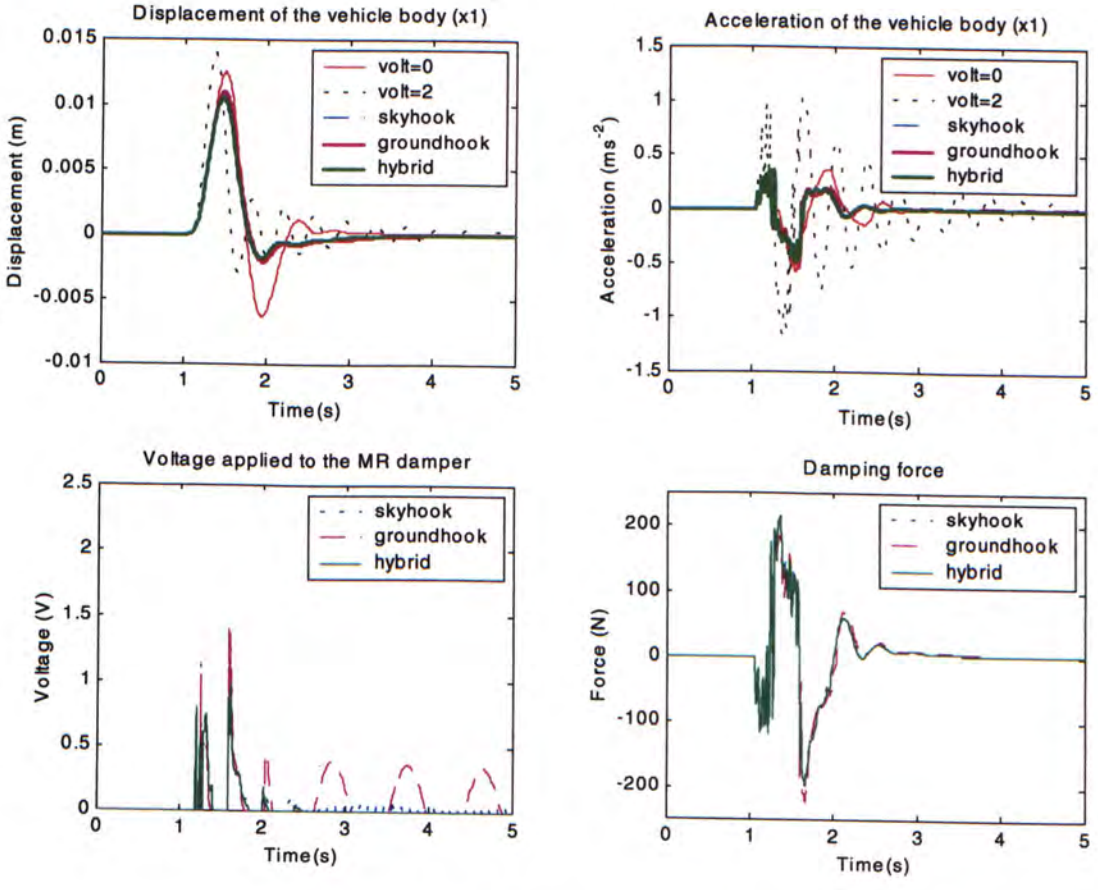

Figure 47 : Responses of bump excitation

4.2.2 Test by Random Excitation (White noise)

The white noise (zero mean) is chosen as the random excitation to the suspension systems, which is shown in the Figure 48. For this random excitation test, the time range is from 0 second to 40 second. In order to have a clear view, all the figures for time domain in this section will be shown by selecting first 5 seconds.

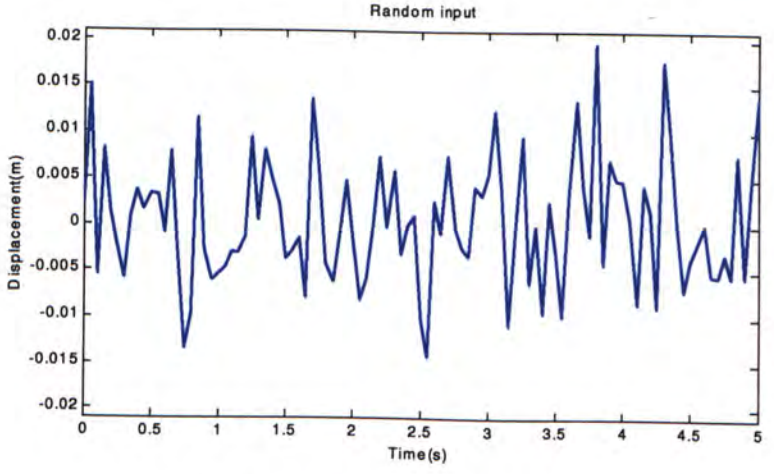

Figure 48 : Random input

The responses of the random excitation are shown in the following figures. For the both displacement and acceleration of the sprung mass will be used the power spectral density to analysis in frequency domain. Figure 49 shows the power spectral density of the sprung mass displacement. Figure 50 shows the power spectral density of the sprung mass acceleration. Figure 51 shows the voltage input of the controlled systems.

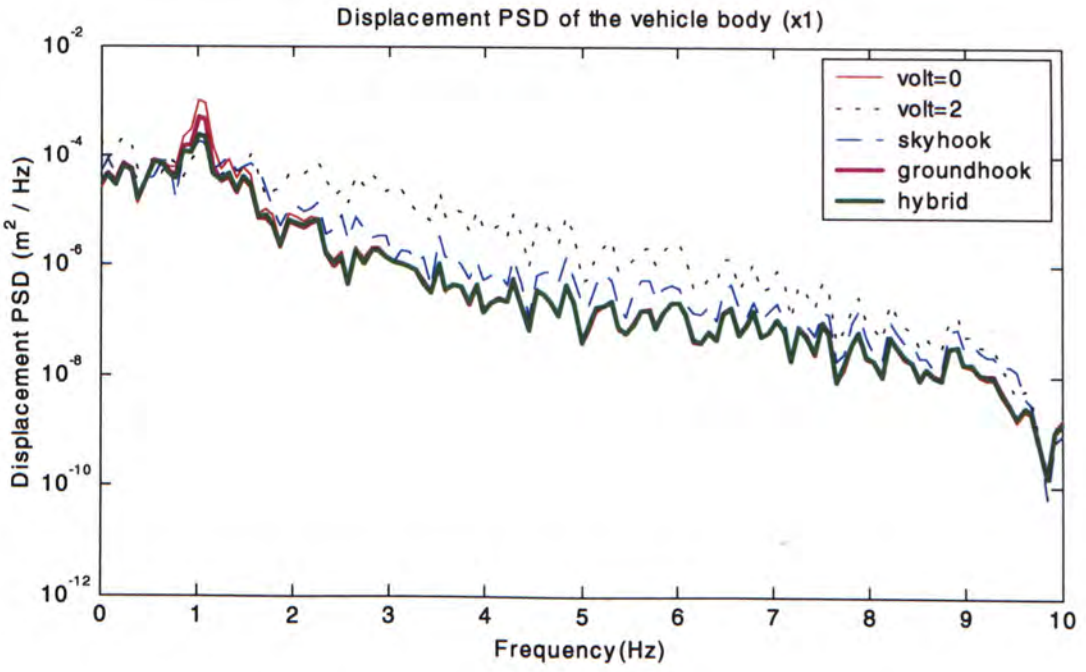

Figure 49 : Displacement PSD of the sprung mass

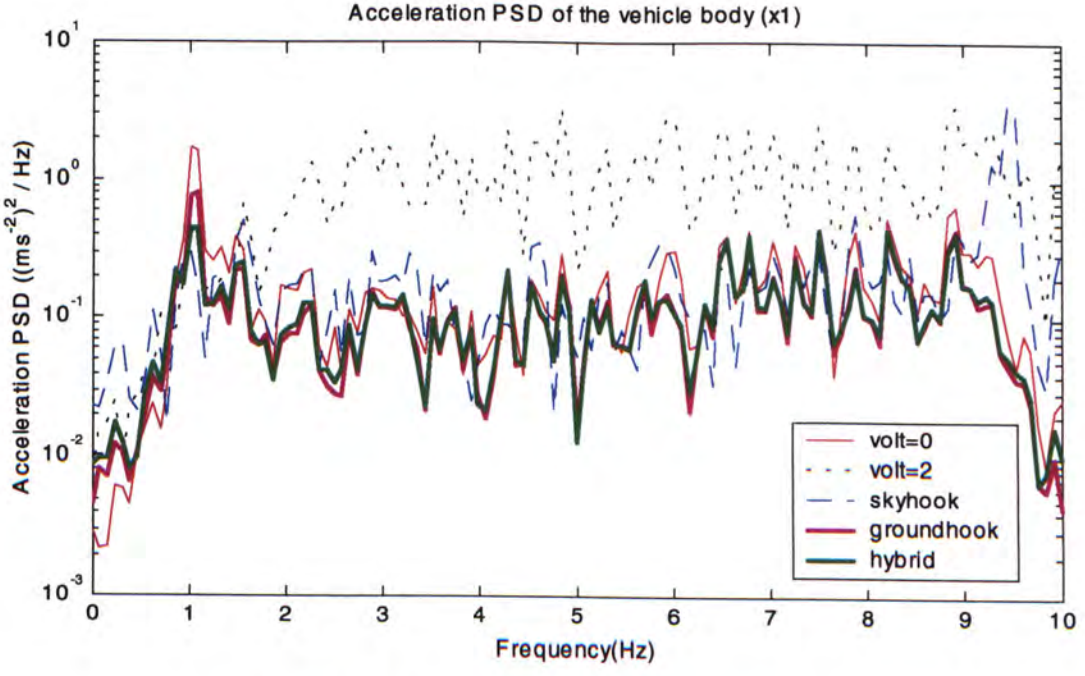

Figure 50 : Acceleration PSD of the sprung mass

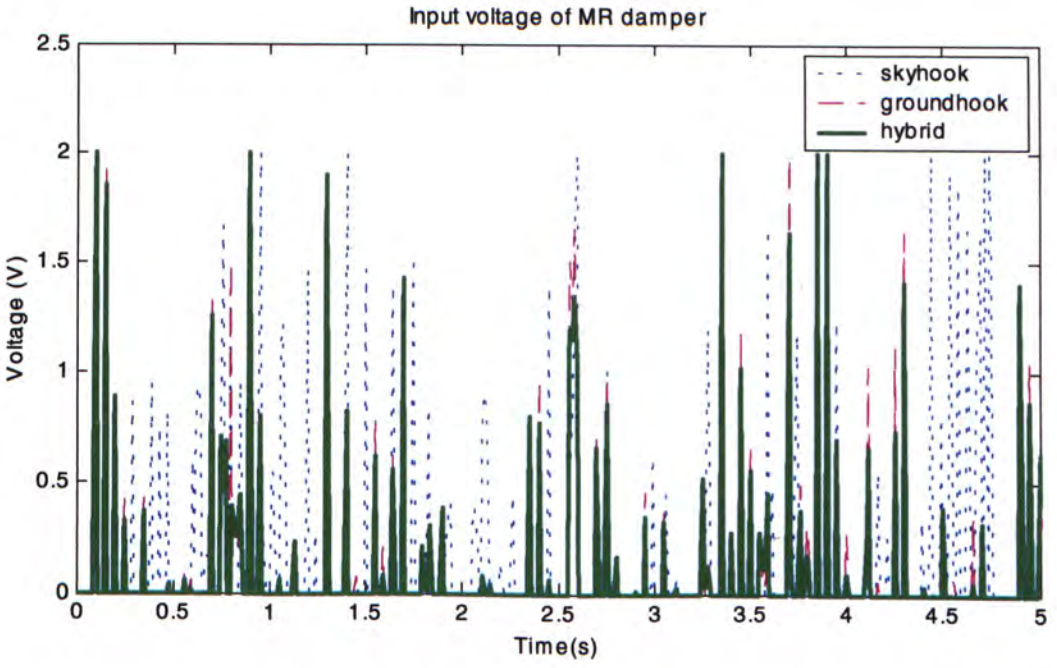

Figure 51 : Voltage inputs of controlled systems

Above figures are shown the frequency responses of the suspension systems under the random excitation. In Figure 49 and Figure 50, the displacement and acceleration are reduced for the frequency range from 0 to 10 Hz for three controlled systems when comparing to the 0 V and 2 V cases. Around the frequency at 1 Hz, there is a peak for both displacement and acceleration. The groundhook case is much higher than the skyhook and hybrid case at that frequency (1 Hz). This results matched to the section 2.1 and section 4.1. The transmissibility level of the groundhook system around the natural frequency is much higher than the skyhook system and hybrid system around the first natural frequency. The Figure 51 shows the input voltage of the controlled MR suspension systems. It shows that the groundhook and hybrid cases have lower voltage level. Therefore, the hybrid system has less power consumption for provide good vibration isolation.

To quantify the system performance under the random excitation, the root-mean-square (RMS) values of the responses are shown in Table 11. It is shown again that the displacement and acceleration of the sprung mass can be reduced effectively by using the controlled MR damper. For the sprung mass with uncertainty, the sprung mass displacement of the controlled systems (for skyhook, groundhook and hybrid reference models) comparing to 0 V case are improved by 22%, 24% and 31% respectively. However, for acceleration, only groundhook and hybrid cases have improvement because there is peak amplitude around the frequency 8.9 Hz for skyhook case. The improvements of the groundhook and hybrid cases are both 19%. In addition, the power consumptions of the groundhook and hybrid cases are both 94.5% less than that of the system with constant 2 V input voltage. As a result, comparing the performance of displacement, acceleration and power consumption of three controlled systems, the systems with sliding model controller using hybrid reference model is the most effective in suppressing vibration under random excitation.

Table 11 : Comparisons of 0V, 2V and controlled cases under random excitation

	RMS values of displacement (m)	RMS values of acceleration (ms^{-2})	Average input voltage (V)	Average power consumption (W)
0 volt	0.0051	0.4437	0	0
2 volt	0.0049	1.0628	2	0.8
Skyhook	0.004	0.4833	0.9580	0.4589
Groundhook	0.0039	0.3610	0.2945	0.0434
Hybrid	0.0035	0.3610	0.2960	0.0438

4.2.3 Test by Road Elevation Profile

The road elevation profile is provided by [42], which is shown in the Figure 52. Originally, the road elevation profile is implemented by that the car is across 100m with the speed 80km/h. In this study, the road elevation profile is described in time domain from 0 second to 4.5 second. Based on this road elevation profile, the MR suspension systems can be evaluated by the realistic excitation.

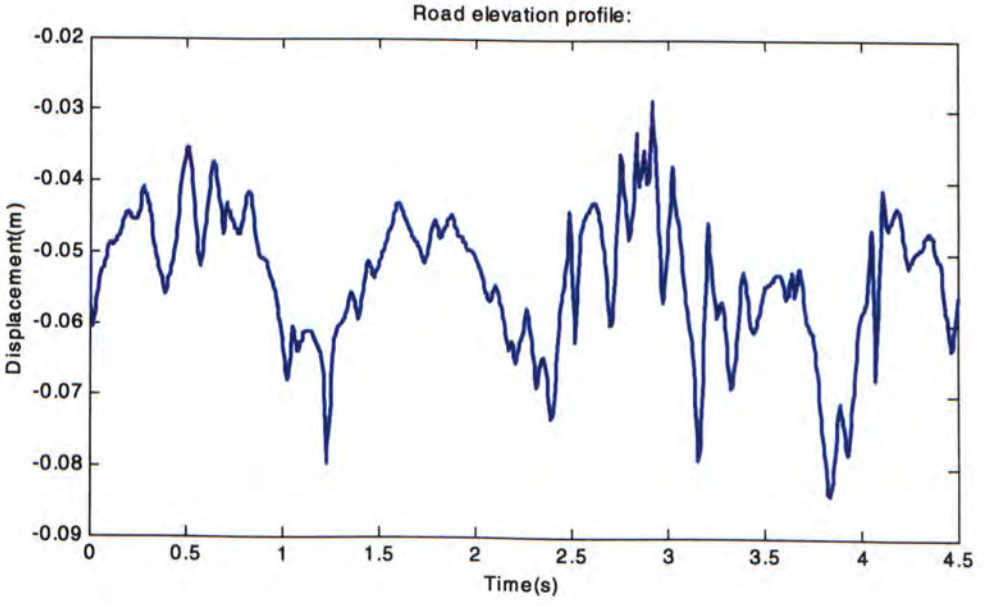

Figure 52 : Road elevation profile

The responses of the road elevation profile are shown in the following figures. For the both displacement and acceleration of the sprung mass will be shown in Figure 53 and Figure 54 in time domain (from 0 second to 4.5 second with sampling time 0.005 second). Figure 55 shows voltage input of the controlled systems.

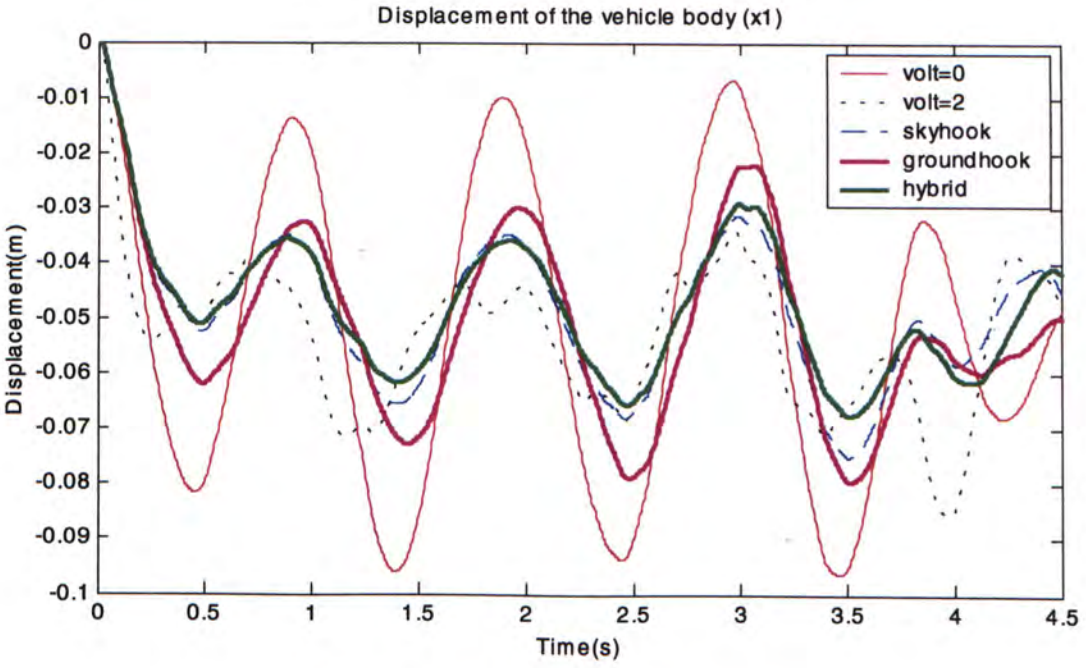

Figure 53 : Displacement of the sprung mass

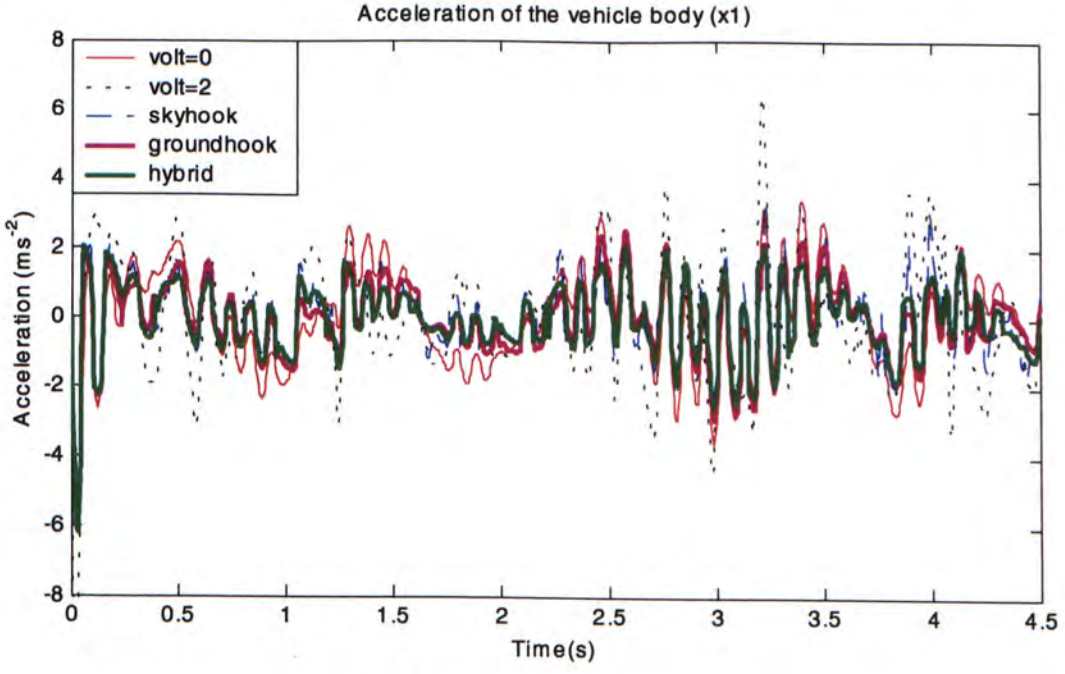

Figure 54 : Acceleration of the sprung mass

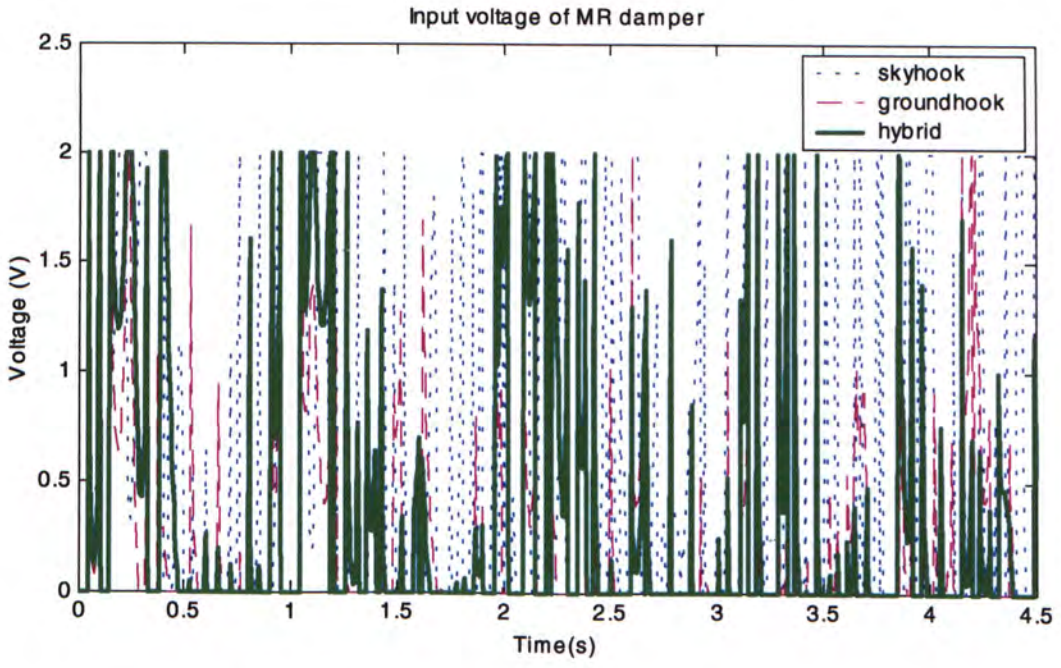

Figure 55 : Voltage input of the controlled systems

In Figure 53 and Figure 54, the displacement and acceleration of three controlled systems are reduced when comparing to the 0 V and 2 V cases. For comparing the three controlled systems, the hybrid system has the most significant improvement for the vibration reduction. To quantify the system performances, the root-mean-square (RMS) values of the responses are shown in Table 12. The sprung mass displacement of the controlled systems with the sliding mode controller with skyhook, groundhook and hybrid reference models comparing to 0 V case are improved by 14%, 9% and 16% respectively. And also, the sprung mass acceleration of the controlled systems comparing to 0 V case are improved by 20%, 22% and 26% respectively. In addition, the power consumptions of the controlled systems are 51.85%, 85.95% and 70.91% less than that of the system with constant 2 V input voltage respectively.

Table 12 : Comparisons of 0V, 2V and controlled cases under road profile

	RMS values of displacement (m)	RMS values of acceleration (ms^{-2})	Average input voltage (V)	Average power consumption (W)
0 volt	0.0590	1.4423	0	0
2 volt	0.0548	1.9001	2	0.8
Skyhook	0.0506	1.1559	0.8777	0.3852
Groundhook	0.0539	1.1230	0.4742	0.1124
Hybrid	0.0495	1.0663	0.6823	0.2327

As a result, comparing the performance of displacement, acceleration and power consumption of three controlled systems among the bump excitation test, random excitation test and the road elevation profile test, the system with sliding model controller using hybrid reference model is the most effective in suppressing vibration under random excitation.

Chapter 5

CONCLUSIONS AND FUTURE WORK

5.1 Summary

A quarter car model with passive, skyhook, groundhook and hybrid systems has been proposed and the characteristics of each system have been investigated. Based on this analysis, it has been shown that the Ideal hybrid system has the optimal performance for vibration suppression of the car suspension system. The stability of the passive suspension system and three semi-active suspension systems have been discussed. The optimal hybrid gain of the hybrid system has also been found.

The 2DoF quarter car model is considered and the Bouc-Wen model for MR damper is adopted. For vibration control of the car suspension system, sliding mode controller has been used as the system controller in order to handle the mass uncertainty. The three Ideal semi-active systems are chosen to be the reference models. The sliding mode control algorithms with these three semi-active reference models have been developed. On the other hand, the continuous-state damper controller has been designed to adjust the appropriate input voltage to the MR damper.

The transmissibilities of the MR suspension systems have been investigated. Moreover, the performances of the car suspension systems under three road excitations have been evaluated through computer simulation. Under the bump excitation, the displacement of the vehicle body has been reduced and the settling time is faster comparing to the passive system (0 V case). Under the random excitation, the suspension systems with the controlled MR damper can significantly reduce the root-mean-square values of both acceleration and displacement, as compared to the passive system. It should be noted that the power consumption for the controlled MR damper is much less than that of the system with constant voltage. For the road elevation profile, the controlled suspension systems can improve both displacement and acceleration of the sprung mass with a little power consumption. These results again show that the controlled MR suspension system can improve the ride comfort quite effectively.

5.2 Future Work and Further Development

5.2.1 Parametric study of the MR suspension system

The parametric study of the semi-active systems has been performed in this thesis. However, the characteristics of the parameters between the suspension systems and the MR damper can be another issue of interest. If the relationship between the system and the MR damper can be known, it would be valuable for designing an effective controller. However, there are fourteen parameters in the MR damper model and five parameters for the suspension system, the relationship between those

parameters could be very complicated. Another future work is to develop a simpler mathematical model for the MR damper with less number of parameters but better accuracy. Then it could be easier to study the parametric relationship for the MR suspension system. On the other hand, characteristics of the MR suspension system can be affected by the location of the MR damper. In this study, the MR damper is installed between the sprung and unsprung masses for the automotive suspension system. However, the MR damper could be installed between the base of the system and the unsprung mass such as a seat suspension system. To find the influence of the position of the MR damper to the suspension system is another valuable task for future development.

5.2.2 Systematic method for selecting control gains

In this study, the gains of the damper controller are determined by trial-and-error method. For different systems, it is time consuming for designing different controllers by using trial-and-error method. It would be better to find a systematic method to determine the damper controller gains.

5.2.3 New control algorithm

In order to handle the loading uncertainty, the sliding mode control is selected to be the system controller. However, there are other control methods that could be more effective to control the system. For different systems and working conditions, it could be desired to develop different system controllers for the MR suspension systems.

5.2.4 *Extension to half and full car models*

In this study, the 2DoF quarter car model is considered. It can be extended to more general systems such as half and full car models. These systems will include more degrees of freedom such as pitch and roll motions. By doing that the handling performance of the car can also be investigated. Since the 2DoF quarter car model can only consider vertical motion, the handling problem involving other motions cannot be studied. For the half and full car systems, the design of the controller should balance the trade-off if any between the effectiveness of vibration suppression and the handling performance.

5.2.5 *System implementation*

Besides the analysis and simulation, it is valuable to implement the closed-loop systems. It has been shown that the effectiveness of the MR suspension system with SDoF skyhook reference model for a sliding mode controller is demonstrated via Hardware-In-the-Loop Simulation (HILS) [40]. For future development, the MR suspension systems with different reference models (skyhook, groundhook and hybrid reference models) can also be validated by HILS. The overall controlled suspension systems with MR dampers could also be implemented if corresponding facilities are available.

APPENDIX

A.1 Additional information of the transmissibility of unsprung mass

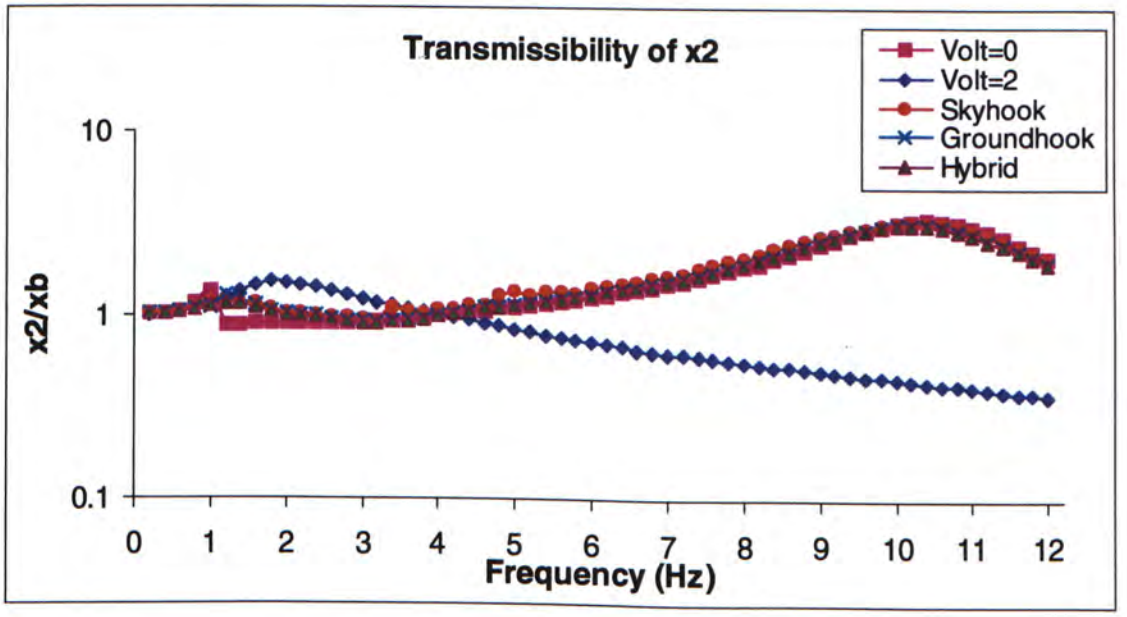

Figure 56 : Displacement transmissibility of unsprung mass

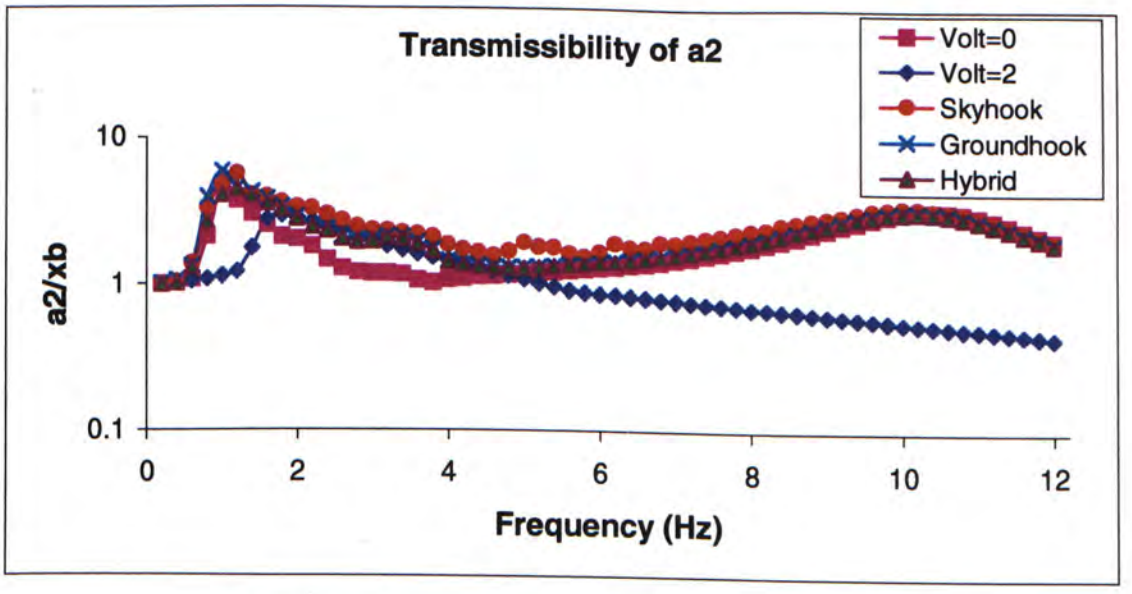

Figure 57 : Acceleration transmissibility of unsprung mass

A.2 Additional figures of the random excitation test:

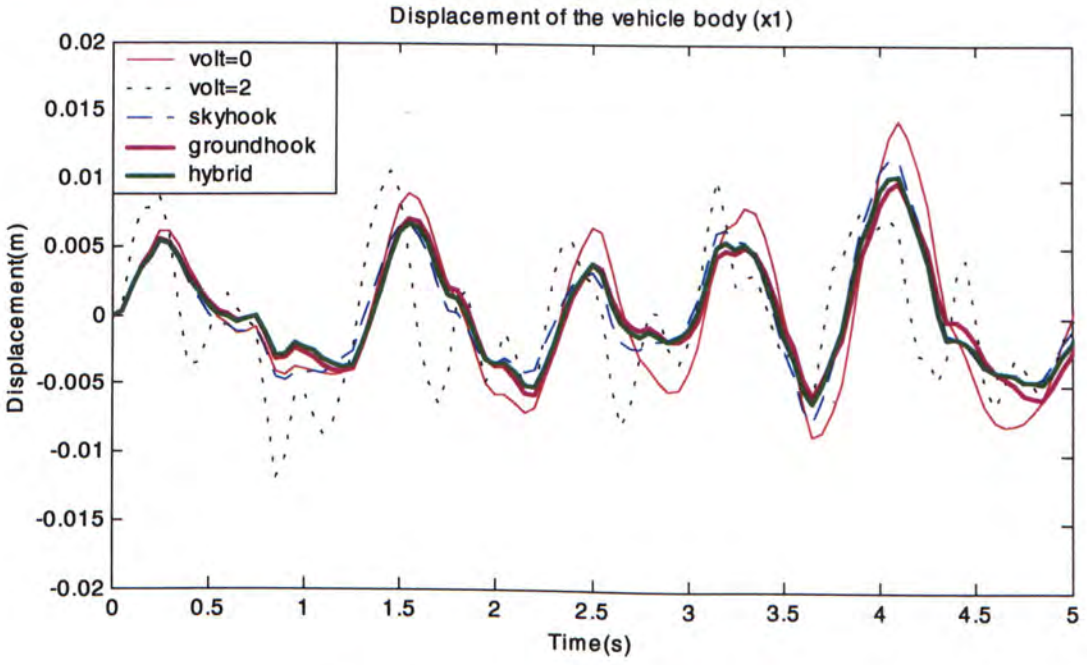

Figure 58 : Displacement of the sprung mass

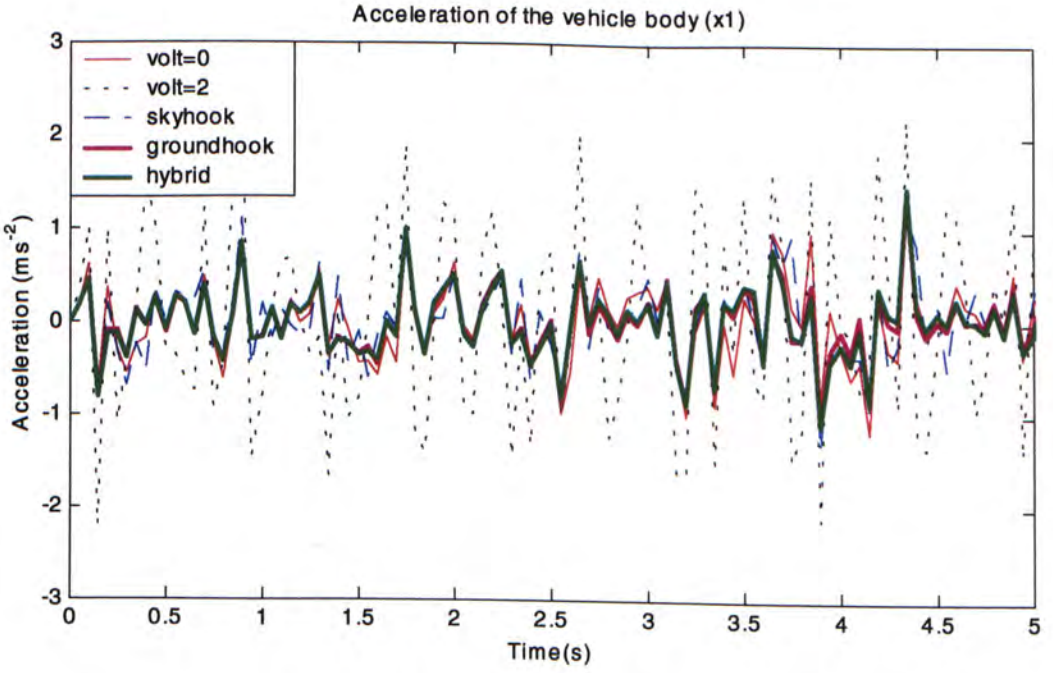

Figure 59 : Acceleration of the sprung mass

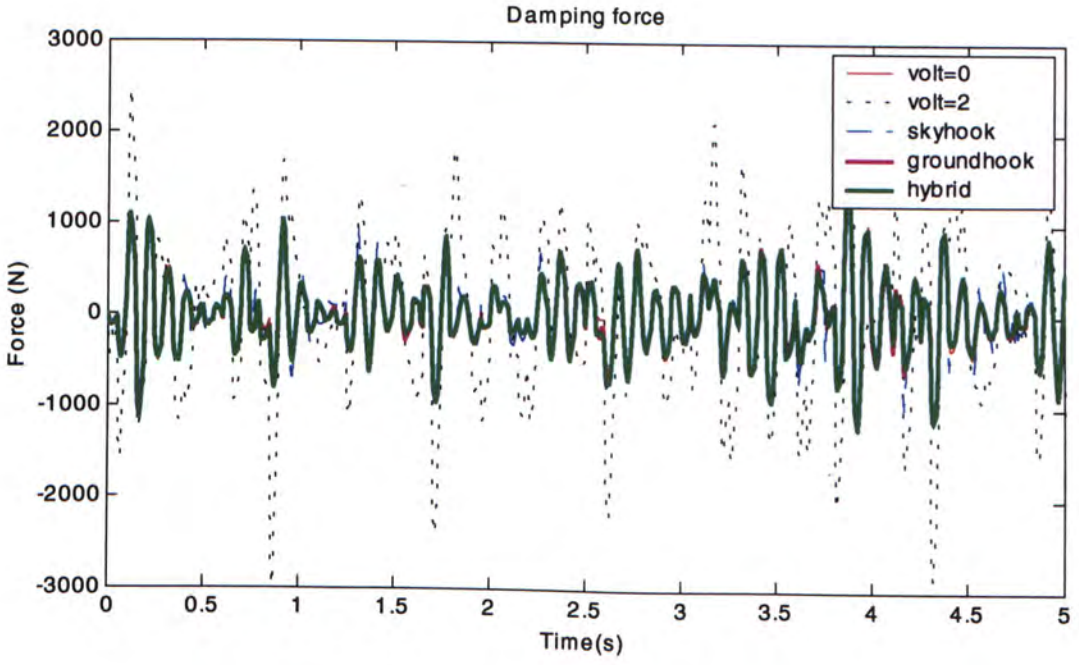

Figure 60 : Damping force of the MR damper

BIBLIOGRAPHY

[1] R. A. Williams, "Automotive active suspensions Part I: basic principles," *Proceedings of the Institution of Mechanical Engineers Part D, Journal of Automobile Engineering*, Vol. 211, pp. 415-426, 1997.

[2] R. A. Williams, "Automotive active suspensions Part II: practical considerations," *Proceedings of the Institution of Mechanical Engineers Part D, Journal of Automobile Engineering*, Vol. 211, pp. 427-444, 1997.

[3] J. S. Lin and I Kanellakopoulos, "Nonlinear design of active suspensions," *Proceedings of 34th IEEE Conference on Decision and Control*, pp. 45-58, 1997.

[4] S. Ikenaga, F. L. Lewis, L. Davis, J. Campos, M. Evans, and S. Scully, "Active suspension control using a novel strut and active filtered feedback: design and implementation," *Proceedings of the 1999 IEEE International Conference on Control Applications*, pp. 1502-1508, 1999.

[5] M. Satoh, N. Fukushima, Y. Akatsu, I. Fujimura, and K. Fukuyama, "An active suspension employing an electrohydraulic pressure control system," *Proceedings of the 29th IEEE Conference on Decision and Control*, Vol. 4, pp. 2226-2231, 1990.

[6] H. D. Taghirad and E. Esmailzadeh, "Automobile passenger comfort assured through LQG/LQR active suspension," *Journal of Vibration and Control*, Vol. 4, pp. 603-618, 1998.

[7] J. J. Kok, J. G. A. M. van Heck, R. G. M. Huisman, J. H. E. A. Muijderman, and F. E. Veldpaus, "Active and semi-active control of suspension systems for commercial vehicles based on preview," *Proceedings of the American Control Conference*, pp. 2992-2996, 1997.

[8] J. Lieh, "Semiactive and active suspensions for vehicle ride control using velocity feedback," *Journal of Vibration and Control*, Vol. 3, pp. 201-212, 1997.

[9] L. R. Miller, "Tuning passive, semi-active, and fully-active suspension systems", *Proceedings of the 27th IEEE Conference on Decision and Control*, Vol. 3, pp. 2047-2053, 1988.

[10] A. H. Nizar, A. Bajwa, and D. S. Joo, "Computer controlled individual semi-active suspension system", *Proceedings of the 36th Midwest Symposium on Circuits and Systems*, Vol. 1, pp. 208-211, 1993.

[11] K. Yi and B. S. Song, "A new adaptive sky-hook control of vehicle semi-active suspensions," *Proceedings of the Institution of Mechanical Engineers*, Part D, Vol. 213, pp. 293-303, 1999.

[12] F. Sadek and B. Mohraz, "Semiactive control algorithms for structures with variable dampers", *Journal of Engineering Mechanics*, Vol. 124(9), pp. 981-990, Sept. 1998.

[13] T. J. Gordon and R. S. Sharp, "On improving the performance of automotive semi-active suspension systems through road preview," *Journal of Sound and Vibration*, Vol. 217(1), pp. 163-182, 1998.

[14] H. C. Sohn, K. S. Hong and J. K. Hedrick, "Semi-active control of the macpherson suspension system: hardware-in-the-loop simulations," *Proceedings of the 2000 IEEE International Conference on Control Applications*, pp.982-987, 2000.

[15] D. Cebon, F. H. Besinger, and D. J. Cole, "Control strategies for semiactive lorry suspensions", *Proceedings of the Institution of Mechanical Engineers*, Part D, Vol. 2(2), pp. 161-178, 1996.

[16] M. Ahmadian, "On the isolation properties of semiactive dampers," *Journal of Vibration and Control*, Vol. 5, pp. 217-232, 1999.

[17] M. Ahmadian, "Semiactive control of multiple degree of freedom systems," *Proceedings of 1997 ASME Design Engineering Technical Conferences*, DETC97/VIB-4123, pp. 1-10, 1997.

[18] N. Yagiz, V. Ozbulur, N. Inanc, and A. Derdiyok, "Sliding modes control of active suspensions", *Proceedings of the 12th IEEE International Symposium on Intelligent Control*, pp. 349-353, 1997.

[19] B. Mohan and S. B. Phadke, "Variable structure active suspension system", *Proceedings of the 1996 IEEE IECON 22nd International Conference on Industrial Electronics, Control, and Instrumentation*, Vol. 3, pp. 1945-1948, 1996.

[20] R. A. Decarlo, S. H. Zak, and G. P. Matthews, "Variable structure control of nonlinear multivariable systems: a tutorial", *Proceedings of the IEEE*, Vol. 76(3), pp. 212-232, 1988.

[21] C. Kim and P. I. Ro, "A sliding mode controller for vehicle active suspension systems with non-linearities," *Proceedings of the Institution of Mechanical Engineers Part D, Journal of Automobile Engineering*, Vol. 212, pp. 79-92, 1999.

[22] S. B. Choi, Y. T. Choi, and D. W. Park, "A sliding mode control of a full-car electrorheological suspension system via hardware in-the-loop simulation," *Journal of Dynamic Systems, Measurement, and Control*, Vol. 122, pp. 114-121, 2000.

[23] S. B. Choi, B. K. Lee, M. H. Nam, and C. C. Cheong, "Vibration control of a MR seat damper for commercial vehicles," Proceedings of SPIE Conference on Smart Structures and Materials, SPIE Vol. 3985, pp. 491-496, 2000.

[24] M. R. Jolly, J. W. Bender and J. D. Carlson, "Properties and applications of commercial magnetorheological fluids," *Proceedings of SPIE Conference on Smart Structures and Materials*, SPIE Vol. 3327, pp. 262-275, 1998.

[25] J. D. Carlson and K. D. Weiss, "A growing attraction to magnetic fluids", *Machine Design*, pp. 61-64, Aug 1994.

[26] O. Ashour, D. Kinder, V. Giurgiutiu, and C. Roger, "Manufacturing and characterization of magnetorheological fluids", *Proceedings of SPIE Conference on Smart Structures and Materials*, SPIE Vol. 3040, pp. 174-184, 1997.

[27] O. Ashour, C. A. Rogers, and W. Kordonsky, "Magnetorheological fluids: materials characterization, and devices", *Journal of Intelligent Material Systems and Structures*, Vol. 7, pp. 123-130, 1996.

[28] T. G. Lazareva and I. G. Shitik, "Magnetic and magnetorheological properties of flowable compositions based on barium and strontium ferrites and iron oxide", *Proceedings of SPIE Conference on Smart Structures and Materials*, SPIE Vol. 3045, pp. 185-189, 1997.

[29] R. Bolter and H. Janocha, "Design rules for MR fluid actuators in different working modes", *Proceedings of SPIE Conference on Smart Structures and Materials*, SPIE Vol. 3045, pp. 148-159, 1997.

[30] J. D. Carlson, D. M. Catanzarite, and K. A. St. Clair, "Commercial magnetorheological fluid devices", *International Journal of Modern Physics B*, Vol. 10, No. 23-24, pp. 2857-2865, 1996.

[31] B. F. Spencer Jr., S. J. Dyke, M. K. Sain, and J. D. Carlson, "Phenomenological model of a magnetorheological damper," *ASCE Journal of Engineering Mechanics*, Vol. 123, pp. 230-238, 1997.

[32] S. J. Dyke, B. F. Spencer Jr., M. K. Sain, and J. D. Carlson, "Modeling and control of magnetorheological dampers for seismic response reduction," *Smart Materials and Structures*, Vol. 5, pp. 565-575, 1996.

[33] P. Li, G. M. Kamath, and N. M. Wereley, "Dynamic characterization and analysis of magnetorheological damper behavior", *Proceedings of SPIE Conference on Smart Structures and Materials*, SPIE Vol. 3327, pp. 284-302, 1998.

[34] W. H. Li, G. Z. Yao, G. Chen, S. H. Yeo, and F. F. Yap, "Testing and steady state modeling of a linear MR damper under sinusoidal loading", *Smart Materials and Structures*, Vol. 9, pp. 95-102, 2000.

[35] N. D. Sims, R. Stanway, A. R. Johnson, D. J. Peel, and W. A. Bullough, "Feedback control of an electrorheological long-stroke vibration damper," *Proceedings of SPIE Conference on Smart Structures and Materials*, SPIE Vol. 3672, pp. 73-81, 1999.

[36] R. Majjad, "Estimation of suspension parameters," *Proceedings of the 1997 IEEE International Conference on Control Applications*, pp. 522-527, 1997.

[37] C. Kim, P. I. Ro and H. Kim, "Effect of the suspension structure on equivalent suspension parameters," *Proceedings of the Institution of Mechanical Engineers Part D, Journal of Automobile Engineering*, Vol. 213, pp. 457-470, 1999.

[38] C. Kim and P. I. Ro, "Reduced-order modeling and parameter estimation for a quarter-car suspension system," *Proceedings of the Institution of Mechanical Engineers Part D, Journal of Automobile Engineering*, Vol. 214, pp. 851-864, 2000.

[39] C. Y. Lai and W. H. Liao, "Vibration control of a suspension system via a magnetorheological fluid damper," *Proceedings of the 5th European Conference on Smart Structures and Materials*, SPIE, Vol. 4073, pp. 240-251, 2000.

[40] H. F. Lam and W. H. Liao, "Semi-active control of automotive suspension systems with magnetorheological dampers," *Proceedings of SPIE's 8th Annual International Symposium on Smart Structures and Materials*, Vol. 4327, 2001.

[41] J-J. E. Slotine and W. Li, Applied Nonlinear Control, Prentice-Hall, New Jersey, pp. 276-310,1991.

[42] J. Y. Wong, Theory of Ground Vehicles, John Wiley & Sons, Inc., 1993.

[43] G. Genta, Motor Vehicle Dynamics: Modeling and Simulation, World Scientific Publishing Co. Pte. Ltd., 1997.

[44] P. C. Muller and W. O. Schiehlen, Linear vibrations, Martinus Nijhoff Publishers, 1985.

[45] S. S. Rao, Mechanical Vibrations, Addison-Wesley Publishing Company, 1995.

[46] D. J. Inman, Engineering Vibration, Prentice Hall International, Inc., 1996.